IONISATION IN FLAMES WITH ADDITIVES

by

MONER ABD-EL-EZIZ MORSY, B.Sc.

A thesis submitted for
the Degree of Doctor
of Philosophy in
The University
of Aston in
Birmingham

December, 1979

PREFACE

This dissertation, which is being submitted for the Degree of Doctor of Philosophy in the University of Aston in Birmingham, is an account of the work done under the supervision of Professor F.M. Page, B.A., Ph.D., Sc.D. in the Department of Chemistry of the University of Aston in Birmingham from October, 1976 to August, 1979. Except where references are given in the text the work described herein is original and has not been submitted for a degree at any other University.

I wish to express my gratitude to Professor F.M. Page for his continued stimulus, guidance and encouragement during these years, and to all the members of the staff of the department and other departments for their assistance.

Ionisation in Flames with Additives

Submitted for the Degree of Ph.D., December 1979

Moner Abd-El-Aziz MORSY

SUMMARY

The addition of phosphorus to a series, at atmospheric pressure, of alkalimetal-seeded $H_2/O_2/N_2$ flames results in the formation of negative ions accompanied by a decrease in free electron concentrations.

Observations were made of the effects of phosphorus on the ionisation of sodium, potassium, rubidium and caesium. The ionisation of lithium is reduced by extensive hydroxide formation, and was too small for accurate measurements.

The construction of the measuring system is described, together with a discussion of the principles involved in its use. The concentrations of electrons, positive ions and hydrogen atoms, have been measured using the microwave resonant cavity, the rotating electrostatic probe and the spectrophotometer, respectively, to investigate the effect of phosphorus on both the charged and the neutral species. Phosphorus has been introduced as dimethylphosphite.

These flames collectively span a temperature range from $2000^{o}K$ to $2500^{o}K$. Temperatures have been measured by the sodium-line reversal technique.

From the results obtained, it has been shown that phosphorus raises the degree of ionisation of alkali metals which is the reason of increasing the positive ion concentration uniformly as the partial pressure of phosphorus increases and at sufficiently high values of total phosphorus, the electron concentration decreases.

The concentration of electrons is linearly proportional to the concentration of hydrogen atoms which decreases as height increases.

The electron affinity of PO_2^- has been obtained throughout the course of this work, (E.A. of PO_2^- = 3.1 eV).

Key Words:
MHD Magnetohydrodynamic generation of electricity
FID Flame ionisation detectors
EA Electron affinity

CONTENTS

CONTENTS, continued

CONTENTS Continued Page

LIST OF DIAGRAMS

LIST OF DIAGRAMS Continued

LIST OF TABLES

1. INTRODUCTION

It has been remarked by many authors[4, 44] that an exact definition of what is meant by the word flame is difficult to compose, and they suggest that certain properties such as the emission of light, the rapid attainment of high temperatures, and the occurrence of rapid reactions such as oxidation processes, which being common to many flames, are not universally present and do not form a complete definition. In the present context however, the flame used, in which mixtures of hydrogen oxygen and nitrogen were burnt at atmospheric pressure, are properly described as such, and would appear so even to the casual observer.

It has long been known that flames are conductors of electricity, although until about thirty years ago the ionisation in flames was a scientific curiosity rather than a subject of great importance. Since that time interest has grown rapidly, and a great number of detailed investigations into the nature and properties of ions in flames have been reported due to several circumstances. The first is the demonstration that electrically conducting flames may be used for magnetohydrodynamic (M.H.D.) power generation. Also, rocket exhaust plumes can have electron concentrations high enought to impede and distort radio guidance signals.

The principle[2] of the M.H.D. generator is illustrated in Figure (1.1). Ionised gas is passed at a velocity of U m/s in the y-direction across a magnetic field of B Wb/m^2 in the z-direction. A charge, e, within the gas experiences a force (eU x B) owing to its motion through the magnetic field. For the given configuration, this is equivalent to an effective

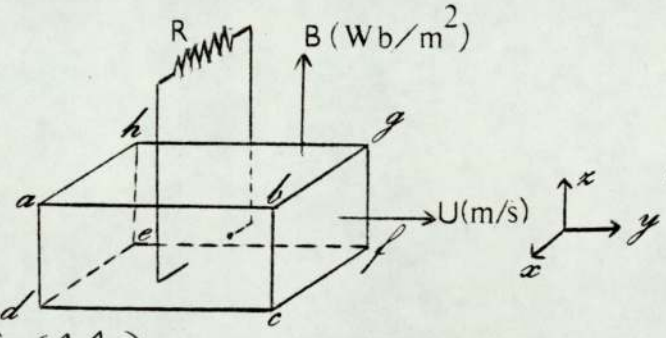

FIG. (1.1) D.C. MHD generator.

electric field of (UB) volts per metre in the x-direction. Thus, if the faces abcd and efgh are made electrodes and connected through a load, R, a current will flow under the action of the induced field, i.e. power will be generated.

The other major reason is concerning the present generation of rocket vehicles which depends on the chemical energy released from a fuel by combustion. Unfortunately the flame emerging from the throat of a rocket will usually contain large concentrations of electrons, which will seriously attenuate any radio-frequency signals whose path to the rocket lies within the flame and then disturb communication with the vehicle, communications blackout being particularly serious when the so-called high-energy propellants are used. This term refers to propellant formulation to which light metals, particularly aluminium, have been added, largely to make use of the very high heat of combustion of the metal. This beneficial property carries the corollary that the combustion products will be highly stable, condensed-phase substances, resulting in the case of aluminium in the appearance of micron sized alumina particles in the rocket exhaust. It is found that aluminised propellants are particularly troublesome in regard to communications, and it has been suggested that electron emission from hot alumina particles is contributory to the high levels of ionisation observed[3].

The great importance of the subject has led to extensive investigations not only in the two major applied fields, but also in laboratory flames to explain the formation and decay of ions.

Organic compounds yield ions when burned in a flame, and, if two electrodes at a potential difference of about 150 V are

inserted in it, differences in the conductivity of the flame can be measured as the solutes elute from the chromatographic column and are burned. This is the principle of the very sensitive and widely used flame ionisation detector (F.I.D.) for gas chromatography.

In operation, nitrogen or similar inert gas is used as the mobile phase for chromatography. The column effluent is mixed with hydrogen, and this mixture fed into the flame jet of the detector. The jet is a thin-walled metal tube which also acts as an electrode. The other electrode is a metal filament held a few millimeters above the flame. A current of filtered sweep air is passed through the detection chamber to remove dust particles and water of combustion. As organic compounds pass through the detector, they are burned in the flame and give rise to an ionisation current which is measured and recorded. Background current is of the order of 10^{-11} amp, depending on detector design.

The F.I.D. has proved very useful in gas chromatography. It is sufficiently sensitive for use with capillary columns or conventional columns prepared at low packing ratios, and at the same time its response is not quenched by the presence of water vapour or oxygen in the gas stream as is the case with the argon detector. Unlike the latter, it responds to low-molecular-weight organic compounds such as methane and ethane but is essentially insensitive to all inorganic gases. In most cases, it would be the detector of choice for a laboratory limited to a single instrument.

The flame ionisation method yields moderately consistent results for hydrocarbons when computations are made on a weight basis, the response per mole increasing roughly with carbon

number. However, much lower responses per unit weight are obtained from alcohols and chlorinated hydrocarbons so that once more rather extensive calibration is required to obtain quantitative data.

The ionisation in flames containing organic compounds, which is the basis of operation of the hydrogen flame detector, cannot be explained on a purely thermal basis using the ionisation potentials of any of the known stable gaseous species or likely intermediates in the flame, and early effort was centred on attempts to account for the observed ionisation in terms of some new species with a low ionisation potential. It was suggested by Stern[115] that such a species might be a solid carbon aggregate, with an ionisation potential approaching the work function of solid graphite, 4 ev, which is sufficiently low to afford the order of magnitude of ionisation observed; when the hydrogen flame ionisation detector was developed, the carbon aggregate theory was uncritically employed[116, 117] even though the formation of the aggregates in such a carbon-lean flame is extremely improbable.

Calcote in a series of papers[94, 118, 20] has reopened the question of mechanism of ion formation in flames, and his work has quite definitely established that chemi-ionisation, not thermal ionisation, must be responsible.

As Calcote has indicated, the greatest hope for clearly identifying the actual processes of importance probably lies in application of direct mass spectrographic sampling to the flame gases. Studies of this type are being undertaken by groups led by Sugden[119], van Tiggelen[120] and Calcote.

Flame ionisation is really a subdivision of plasma physics, yet it has developed independently because generally flames are

at a much lower temperature than plasmas, also the composition of flame gases leads to a great variety of possible reactions than is generally the case in plasmas.

The study of ionisation[4] in flames demands an analytical technique for the determination of the concentration of ions. It is customary to determine the electron concentration by a.c. conductivity, the positive ion concentration by diffusion limited d.c. conductivity, and to apply mass spectrometry to a more specific analysis both of positive and negative ions.

The idea that a flame could be used as a high thermostat in which to study the equilibria between ions, molecules and electrons, was used by Rolla and Piccardi[5] who studied the thermal ionisation of a number of substances[6, 7, 8] deducing values for the ionisation potentials of a number of elements, and claiming to have measured the electron affinities of several compounds. The results for the determination of ionisation potentials quoted are in very good agreement with the values obtained by other methods.

The early attempt to apply chemical arguments to the experimental data on ionisation in a flame was made by Page[9]. Other early studies of ionisation in flames by methods based on D.C. conductivity[10] had shown that the ionisation was qualitatively in agreement wiht the equation proposed by Saha[11] but there was some indication that the electron concentration was lower than that predicted.

A study of ionisation[12, 13] showed that a detailed physicochemical analysis of any combustion system could be made on the basis of the electron concentration, assuming thermodynamic equilibrium. It was therefore proposed that a general study be made of the effects of electron acceptors on

both the charged and the neutral species in flames containing alkali metal. In the present work the proper diagnostic techniques have been utilized in a study of the effects of phosphorus on both the neutral and the charged species in premixed H_2-rich-N_2-O_2 flame containing different alkali metals.

The Karmen-Guiffrida detector[14, 15, 16] is now well known to gas chromatographers and is available commercially. Its main value is its extraordinary sensitivity to phosphorus, but it can be very useful for other elements.

As a matter of fact, the mechanism of the Karmen-Guiffrida detector in dispute and may not be simple. The detector entails a flame and ionisation; but the ions may not be thermionic and an alkali metal is not indispensable. However, there has to be an additive, activator or sensitizer of some sort.

Karmen believed thatin his original detector[14] phosphorus raises the rate of vaporization of alkali metal from the sensitizer into the flame. In his later review[17] he stressed the probable multiplicity of the mechanism and mentioned the contending view that phosphorus (or other response-eliciting analyte) does not raise the volatility of the sensitizer but instead raises the degree of ionisation of sensitizer vapour already present in the flame. This must be the case in the arrangement described by Aue and Gehrke[18], who fed a constant concentration of alkali metal vapour in helium into the hydrogen flame; phosphorus (or chlorine) raised the ionisation while depressing the alkali emission. At the same meeting, Saturno and Cooke[19] presented similar evidence and attributed it to the phenomenon explained by Padley, Page and Sugden[20]:

when a halogen X and an alkali metal M enter a hydrogen flame, the two reactions $M+X \rightarrow M^{+}+X^{-}$ and $X^{-}+H \rightarrow HX+e^{-}$ raise the concentration of electrons above what it would be from the thermal ionisation of M alone, since the concentration of H is abnormally high. Page and Woolley[21] further discussed this mechanism for the halogens and suggested that the response to phosphorus may be similarly explained.

Most flames containing phosphorus emit a conspicuous continuum. Such a continuum has been reported by Guest[22] and Miller[23]. It looks white with perhaps a greenish-yellow tint. This continuum is strong in the primary flame of all burners emitting the HPO spectrum.

Fenimore and Jones[24] measured the emission due to HPO from methyl phosphate in fuel-rich hydrogen-oxygen-argon flames at 50, 100 and 760 torr and 1000-1380°K. They undertook to relate the HPO intensity to the temperature and to the concentrations of atomic and molecular hydrogen and oxygen. They found the emission to be proportional to the 0.4 power of the phosphorus concentration; but all who have used the HPO emission for practical analysis report linearity over a wide range of concentrations. This discrepancy impairs Fenimore and Jones's main conclusion, viz., that the phosphorus is present mostly as P_2 in the region of the glow. They observed that atomic H was the dominant radical in the burnt gas (ranging around 0.03 micromole per ml).

William J. Miller[25] added phosphorus to a series of potassium-seeded $H_2/O_2/N_2$ flames and identified the formed negative ions mass spectrometically as PO_2^{-}.

This dissertation reports the studies of the effect of phosphorus on both the charged and the neutral species in a

series of flames containing alkali metals.

These studies which although complementary to each other appear separately in the text for the sake of clarity. They are measuring the concentrations of electrons, positive ions and hydrogen atoms.

2. LAMINAR PREMIXED H_2-rich-N_2-O_2 FLAMES

2.1. INTRODUCTION:-

A number of isothermal sets of hydrogen flames were chosen at a series of temperatures distributed through the range for the work to be described. The flames used were laminar, premixed hydrogen-oxygen flames, containing nitrogen as dilutent. All gases were obtained from commercial cylinders.

2.2. LAMINAR PREMIXED FLAME:-

This flame is generally characterized by its homogeneous properties and stable form when the flow velocity of the supply gas exceeds the burning velocity. Three zones can be clearly distinguished:

(i) The PRIMARY COMBUSTION OR REACTION ZONE (or inner cone) where the fuel-oxidant mixture that has left the burner is ignited. With a Meker burner, this zone is split up into a number of little cones, one for each cylindrical hole in the burner top. In this very thin zone (thickness is of the order of 0.1 mm) the combustion reactions proceed rapidly to near completion, as far as sufficient oxygen is available in the supplied gas-mixture. In this zone, i.e. during the combustion, thermal and chemical equilibrium do not exist, so that a general temperature cannot meaningfully be defined here.

(ii) In the INTERMEDIATE ZONE above and immediately adjacent to the reaction zone, the flame gases are usually found in a state of thermal and chemical equilibrium. They attain here, practically, their final temperature, which depends on the kind of fuel and oxidant gases used and on

their mixture strength. A maximum temperature is usually attained when the gas-oxidant ratio is slightly above the stoichiometric ratio. The actual maximum temperature is often somewhat lower owing to heat losses, incomplete combustion, etc.

(iii) The latter zone is surrounded by the SECONDARY COMBUSTION OR REACTION ZONE (or outer cone) where the flame comes into contact with the ambient air. The infusion of air and its turbulent mixing with the flame gas causes on the one hand a cooling effect and on the other hand, the additional, gradual supply of fresh oxygen gives rise to further combustion of the flame gases. This secondary combustion takes place in a rather diffuse zone at the flame border, whose width increases with height in the flame.

2.3. THE HYDROGEN FLAME:-

The simple flame of hydrogen burning in clean air is practically non-luminous in the visible region of the spectrum, although the flame as usually obtained in the laboratory is coloured slightly orange by various impurities in the dust of the air, chiefly NaCl and $CaCO_3$. The yellow colour often observed at the tip of flames surrounded by air is apparently associated with the presence of nitrogen and is believed to be caused by continuous radiation due to the reaction involving nitric oxide and oxygen. Higher temperature flames, however, appear to be coloured in their own right.

Although in flame photometry hydrogen flames ordinarily are less efficient in atomization, exhibit more chemical interferences, and are less efficient in excitation; it has the major advantage which is the improved signal-to-noise ratio for some elements due to the low background intensity

of this flame.

The only radiation is from the OH bands and also some faint-banded structure at the red end which is due to the pure vibration-rotation spectrum of water. The latter is almost absent in hydrogen-air flames but is quite strong in hydrogen-oxygen flames. The OH radiation appears fairly uniform over the length of the flame without any marked strengthening in the reaction zone, as with many other flames.

The inner cone is not obvious in hydrogen flames, there is an inner, cone-shaped, dark region, but there is no increase in luminosity at the same front.

Hydrogen-rich flames always give more ionisation than an oxygen-rich one of the same temperature.

The ionisation energy of the molecules and radicals contained in the metal free flame gas is comparatively high (8eV, or more). In thermal equilibrium, ions are therefore not expected to occur in noticeable concentrations in flames which are not seeded by metal vapour. In H_2, natural flame ions are practically absent.

By contrast with a hydrocarbon flame, the hydrogen flame cannot produce carbon deposits around the burner orifices.

Several flames have hydrogen as the fuel. The oxidant gas may be oxygen, various mixtures of oxygen and nitrogen, halogens, or perchloryl fluoride.

To lower the temperature as required, an inert gas is added to the hydrogen-oxygen flame. Nitrogen is usually used, but helium, argon, carbon dioxide and excess hydrogen serve just as well. The flame velocity is also decreased.

Friedman[26] has studied the relationship between flame extinction distance and nitrogen content for these flames,

and his results furnish valuable data for the design of burners to be used with premixed gases. Some of his results show that the extinction distance increases exponentially with increase in nitrogen content, and the flame temperature decreases with increasing nitrogen content. He also found that helium gives a smaller decrease in the flame velocity than nitrogen, on account of its higher heat conductivity.

2.4. CHEMISTRY OF HYDROGEN FLAMES:-

The oxidation of hydrogen in a flame does not take place by a single step, but by a chain mechanism, the first step in the chain is the reaction[27].

$$H_2 + O_2 \xrightarrow{k_1} H + HO_2 \qquad \overset{\Delta H}{+55 \text{ kcal}} \qquad (2.1)$$

which proceeds at an extremely low rate. Experiments by Dixon-Lewis and Williams[28] indicate that this step may be affected by the water present in the flame.

The H radicals formed in reaction (2.1) react with the oxygen to produce new radicals, one of which - the O radical - causes chain branching:

$$H + O_2 \xrightarrow{k_2} OH + O \qquad \overset{\Delta H}{+ 15 \text{ kcal}} \qquad (2.2)$$

$$OH + H_2 \xrightarrow{k_3} H + H_2O \qquad - 14 \text{ kcal} \qquad (2.3)$$

$$O + H_2 \xrightarrow{k_4} OH + H \qquad 0 \text{ kcal} \qquad (2.4)$$

The chain-supporting radicals recombine on the walls of the burner or in collision with species that can take up energy without forming new radicals. The rates of reactions (2.2), (2.3) and (2.4) have been investigated by a number of authors. The slowest is reaction (2.2) and the fastest, which leads to chain branching, is reaction (2.4). The rate

constants are in the ratio $k_1:k_2:k_3 = 1:100:1000$, from which it is evident that reaction (2.2) is the rate determining step. Since the rate depends on the concentrations of the reactants, and the final stable product is water:

$$\frac{d[H_2O]}{dt} = k_2 [O_2][H] \qquad (2.5)$$

Of the two components of the reaction, the hydrogen radical is of decisive importance since its concentration is very low right at the start but increases in the course of the reaction as a result of the side-chains. If for the time being we disregard the recombination of radicals, we have, by addition of reactions (2.2), (2.3) and (2.4):

$$H + O_2 + 2H_2 \longrightarrow OH + 2H + H_2O \qquad (2.6)$$

Taking into account reaction (2.3) between the OH radical and hydrogen, we have:

$$H + O_2 + 3H_2 \longrightarrow 3H + 2H_2O \qquad (2.7)$$

Thus trebling the number of H radicals in one cycle.

These reactions take place in the combustion zone of the flame. For both laminar and turbulent flames, this zone occupies quite a narrow space, above which there are high-temperature gases. The chain members taking part in the combustion reaction get into this high-temperature zone, where they are mixed with the reaction products. Ideally, for a stoichiometric mixture, only water is found in addition to the radicals. At the edge of the flame, however, as a result of diffusion and convection there will be oxygen and nitrogen present as well (the minor components of air can be neglected). If the flame does not contain such substances as smoke, then the radicals can only

recombine by interaction with polyatomic molecules. These polya molecules may themselves undergo thermal dissociation in the high-temperature zone of the flame. In the case of a hydrogen-oxygen flame, the chain-supporting radicals and the final reaction product (water) are in a thermal dissociation equilibrium[29, 30] reached by either of the reactions:

$$H_2O \rightarrow H + OH \tag{2.8}$$

$$2H_2O \rightarrow 2H_2 + O_2 \tag{2.9}$$

Reaction (2.9) however, occurs to only a small extent.

Consider the possible reactions of OH radicals produced in the flame:

$$OH + OH \underset{k_{-5}}{\overset{k_5}{\rightleftharpoons}} H_2O + O \tag{2.10}$$

$$OH + H_2 \underset{k_{-6}}{\overset{k_6}{\rightleftharpoons}} H_2O + H \tag{2.11}$$

$$OH + O \underset{k_{-7}}{\overset{k_7}{\rightleftharpoons}} O_2 + H \tag{2.12}$$

$$OH + H \underset{k_{-8}}{\overset{k_8}{\rightleftharpoons}} H_2 + O \tag{2.13}$$

At each flame temperature there will be a different equilibrium concentration of OH radicals, but in the combustion zone, as a result of the high rate of side-chain formation, there will be a considerably higher concentration of radicals than the equilibrium concentration in the high-temperature zone. The relative concentrations of H and OH radicals in the reaction zone will be governed[31] by

$$H + H_2O \underset{k_{-9}}{\overset{k_9}{\rightleftharpoons}} H_2 + OH \tag{2.14}$$

which is a simple exchange reaction, and consequently very

fast. (The rate constants[32] in $ml.mole^{-1}.sec^{-1}$ are $k_9 = 1x10^{15}\ e^{-25000/RT}$, $k_{-9} = 2.5 \times 10^{14}\ e^{-10000/RT}$ and $t_{\frac{1}{2}} = 1/3$ μsec.) The ratio of the concentrations of H and OH radicals over the whole of the flame is therefore the equilibrium ratio, but the absolute concentrations are far from the equilibrium value predicted by reaction (2.8). The radicals formed in the combustion zone can only recombine by a three-body collision with a species possessing enough degrees of freedom to be able to absorb the surplus energy. The radical concentration approaches the equilibrium value corresponding to the flame temperature by the reaction:

$$H + H + M \rightarrow H_2 + M \qquad (2.15)$$

or

$$OH + H + M \rightarrow H_2O + M \qquad (2.16)$$

which tend to reduce the disequliibrium downstream of the reaction zone. It has been shown however, these radicals may maintain equilibrium proportions with respect to each other by the more rapid bimoleculor exchange process:

$$H_2O + H \rightleftharpoons H_2 + OH \qquad (2.3)$$

$$H_2 + O \rightleftharpoons OH + H \qquad (2.4)$$

The radical species H, O and OH do not produce any appreciable amounts of natural ionisation such that the burnt gas region of hydrogen flames have been extensively used for the study of nonequilibrium ion chemical kinetics of metal additives.

3. FLAMES WITH ADDITIVES

3.1. INTRODUCTION:

3.1.a. General Remarks

It is well known that the addition of small amounts of substances of low ionisation potential, such as alkali or alkaline earth metals, can greatly enhance ionisation in the product gases of flames. As regards practical considerations, this can be either a nuisance or an advantage depending upon the circumstances. For example, in rocket exhausts it can cause interference with radio communications, whilst deliberate seeding with alkali metals has been used to raise the electrical conductivity of combustion products to the level required to operate M.H.D. generators.

Ionisation usually requires considerable energy, the ionisation potentials for most atoms and molecules falling within the range 4-20 eV.

There are many processes that results in ionisation:

(i) Ionisation by collision

$$A+B \rightarrow A^+ + B + e^-,$$

$$A + e^- \rightarrow A^+ + e^- + e^-.$$

(ii) Electron teransfer

$$A + B \rightarrow A^+ + B^-.$$

(iii) Ionisation by transfer of excitation energy

$$A + B^* \rightarrow A^+ + B + e^-$$

(iv) Chemi-ionisation

$$A + B \rightarrow C^+ + D + e^-,$$

$$A + B \rightarrow C^+ + D^-.$$

Positive ions can recombine with either electrons or negative ions, according to some processes, such as:

(i) Three-body recombination

$$A^+ + e^- + M \rightarrow A + M$$

(ii) Dissociation recombination

$$AB^+ + e^- \rightarrow A + B$$

(iii) Mutual neutralization

$$A^+ + B^- \rightarrow A^* + B^*$$

However, many species are capable of forming stable negative ions. There are three principal gas-phase mechanisms:

(i) Radiative attachment

$$e^- + A \rightarrow A^- + h\nu$$

(ii) Three-body attachment

$$e^- + A + M \rightarrow A^- + M$$

or:

$$e^- + A \rightarrow (A^*)^-$$

followed by:

$$(A^*)^- + M \rightarrow A^- + M$$

(iii) Dissociative attachment

$$AB + e^- \rightarrow A + B^-$$

In the flame, neutral atoms or molecules may be split, giving a positive ion and a free electron (or a negative ion). The higher the flame temperature and the lower the ionisation energy, the larger will be the proportion of ions produced. The ionisation energy is the minimum amount of energy required to remove an electron from the atom or molecule. As a consequence of ionisation, the fraction of element present as neutral species will be reduced and the spectral lines emitted by this species will be weakened. With some elements the ionic species may also emit spectral lines in the flame, but these occur at wavelengths other than those of the neutral species. Double ionisation, i.e. stripping of two electrons

from one neutral atom or molecule has not yet been reported in commonly used flames.

The tendency to form ions is especially strong for most of the alkali atoms; this tendency decreases in the order: Cs, Rb, K, Na, and Li, corresponding to an increase in ionisation energy in the same order from 3.89 to 5.39 electron volt (eV).

Some elements (for instance: Na and Cu) are, virtually FULLY ATOMIZED. They occur mainly as free atoms in the flame. However, some of them may be partially ionised in the hotter flames.

3.1.b. Excitation of Metal Spectra in H_2-N_2-O_2 Flames

When metal salts are sprayed into hydrogen flames the resonance lines of the metal atoms usually appear in emission, and in some cases band systems of oxides, hydrides or hydroxides are also observed. Sugden and colleagues at Cambridge between 1955 and 1960 published a long and valuable series of papers on measurements of the strengths of these metal lines and bands in hydrogen-oxygen-nitrogen flames, making quantitative measurements in flames of various compositions and temperatures and also studying the effect of height in the flame.

Usually the metallic line spectrum is restricted to a few resonance lines with the lowest excitation energy, especially resonance lines like the extremely persistent yellow lines of sodium or the infra-red resonance lines of potassium.

Flames containing alkali metals show strong resonance lines and continuous emission. Some very old papers by Hartley[33, 34] give a clear account of the spectra of these flames.

The continua were previously attributed by Gaydon[35] to ion-electron recombination processes of the type:

$$Na^+ + e^- = Na + h\nu$$

but it is now known that the main reaction is of the type[35]:

$$Na + OH = NaOH + h\nu$$

3.1.c. Molecular Metal Species in the Flame

Significant proportions of some alkali elements may be bound as monohydroxides in flames that contain hydrogen as a major component. The tendency to form hydroxides is especially strong for Li whose atomic fraction is often reduced to below 10%. This tendency is much less strong for Cs, Rb, and K. The formation of NaOH is usually negligible. Values of the ratio ϕ (= [MOH]/[M]) of the concentration of hydroxide and free metal atoms are very much less than 1 for Na, and in the ranges 0.05 for K, 0.06-0.8 for Rb, 1.4-7.0 for Cs and 10-470 for Li.

None of the alkali hydroxides emits spectral bands in the visible or ultraviolet portion of the spectrum.

3.2. THE CHEMICAL THEORY OF THE IONISATION IN FLAMES:

3.2.a. Ionisation of Alkali Metals

Occurrence of ionisation from traces of metal vapours, especially of alkali metals, in a flame is well known. Ions are formed in the reaction zone of a flame by thermal means. The ionisation of an atom A to its positive ion A^+ and a free electron e^- may be treated like a diatomic dissociation process basically governed by the equation:

$$A \rightleftarrows A^+ + e^- \qquad (3.1)$$

In equilibrium the ionisation and recombination rates are balanced. The concentrations of the species involved in

process (3.1) are then related to one another by the equation (3.2) which is a kind of mass action law for the dissociation of a neutral particle into two ionised particles[36, 37, 38]. This equation reads:

$$K_1 = \frac{[A^+]\ [e^-]}{[A]} \qquad (3.2)$$

The ionisation constant K_1 is specific for the species considered and depends only on T. Its value can be calculated from statistical mechanics according to Saha equation:

$$\log K_1 = \frac{-5050\ V}{T} + \frac{5}{2} \log T - 6.49 + \log \frac{g_A^+\ g_e^-}{g_A} \qquad (3.3)$$

where V is the ionisation potential in electron volts, T is expressed in degrees kelvin on the absolute scale, K_1 in atmospheres, and the g terms are the statistical weight of the ionised atom, the neutral atom, and the electron. For alkali metals the final term is zero.

The dependence of the equilibrium constant on the flame temperature is governed mainly by the first term containing V in equation (3.3). For a typical value of V (4-5 eV) at a medium flame temperature of 2500°K, the absolute value of the first term is of the order of 10. Lowering V by 0.5 eV appears to raise K_1 about 10-fold, all other parameters remaining constant. The same increase in K_1 is achieved through a temperature increase of approximately 250°C.

If the total ionisation is small, that is, $[A^+] \ll [A]$, so that $[A_o] = [A]$, where $[A_o]$ represents the total quantity of metal added and expressed as a partial pressure, and if the effects of anion formation are slight, equation (3.2) reduces to:

$$[A^+]^2 = [e^-]^2 = K_1\ [A_o] \qquad (3.4)$$

A plot of log $[A^+]$ or log $[e^-]$ against the logarithm of the molarity of the salt solution should be a straight line of slope 0.50. Zero slope indicates no ionisation.

Using equation (3.3), and assuming the partial pressure of metal atoms in the flame to be 10^{-6} atm, the percent ionisation for the alkali metals at 2450°K in hydrogen-oxygen flame is shown in Table (3.1)[39].

Table (3.1). Percent ionisation of alkali metals at 2450°K in H_2/O_2 flame

Element	Ionisation potential	Percent ionisation
Lithium	5.37	0.9
Sodium	5.12	5.0
Potassium	4.32	31.9
Rubidium	4.16	44.4
Caesium	3.87	69.6

Page and Sugden[40] have measured the number of electrons per cubic centimeter in a column of flame gases resulting from the combustion of hydrogen and air in a premixed flame. Measurements were accomplished through the attenuation of 3-cm (microwave) radiation passing through the flame gases horizontally. Salts of sodium, potassium, and lithium were sprayed into the flame. These investigators found a marked increase of electron concentration with increasing height above the burner base. The variation with height is not very temperature-dependent although it is more pronounced for gas mixtures nearer stoichiometric. Results for sodium and potassium were similar, but when lithium solutions were sprayed

into the flame, the concentration of electrons remained almost independent of the height above the burner.

According to equation (3.3), a plot of the logarithm of the proportionality constant K_1 between $[e^-]^2$ and $[A_o]$ against 1/T for a given metal in a series of flames should be a straight line of slope - 5050V. Similarly, a plot of the logarithm of K_1 against V for various metals should be a straight line of slope - 5050/T when the temperature is held constant. Neither of these predictions was found to be true in the case of the alkali metals. The deviations from the predicted ionisation have been noted by other workers but no satisfactory explanation was offered until Smith and Sugden suggested that the ionisation which occurs is explicable on the basis of equilibrium between the metal, its positive ion, and free electrons, provided that reasonable account is taken of the side reactions involving the free radicals of the flame gases to give the hydroxide of the metal and negative hydroxyl ions, also in equilibrium amounts. The equilibria that are considered to be important in flame gases containing a small amount of added alkali metal are given by equations (3.1) and (3.2) and the following:

$$AOH = A + OH \qquad (3.5)$$

$$K_2 = \frac{[A]\ [OH]}{[AOH]} \qquad (3.6)$$

$$OH^- = OH + e^- \qquad (3.7)$$

$$K_3 = \frac{[OH]\ [e^-]}{[OH^-]} \qquad (3.8)$$

To these equations must be added that for charge balance

$$[A^+] = [e^-] + [OH^-] \qquad (3.9)$$

and the mass balance for A

$$[A_o] = [A] + [AOH] + [A^+] \qquad (3.10)$$

Below 2200°K the ionisation is small, and the last term of equation (3.10) may be ignored. As earlier, $[A_o]$ represents the total alkali metal added, free or combined.

The solution of these equations had been demonstrated mathematically by Page[9], for the partial pressure of electrons, to show:

$$K_1 [A_o] = [e]^2 (1+\phi) (1+\phi^-) \qquad (3.11)$$

if the degree of ionisation is small, and

$$[A_o] = [e] (1+\phi^-) \qquad (3.12)$$

if the alkali metal is largely ionised. ϕ and ϕ^- are two flame parameters dependent only on the composition of the flame gases and defined by the equations:

$$\phi = [AOH]/[A] \qquad (3.13)$$

$$\phi^- = [OH^-]/[e] \qquad (3.14)$$

3.2.b. Ionisation of Alkali Metals in Presence of an Electron Acceptor:

In a system at equilibrium, the condition, $[A^+] = [e^-]$ is not fulfilled when the flame is supplied with an electron acceptor B, that is partly converted into negative ions B^-, and into AB, the number of free electrons is now lowered, since a certain fraction of them is bound to B, and an increase in metal ionisation must be expected.

Padley, Page and Sugden[20], observed that, under certain conditions, the addition of halogen to flame gases containing traces of alkali metals may result in a pronounced increase in the concentration of electrons present in the system. They explained this unexpected result on the hypothesis that

whereas the production of electrons in the absence of halogen is governed by a steady state of the reaction:

$$(1) \quad A + X \underset{k_{-1}}{\overset{k_1}{\rightleftharpoons}} A^+ + e + X, \qquad K_1$$

where A and X represent an atom of alkali metal and any third body respectively, the introduction of a halogen B allows the reactions:

$$(2) \quad A + B \underset{k_{-2}}{\overset{k_2}{\rightleftharpoons}} A^+ + B^- \qquad K_2$$

$$(3) \quad B^- + H \underset{k_{-3}}{\overset{k_3}{\rightleftharpoons}} HB + e \qquad K_3$$

to occur, with consequent effects on the steady state determining [e].

The initial increase and the subsequent decrease of [e] have been explained by the transition between the steady-state without halogen and the shifted steady-state caused by the halogen.

Sugden and Hayhurst[41] later showed that the analysis could be made even more general. They considered the last three chemical processes, (1), (2), and (3), and the following:

$$(4) \quad HB + H \underset{k_{-4}}{\overset{k_4}{\rightleftharpoons}} H_2 + B \qquad K_4$$

$$(5) \quad AOH + H \underset{k_{-5}}{\overset{k_5}{\rightleftharpoons}} A + H_2O \qquad K_5$$

$$(6) \quad AB + H \underset{k_{-6}}{\overset{k_6}{\rightleftharpoons}} A + HB \qquad K_6$$

$$(7) \quad H_2O + H \underset{k_{-7}}{\overset{k_7}{\rightleftharpoons}} H_2 + OH \qquad K_7$$

and the three conservation equations

(8) $[A_o] = [A] + [AOH] + [AB]$

(9) $[B_o] = [B] + [HB] + [AB]$

(10) $[A^+] = [e] + [B^-] + [OH^-]$

In the actual analysis, [AB] was omitted in equation (9) and $[OH^-]$ in equation (10), as being small.

The rates of direct ionisation (process 1) and indirect ionisation (processes 2 and 3) were related by defining the ratios:

$$R_2 = k_{-2}/k_{-1} \qquad (3.15)$$

$$R_3 = k_{-3}/k_{-1} \qquad (3.16)$$

also:

$$K_1 = k_1/k_{-1} \qquad (3.17)$$

Attention was confined to processes 1-3, as the others were all considered, from flame photometric evidence, to be fast and balanced at all times.

Certain distribution parameters were defined and related to elementary equilibrium constants.

$\eta = [B^-]/[e]$; $\quad \eta_e = [B]_e/K_\eta$; $\quad \eta/\eta_e = \gamma^{-1}$

$\phi = [OAH]/[A]$; $\quad \phi_e = [OH]_e/K_\phi$; $\quad \phi/\phi_e = \gamma^{-1}$

$\theta = [HB]/[B]$; $\quad \theta_e = [H]_e/K_\theta$; $\quad \theta/\theta_e = \gamma^{-1}$

$\xi = [AB]/[A]$; $\quad \xi_e = [B]_e/K_\xi$; $\quad \xi/\xi_e = \gamma^{-1}$

where γ is the disequilibrium parameter $[H]/[H_e]$. Processes 1-3 are assumed to have brought ions and electrons to a steady state.

$$d[A^+]/dt = k_1[A][X] - k_{-1}[A^+][e][X] + k_2[A][B] - k_{-2}[A^+][B^-] = 0$$

$$d[B^-]/dt = k_2[A][B] - k_{-2}[A^+][B^-] - k_3[H][B^-] + k_{-3}[HB][e] = 0$$

$$d[e]/dt = k_1[A][X] - k_{-1}[A^+][e][X] + k_3[H][B^-] - k_{-3}[HB][e] = 0$$

Taking the negative ions first:

$$\{k_2[A] + k_{-3}[e]\theta\}[B] = \{k_{-2}[A^+] + k_3[H]\}[B^-]$$

$$\frac{[B^-]}{[B]} = \frac{k_2[A] + k_{-3}[e]\theta}{k_{-2}[A^+] + k_3[H]} = \frac{K_2 R_2 [A] + R_3[e]\theta}{R_2[A^+] + K_3 R_3[H]}$$

For electrons:

$$k_1[A][X] - k_{-1}[A^+][e][X] = k_{-3}[e][B]\theta - R_3 K_3[H][B^-]$$

$$K^-[A] - [A^+][e] = R_3[e][B]\theta - R_3 K_3[H][B^-]$$

$$= R_3[e][B]\theta - K_3[H][B]\left(\frac{K_2 R_1[A] + R_3[e]\theta}{R_2[A^+] + K_3 R_3[H]}\right)$$

$$= R_3[B]\left(\frac{R_2[A^+][e]\theta - K_2 K_3 R_2[H][A]}{R_2[A^+] + K_3 R_3[H]}\right)$$

Noting that:

$$[A^+] = [e] + [B^-] = [e]\ (1 + \eta)$$

$$[B_o] = [B] + [HB] = [B]_e\ (1 + \theta)$$

$$[A_o] = [A] + [AOH] + [AB] = [A](1 + \phi + \xi)$$

the relation becomes:

$$K^-[A] - [e]^2\ (1+\eta) = \frac{R_2 R_3 [B_o]}{(1+\theta)}\left(\frac{[e]^2\theta\ (1+\eta) - K_2 K_3\ [H][A]}{R_2[e]\ (1+\eta) + K_3 R_3[H]}\right)$$

This is a cubic in $[e]$, which is not easy to use in analysing experimental results. The term $R_2[e](1+\eta)$ in the denominator of the R.H.S. can be neglected if R_3 were sufficiently large[41]; the equation now simplifies to a linear equation in $[e]^2$. In doing this, it is useful to relate the real equilibrium constants K_2 and K_3 to the elementary equilibrium constants K_η etc.

$$K_2 = [A^+][B^-]/[A][B] = [A^+][e]\,\eta/[A][B]$$

$$= K^-\eta/[B] = K^-/K_\eta$$

$$K_3 = [HB][e]/[H][B^-] = [HB]/[H]\eta$$

$$= [B]\theta/[H]\eta$$

$$= \theta_e K_\eta/[H]_e$$

The relation then becomes:

$$[e]^2\,(1+\eta)\left(\frac{R_2\,[B_o]}{(1+\theta)}\;\frac{\theta[H]_e}{\theta_e\,K_\eta[H]}+1\right) = [A]K^- + \frac{R_2[B_o]}{(1+\theta)}\,\frac{K^-[A]}{K_\eta}$$

Hence:

$$[e]^2 = \frac{K^-[A]}{(1+\eta)}\left(\frac{1 + R_2[B_o]/K_\eta\,(1+\theta)}{1 + R_2[B_o]/K_\eta\,(1+\theta)\gamma^2}\right)$$

Inserting the value for $A = [A_o]/\,(1 + \phi + \xi)$

and writing: $X = R_2/K_\eta\,(1 + \theta)$

$$[e]^2 = \frac{K^-[A_o](1+X[B_o])}{(1+\eta)(1+\phi+\xi)(1+X[B_o]\gamma^{-2})}$$

If $[e_o]$ is the electron concentration when $[B_o] = 0$, and $E = [e]/[e_o]$

$$E^2 = \frac{(1+X[B_o])(1+\theta)}{(1+X[B_o]\gamma^{-2})(1+\phi+\xi)(1+\eta)} \qquad (3.18)$$

The corresponding expression for $P = [A^+]/[A_o^+]$ is:

$$P^2 = \frac{(1+X[B_o])(1+\theta)(1+\eta)}{(1+X[B_o]\gamma^{-2})(1+\phi+\xi)} \qquad (3.19)$$

On differentiating these expressions, the initial slope of the E^2 or P^2 graph against $[B_o]$ may be determined:

$$\left[\frac{dE^2}{d[B_o]}\right]_{[B_o]=0} = \frac{R_2(\gamma^2-1) - \gamma^2(1+\theta)(1+K_\eta/K_\xi)}{K_\eta\,\gamma^2\,(1+\theta)} \qquad (3.20)$$

$$\left[\frac{dP^2}{d[B_o]}\right]_{[B_o]=0} = \frac{R_2\,(\gamma^2-1) + \gamma^2(1+\theta)(1 - K_\eta/K_\xi)}{K_\eta\,\gamma^2\,(1+\theta)} \qquad (3.21)$$

The conditions for a maximum in the graph may also be evaluated with the results:

$$E^2_{max} = \frac{R_2\,(\gamma^2-1)}{\gamma^2(1+\theta)} \quad \frac{1}{(1+X[B_m]\gamma^{-2})^2} \quad \frac{1}{(1+K_\eta/K_{\bar\xi} + 2[B_m]\,/K_\eta K_{\bar\xi})} \qquad (3.22)$$

where $[B_m]$, $E_{\bar\xi max}$ are the values at the maximum and

$$K_{\bar\xi} = K_\xi(1+\phi)$$

$$P^2_{max} = \frac{R_2(\gamma^2-1)}{\gamma^2(1+\theta)} \left[\frac{(1+\eta_{max})}{(1+X[B_o]\gamma^{-2})}\right]^2 \frac{1}{(K_\eta/K_{\bar\xi} - 1)} \qquad (3.23)$$

Since $\gamma > 1$, a maximum in P will only be observed if $K_\eta > K_{\bar\xi}$: this condition which will not, in general, be satisfied.

These relations have been exploited by Page and Woolley[21] for the case of phosphorus acting as acceptor, though without definite kinetic results, and by Hayhurst and Sugden[41] who studied the halogens as acceptors, and will be applied by the author to the experimental results. Graphs 5.4 & 6.7 show $[e]/[e_o]$ as (E/E_o) & $[A^+]/[A^+_o]$ as (P/P_o).

4. THE APPARATUS

4.1. BURNER DESIGN

The burner used in the studies is shown in Figure (4.1) approximately to scale. The upper chamber allows cooling water to circulate around the hypodermic tubes, a necessary feature as the parts were soldered together. The central chamber supplies the gas for the outer shield flame, and the lower chamber, the gases and additives for the inner flame. The stainless steel hypodermic capillary tubes, 8.1×10^{-4}m internal diameter, were regularly spaced apart with 15×10^{-4}m from centre to centre to allow for lateral expansion of the burned gases and the bundle arranged to give a flame hexagonal in cross-section. The flame rate to the outer flame was the greater, 54 tubes being used to supply the gases, as opposed to 37 to the inner flame. Such water cooled Meker type burners have been used for a number of years in this type of study. The tubes were held in phates by being soldered into three predrilled circular brass plates, themselves held in position inside the outer barrel by rubber "O" rings rather than a more rigid attachment to allow a safety blow off facility. The reaction zone of the flames takes the form of small cones above the individual tubes and the effect of the multitude double flame burner is to produce a flame having a flat, short reaction zone $<1 \times 10^{-3}$m, in height. The burnt gas region moves with piston flow effectively steady in temperature and composition for up to 8×10^{-2}m above the burner surface. Above this distance the effect of entrained air becomes noticeable. The burner assembly was mounted on an adjustable jack, so that the flame could be moved easily in the vertical plane relative to the detection device.

FIG(4.1) THE BURNER

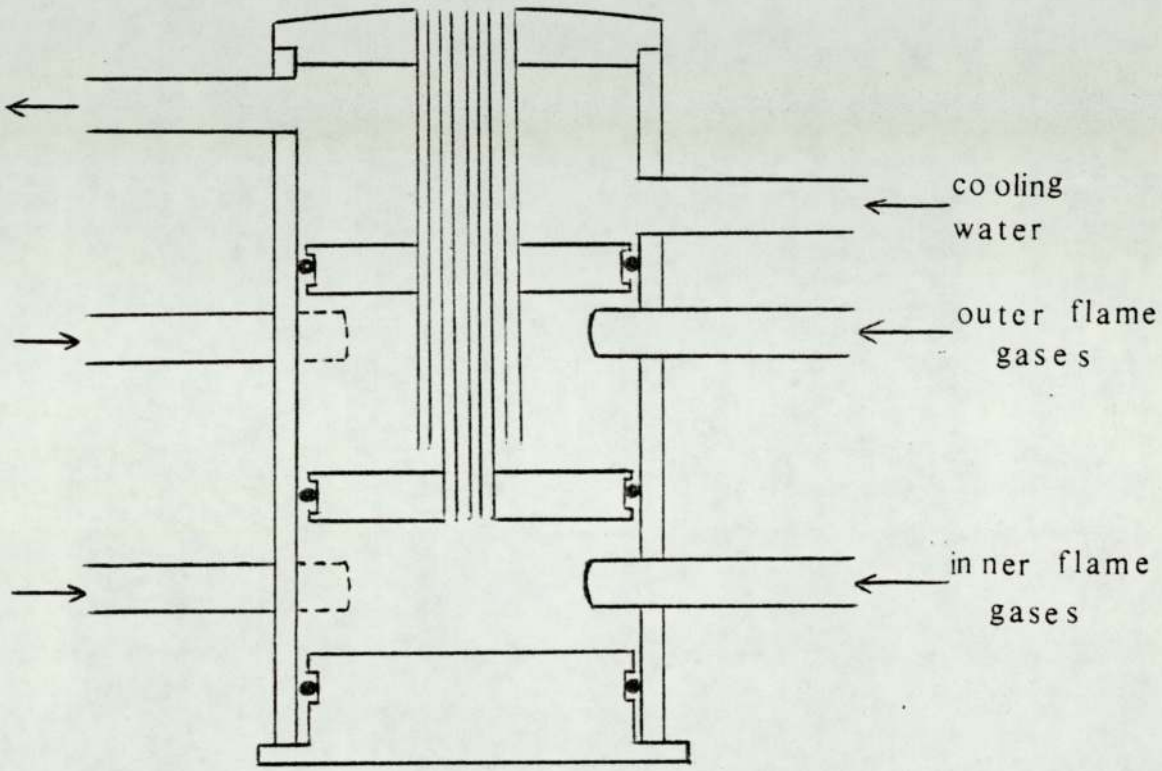

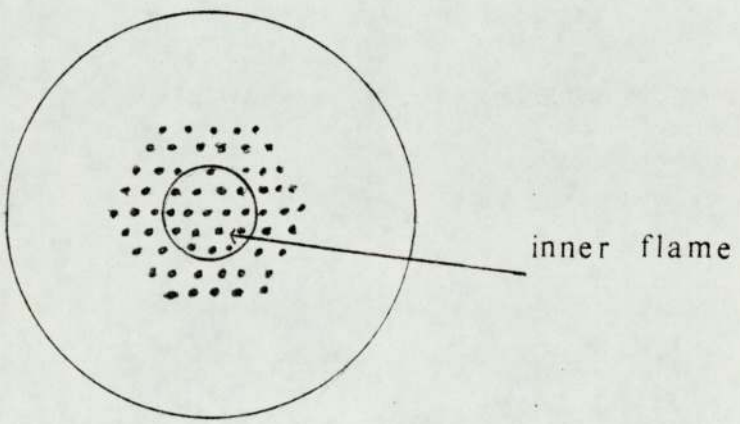

top view

4.2. THE GAS DELIVERY SYSTEM:

Unburnt mixtures of hydrogen, oxygen and nitrogen fed to the flame, were monitored by means of calibrated 'Rotameters' and controlled by 'clockhouse' needle valves in the fuel lines.

In practice two flames were burned, an inner test flame on which measurements were made, surrounded by a sheath flame of similar composition to protect the central region from surrounding air and from wall-cooling and to improve stability. Flow rates to the outer and inner flames were arranged to be such that both had the same convective velocity.

4.3. SUPPLY OF LIQUIDS TO THE FLAME:

Metal salt solutions were introduced into the flame as fine mists from a pneumatic atomiser, Figure (4.2.A), operated by a part of the nitrogen supply to the inner flame. The gas flow across the tip of the jet created a reduced pressure at this point, and solution from the bulb was drawn up to be disintegrated by the high velocity gas stream. A long tube interposed between the atomiser and the burner ensured that only the finest droplets reached the flame. This type of atomiser has been used by many previous workers[42] and has been shown to be linear in operation with concentration over a wide range for most solutions up to 0.25 molar concentrations, above this, blocking of the atomiser nozzle occurred due to salt deposition. In view of this, an independent check on the atomiser delivery was thought to be unnecessary, since the delivery factor can be conveniently obtained during the calibration.

Calibration of the atomiser delivery was achieved along with the calibration of both the probe and the cavity, by

FIG(4.2) THE ATOMISER AND SATURATOR

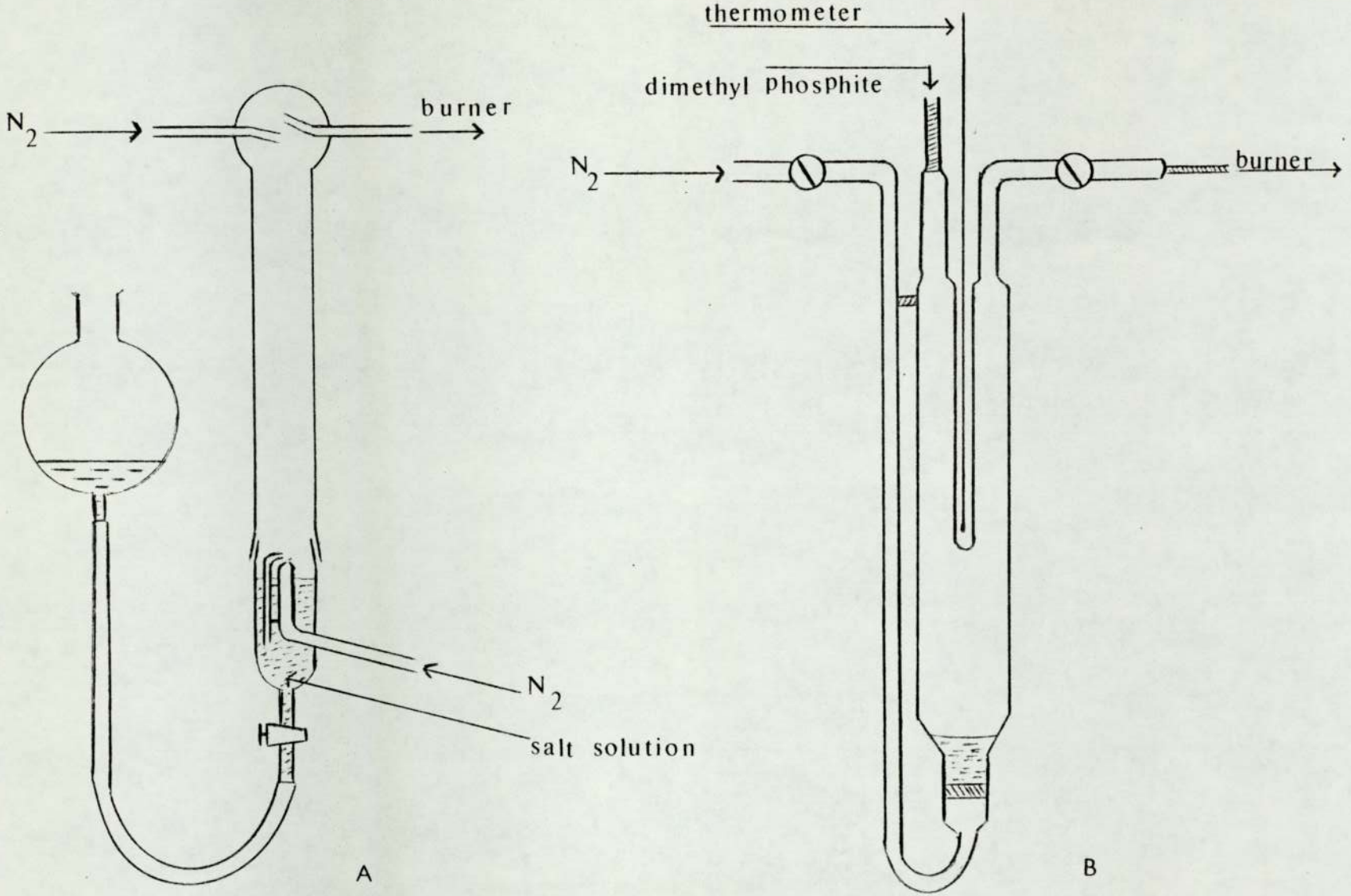

FIG(4.3) GAS DELIVERY SYSTEM

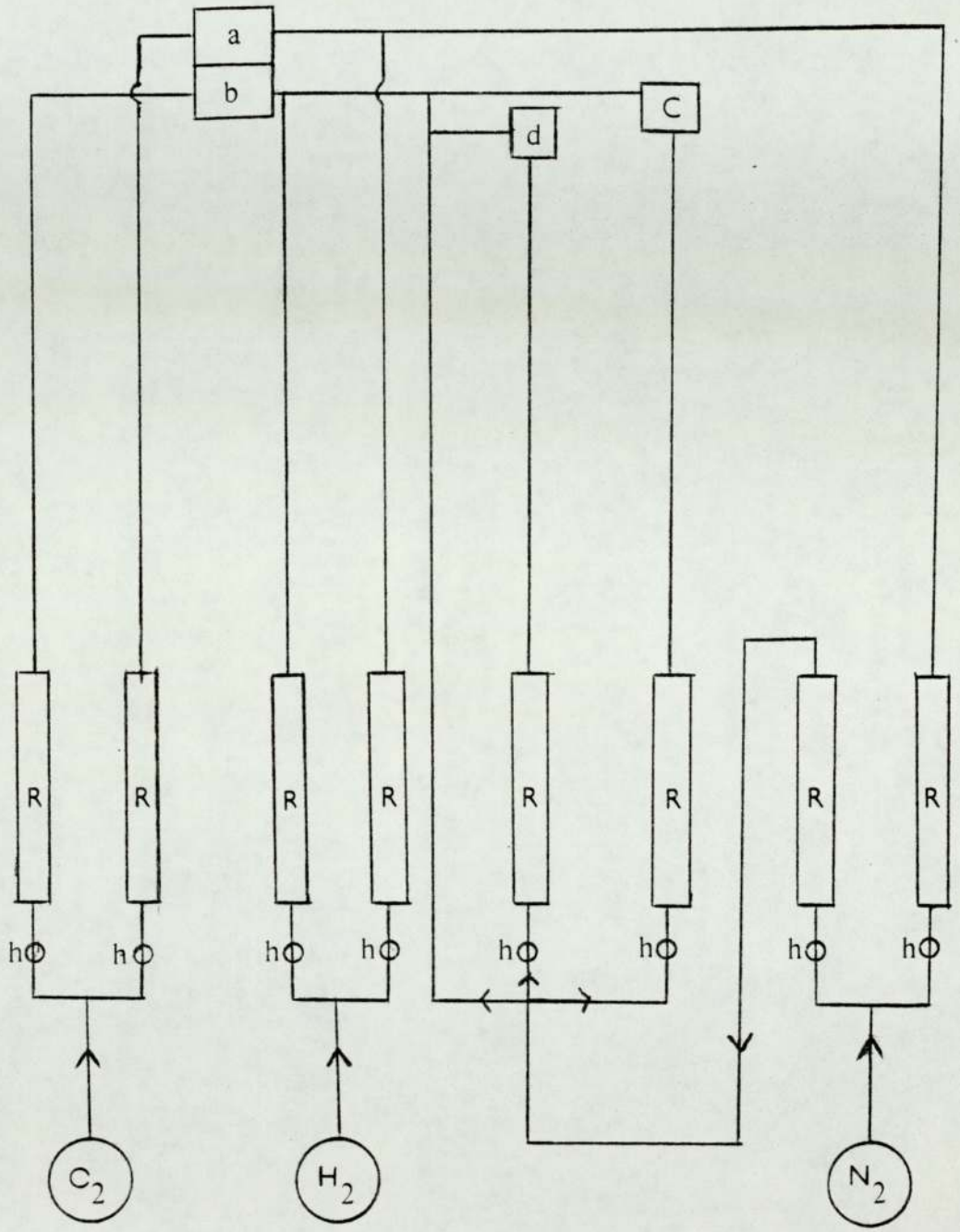

a outer flame

b inner flame

C atomiser

d saturator

R rotameter

h needle valve

matching experimental dilution plots for caesium with theoretical curves obtained using the Saha equation. The calibration procedure is described in sections 5.6 and 6.12.1.b.

Volatile dimethylphosphite was introduced to the flame by passing a portion of nitrogen gas through a saturator immersed in a thermostated bath. The saturator is shown in Figure (4.2.B) .it was normally used with a layer of dimethylphosphite about 5 cm in depth resting on the sinter. The nitrogen stream from the flowmeter is broken up by the sintered glass disc of the saturator into a great number of fine bubbles, which present a very great surface to the liquid, and readily become SATURATED. The body of the saturator is sufficiently long to prevent any liquid being carried over as a spray, and a thermometer suspended inside the body of the saturator showed that under the conditions used, the temperature of the saturated vapour was the same as that of the thermostated bath. Figure (4.3) shows the general scheme of the gas delivery system.

4.4. FLAME TEMPERATURE:

It is difficult, so far, to define the flame temperature because of the departure of the flame gases from equilibrium, this departure is slight for the interconal or burnt gases, but there are major departures from equilibrium in the reaction zone or flame front.

4.4.a. Measurement by the Spectrum-line Reversal Method

The optical methods of measurement only give a mean value along the path of the light beam but have an advantage; that they do not disturb the flame gases. On the other hand

they often have the disadvantage that it is not possible to make a point-by-point study of the temperature distribution through the flame.

4.4.b. The Sodium-line Reversal Method

Alkali-metal atoms all have one electron outside the closed shells. The energy level depends mainly on the value of the principal quantum number n for this electron, but also to some extent on the azimuthal quantum number l, those energy levels for alkali-metal atoms are doubled by the electron spin; this is the cause of the well-known doublets in the spectra, such as the yellow "D-lines" doublet of sodium.

The flame temperatures were measured by the sodium "D" line reversal technique, which is widely used and accepted for these type of flames, and described by several authors[44,4]. The measurement of flame temperatures by this method at atmospheric pressure give flame temperatures usually only 50°C to 100°C below theoretical values, part of this difference may be due to heat losses from the flame, rather than to any lack of equilibrium. This method depends on the line reversal of the emitted resonance radiation of Na atoms, thermally equilibrated with the bulk flame gases, and gives the electronic excitation temperature of Na in the flame, which may be assumed to be equal to the true thermodynamic temperature if there is thermal equilibrium between sodium atoms in their ground state (^2S) and atoms in their first excited states ($^2P_{\frac{1}{2}}$ and $^2P_{3/2}$). That equilibrium does prevail has been established by a number of workers[43], who have shown that temperatures measured by the reversal technique are consistent with values obtained by other methods.

When sodium is introduced into a flame, it emits the two yellow "D" lines at 5890 and 5896 A^{O}. Also, when light from a bright back ground source giving a continuous spectrum is passed through a flame containing sodium vapour, the sodium lines will appear either in absorption, as dark lines, or in emission as bright lines, according to whether the brightness temperature of the background source is higher or lower than the flame temperature.

When the brightness temperature of the background and the flame temperature are exactly the same, then the lines are invisible, having the same brightness as the background. Thus, if we can vary the brightness of the background until the sodium lines just disappear and then measure the brightness temperature of this background with an optical pyrometer, we can determine the flame temperature. The brightness temperature of the lamp for various current values were found from the calibration of the lamp at 6550 A^{O}, against a Leeds and Northrop disappearing filament pyrometer, itself standardised against a black body.

Light from a suitable background source (B), such as a strip-filament tungsten lamp, is focussed with a concave mirror (M) to give an image of the lamp in the centre of the inner flame (F). A lens (L) then forms an image of both flame and lamp on the slit (S) of the constant deviation spectrometer (C). An aperture stop (P) is used to restrict the aperture, so that the solid angle of light taken from the flame is the same as that from the image of the lamp; the correct position for this aperture stop is at the position of the image of the lens (L) formed by the mirror (M). Figure (4.4).

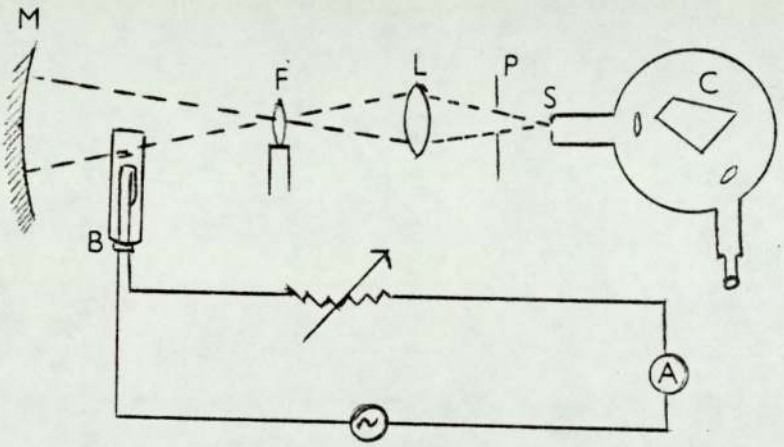

FIG(4.4) THE ASSEMBLY OF FLAME TEMPERATURE MEASUREMENT

Since a tungsten strip lamp is used as background source, and the temperature of this is determined from a calibration against a black body using red light, then a correction[44] must be made to this temperature. The calibration is for the brightness temperature in the red, usually for a mean wavelength of 6550 A^{o}, i.e. the temperature a black body would have to have to give the same light intensity at that wavelength. Now the true temperature of tungsten strip is appreciably higher than its brightness temperature, and when we come to use the yellow sodium line the brightness temperature for this wavelength is rather closer to the true temperature.

This correction can be made quite easily by the use of Wien's law:

$$\frac{1}{T} - \frac{1}{T_{\lambda}} = \frac{\lambda \ln \varepsilon_{\lambda}}{C_2} \qquad (4.1)$$

Where C_2 is the second radiation constant which has the value 1.438 $cm.deg^{-1}$ and ε_{λ} the emissivity at wavelength λ. The radiation data used was taken from International Critical Tables[1] and the values used for the emissivity of tungsten are those given by deVos[45].

The flame temperatures thus measured were found to rise sharply to a constant value at round 2×10^{-2} m above the burner face, and to vary only over $20^{o}K$ or less up to 8×10^{-2}m in the flame. The absolute error is hard to assess, but after considerations of the reproducibility of the measurement, errors of ± $20^{o}K$ at $2300^{o}K$ and below, to ± $25^{o}K$ at $2500^{o}K$ were assigned to the temperatures. Flame compositions used in the investigations, together with their measured temperatures, are shown in Table (4.1).

Table 4.1

The measured temperatures at a fixed height of 3 cm above the tip of the burner.

Flame	% H_2	% O_2	% N_2	Temperature (^{o}K)
1	32	11	56	2000
2	32.68	11	55.62	2030
3	33.36	11	54.24	2065
4	35	12	54	2105
5	35.69	12	53.62	2140
6	36.37	12	52.23	2176
7	38	13	48.8	2200
8	38	13	50	2200
9	39	12	48.8	2200
10	38.8	13	48.4	2250
11	40	13	46	2300
12	41	14	45	2330
13	43	14	43	2382
14	52	14	33	2417
15	41	15	44	2440
16	46	15	39	2470
17	41	16	43	2490
18	46	15	39	2500
19	48	16	36	2500
20	38	13	48	2545

5. MEASUREMENT OF ELECTRON CONCENTRATIONS

5.1. INTRODUCTION:

The a.c. conductivity may be determined from the absorption coefficient for microwaves, or from the alternation in the resonance response of a tuned circuit either in the megacycle region (tank circuit) or in the microwave region (resonant cavity).

Microwave measurements yield a value for the electron concentration in the flame, and are applicable over the range 10^8-10^{12} electrons cm^{-3}. In the most sensitive method, a section of the flame is made part of the dielectric of a cylindrical cavity in which electromagentic waves oscillate at the resonance frequency of the cavity. Electrons in the flame modify the electronic characteristics of the cavity, absorbing power from the radiation and producing a shift in resonance frequency and a change in the quality-factor (Q) of the resonator. The change in Q is a measure of the concentration of electrons in the flame.

Two of the earliest uses of microwave attenuation were by Andrew, Axford and Sugden[46] to determine the number of electrons in the transient flame resulting from the firing of a rifle and by Belcher and Sugden[47], who studied the ionisation of the alkali metals in a coal gas-air flame using the experimental collision frequency and the attenuation coefficient expression deduced by Margenau[48] to evaluate the constant of proportionality between the attenuation in decibels per centimetre and the number of electrons per cubic centimetre of the attenuating medium, the method which has been widely applied to the study of flames by Sugden and his co-workers. The experimental establishment of the method by Belcher and Sugden[49] involved

a demonstration that the observed attenuation depended on the frequency of the microwave radiation in the correct manner, and the determination of the collision frequency of the electron from this dependency.

Microwave techniques have been much used in kinetic studies in flames[50,51], and have been applied to the ionisation produced by carbon particles in flames by Sugden and Thrush[52], and Shuler and Weber[53]. Woolley[54] has applied the technique to the ionisation of a variety of smokes in flames. Because microwave frequencies are the highest that can be used in order to obtain appreciable attenuation, at the electron concentrations found in flames, they have been employed by numerous other workers in the field of combustion; for example, Smith and Sugden[55], Balwanz, Headrick and Ahern[56]. The main difficulty with microwave methods is that of obtaining a sufficient degree of spatial resolution. The holes in the cavity walls which allow the passage of the flame enable the electric and magentic fields to spread into the flame, and the section of flame under observation becomes ill-defined. The best resolution claimed for the method is 3 mm.

5.2. THE THEORY OF THE MICROWAVE CAVITY RESONANCE:

Electromagnetic radiation passing through a gas containing free ions is attenuated because the ions acquire directed momentum by interaction with the electric field of the radiation, which is then randomized by collisions between the ions and the molecules of the gas. This effect, which determined the electrical conductivity of the gas, will be dependent upon three factors; the number density of ions in the gas, the frequency of the radiation and the collision frequency of the ions with molecules. If the number density

of ions of mass 'm' and charge 'e' is 'n' per cc. The conductivity σ is shown by classical electromagnetic theory to be:

$$\sigma = \sum_{\text{ions}} \frac{ne^2}{m} \left(\frac{\omega_c}{\omega^2 + \omega_c^2}\right)$$

where ω_c, is the collision frequency of the ions and ω the angular frequency of the radiation. As σ is inversely proportional to the mass of the ions the effect of even the lightest atomic ions is negligible compared with that of electrons unless heavier ions greatly exceed electrons in number or ω is much less than ω_c, so that

$$\sigma = \frac{ne^2}{m} \left(\frac{\omega_c}{\omega^2 + \omega_c^2}\right) \qquad (5.1)$$

The application of (5.1) requires a knowledge of the electron collision frequency. Belcher and Sugden[49] who compared the attenuation at various values of ω, found this to be 8.8×10^{10} S^{-1}. Later work[57, 58] showed that this was too low by a factor of 3, and that the electron concentrations measured by them, and subsequent workers[53] were therefore too small[59,60]. These low electron concentrations were ascribed to the presence of OH^- ions[55,57,61], and the use of the latter and higher values of the collision theory obviates the necessity of invoking OH^- as a significant ionic constituent. Page[4] has mentioned that Page, Soundy and Williams have examined the temperature dependence of the collision frequency, and shown that the collision frequency is related to the temperature and composition by:

$$\omega_c = [H_2O]\ T^{-3/2} \qquad (5.2)$$

Since they worked in fuel-rich flames at fairly low temperatures, the water concentration will, to a first order,

be proportional to the temperature, so that the collision frequency was proportional to $T^{-1/2}$. These workers argued that the collision cross-section for water was far larger than for any other species at thermal electron energies, but did not carry out a sufficiently wide range of experiments to prove this. Bulewicz and Padley[62], using the allied cyclotron resonance technique examined a wide variety of fuels and deduced composition dependent electron molecule cross-sections which increased as the amount of hydrogen in the fuel, and hence water in the burnt gases, increased.

In flames at atmospheric pressure the attenuation of radiation at microwave frequencies (of the order of 10 kM c/s) is measurable on passing through a flame about 1 cm thick and containing around 10^{12} electrons/cc. In the present system, the flame passes through a cavity resonating at microwave frequencies, and 'damping' of the resonance by electrons is detectable for electron concentrations down to about 10^{8}/cc. This method was first used by Adler[63] to study ionisation in discharge tubes, and first applied to the study of flame ionisation by Sugden and Thrush[55], who offered few advantages over the direct measurement of attenuation.

The efficiency of a resonant cavity is conveniently expressed by the Quality (Q)-factor, defined as:

$$Q = 2\pi \frac{\text{energy stored per cycle}}{\text{energy dissipated per cycle}} = \frac{\omega L}{P} \qquad (5.3)$$

where L is the total electromagnetic energy averaged over one cycle. Normally the dissipation of energy is due to heating of the walls and loading introduced by coupling to the cavity. Denoting the loss due to these causes together with the loss

due to the presence of a 'clean' flame, as P_1 and the further loss which is brought about by causing the flame to become conducting as P_F, the net Q, Q_2, is given by:

$$Q_2 = \frac{\omega L}{P_1 + P_F} \qquad Q_1 = \frac{\omega L}{P_1}$$

$$\therefore \quad \frac{1}{Q_2} = \frac{P_F}{\omega L} + \frac{1}{Q_1}$$

Hence: $$P_F = \frac{\omega L}{Q_1} \left(\frac{Q_1}{Q_2} - 1\right) \tag{5.4}$$

The average energy dissipation by the electrons in the flame is[64]:

$$P_F = \tfrac{1}{2}\sigma \int_{vol} E^2 . dv = \sigma g \tag{5.5}$$

where E is the strength of the electric field vector.

Substituting equations (5.1) and (5.5) into equation (5.4) gives:

$$\frac{ne^2}{m} \left(\frac{\omega_c}{\omega^2 + \omega_c^2}\right) . g = \frac{\omega L}{Q_1} \left(\frac{Q_1}{Q_2} - 1\right) \tag{5.6}$$

The electron density, therefore, is directly proportional to the quantity $(Q_1/Q_2 - 1)^{1/2}$. Q-factors are not readily measureable with any accuracy for cavities with a Q greater than about 1000, but the ratio 't' of power transmitted at resonance by the cavity containing the 'clean' flame to that containing a conducting flame is readily obtained from a measurement of the power attenuation, βdb. Then:

$$\beta = 10 \log t \tag{5.7}$$

It now remains to obtain a relationship between 't' and $(Q_1/Q_2 - 1)$.

The power transmitted through the cavity is given by

relationship[72].

$$t_o = (1 + \frac{Q_i}{Q_o})^2 \qquad (5.8)$$

where t_o is the ratio of the power available to the power output, Q_o is the Q of the unloaded cavity, not coupled to an external circuit but containing a clean flame, and Q_i is the Q introduced by coupling to the external circuit (the iris loading Q).

$$\text{Hence } \frac{1}{Q_1} = \frac{1}{Q_o} + \frac{1}{Q_i}$$

Denoting the Q introduced by virtue of making the flame conducting as Q_F, we may define Q^-:

$$\frac{1}{Q^-} = \frac{1}{Q_o} + \frac{1}{Q_F}$$

and

$$\frac{1}{Q_2} = \frac{1}{Q_1} + \frac{1}{Q_F} = \frac{1}{Q_o} + \frac{1}{Q_i} + \frac{1}{Q_F}$$

thus:

$$\frac{Q_1}{Q_2} = \frac{Q_o\, Q_i + Q_o\, Q_F + Q_i\, Q_F}{Q_F\,(Q_o + Q_i)}$$

In the presence of a conducting flame, t^-, the ratio of the power available to the power output is:

$$t^- = (1 + \frac{Q_i}{Q_1})^2$$

$$= (\frac{Q_o\, Q_F + Q_i\, Q_o + Q_i\, Q_F}{Q_o\, Q_F})^2$$

The power ratio actually measured, $t = \frac{t^2}{t_o}$

$$\text{i.e.} \quad t = \left(\frac{Q_o Q_F + Q_i Q_o + Q_i Q_F}{Q_F (Q_o + Q_i)}\right)^2 = \left(\frac{Q_1}{Q_2}\right)^2 \qquad (5.9)$$

and

$$\eta_e \propto \frac{1}{Q_1} \cdot (t^{\frac{1}{2}} - 1) \qquad (5.10)$$

which agrees with the relationship by Adler[63].

The discussion above[54], applies strictly only to a gas filled cavity.

5.3. THE DESIGN OF THE MICROWAVE RESONANCE CAVITY:

The design of a suitable cavity resonator involves a compromise between selectivity of the length of flame to be studied and sensitivity of the cavity to electrons. Examination of equation (5.6) shows that the desirable features for maximum sensitivity are a high value of Q_1 coupled with a low resonant frequency, and the flame passing through the region of maximum electric field strength. Since equation (5.6) places no restriction on the mode of oscillation of the resonator, it is tempting to consider the use of resonators oscillating in the H_{1mn} modes, for which very high values of Q_1 may readily be obtained. However, resonators of this type have two important disadvantages; the depth of the cavity is proportional to the wavelength of the radiation resulting in measurements being made over rather long sections of the flame and, secondly, the ports in the end walls, which allow the passage of the flame through the cavity, must be sealed electrically to prevent the escape of radiation. This has been achieved by using coarse gauzes, which immediately limit the flame temperature and are a further source of trouble since distortion of the gauzes leads to a change in the depth cavity. Horsfield[65] avoided these problems and developed the loop

coupled cavity designed to oscillate in the E_{010} mode, and the advantages of working with this mode are such that this is now the usual type of cavity employed in flame ionisation studies and it has been applied to the kinetics of flame ionisation by Sugden, Padley and Jensen[66,67]. This cavity is not quantized in the vertical dimension, and can therefore be used to study narrow sections of flame: resolutions as high as 2 mm have been achieved.

It is not essential to work in the microwave region, and Sugden and Smith[58], Knewstubb[68], Williams[69], and Borgers[70] have used tank circuits (Capacitor-inductances) operating at megacycle frequencies in various forms. Only Knewstubb was able to approach the kinetics of ionisation.

Since in the megacycle region $\omega << \omega_c$ the dominance of the electron is lost, and the technique can in principle give information about heavy ions as well. The very poor height resolution, and the field distortion in the more highly conducting flames have, however, restricted the application of this method despite its sensitivity.

In E_{010} cavities the resonant frequency is governed solely by the diameter of the cavity and is given by[64,72].

$$\frac{c}{\omega} = \frac{a}{x_{1m}} \qquad (5.11)$$

where 'a' is the radius of the cavity and 'x_{1m}' is the $m^{\underline{th}}$ root of the Bessel function equation $J_1(x) = 0$. For the E_{010} mode, $x_{1m} = 2.405$. 'Q_1' is strongly dependent on the length of the cavity, being given by:

$$Q_1 = \frac{cx_{1m}}{\omega(1+a/L)\delta} = \frac{a}{(1 + a/L)\delta} \qquad (5.12)$$

where 'L' is the length of the cavity and 'δ' is the 'skin

depth' of the material from which the cavity is constructed.

The field equations for the E_{010} mode are:

$$\left.\begin{aligned} E_r = E_\theta = 0 \qquad & E_z = K^2 J_o (k\rho) \\ H_r = H_z = 0 \qquad & H_\theta = \frac{-i\omega\varepsilon k J_o'}{C} (k\rho) \end{aligned}\right\} \qquad (5.13)$$

The distributions of these fields are shown in Figure (5.1.b). The electric field vector is at a maximum at the centre of the resonator, giving a region in which power dissipation by electrons will occur almost uniformly through the flame, and the magnetic field vector is zero at the centre, so that holes cut in the walls at the centre will result in little loss of radiation from the cavity, obviating the need to seal the holes electrically with gauzes.

5.4. CONSTRUCTION OF THE RESONANT CAVITY:

The cavity, shown in Figure (5.1.a), consists of a copper cylinder, internal diameter 7.99 cm and length 1.2 cm, with axial flame ports 1.72 cm in diameter cut in the end plates. It was manufactured in three sections, consisting of two end-plates and a spacing-ring, which are tightly held together by means of six symmetrically placed screws in each end plate. This is important as the wall currents rise to a maximum at the corners of the cavity so that good electrical contact is essential to ensure efficient functioning of the cavity. As the Q-factor was reduced, both by the decrease in length of the cavity and by increased radiation losses from the ports[71]. The end-plates are fitted with cooling chambers through which water at 65°C was circulated. This prevents local overheating of the cavity and condensation of water vapour from the flame gases onto its cooler surface, both of which effects seriously affect its performance. The cavity

FIG(5.1) THE MICROWAVE RESONANT CAVITY

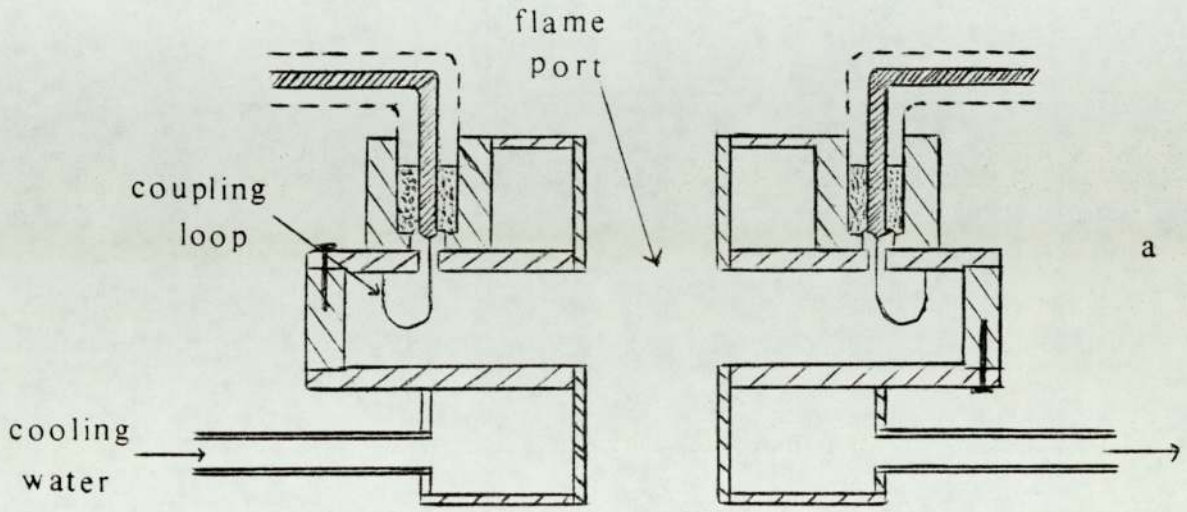

a

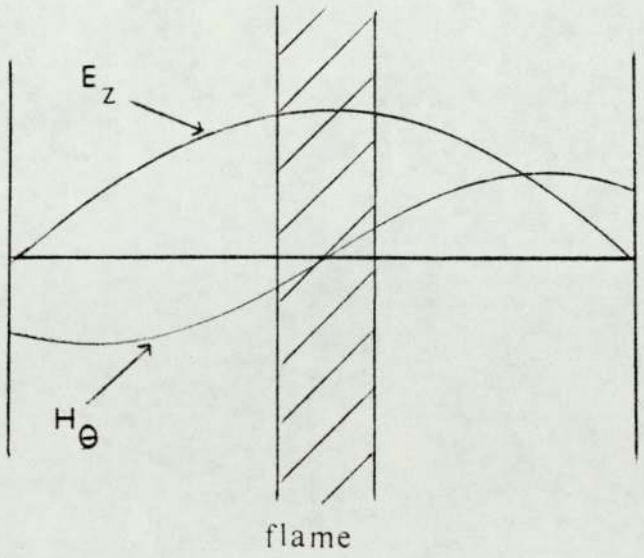

b

field configurations

FIG(5.2) BLOCK DIAGRAM OF THE MICROWAVE APPARATUS

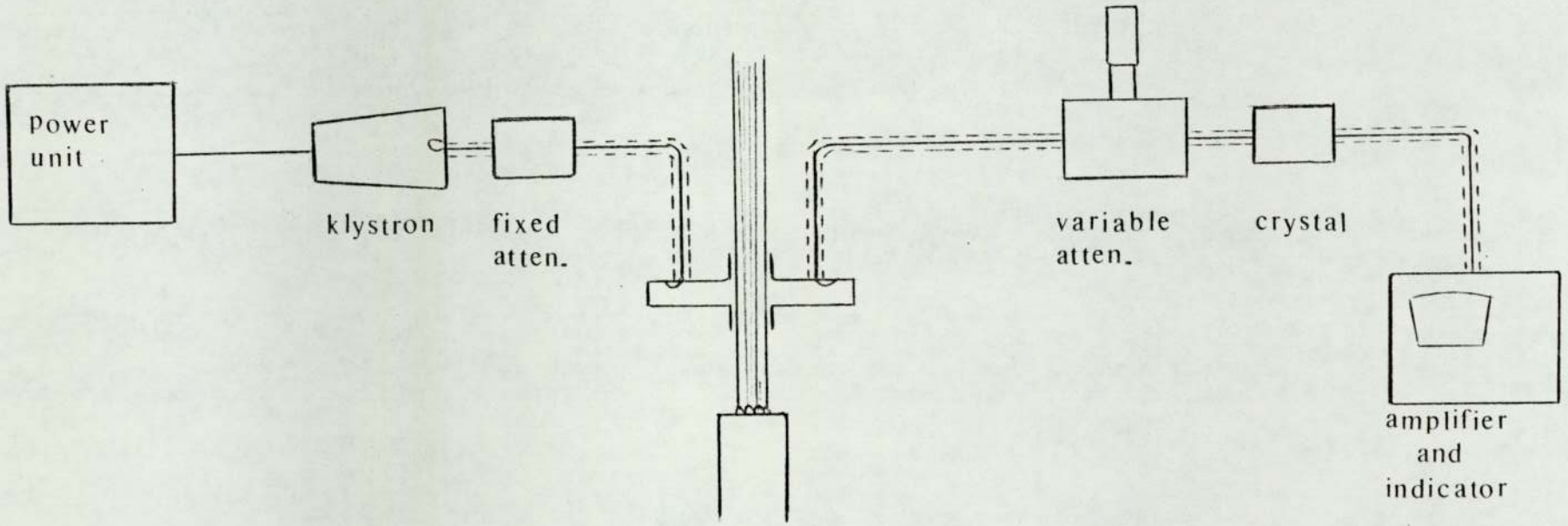

was coupled to the external circuit by means of two symmetrically placed platinum loops, orientated to intersect the magnetic flux and led out via small holes in the end plate to B.N.C. sockets. No provision was made for mechanical tuning of the cavity since fine tuning could be accomplished by adjustment of the klystron reflector voltage.

The 'Q', calculated from 5.12 using a value for the skin-depth of 5.10^{-3} cm[72] is low, only a little over 200, but this is compensated for by the relatively low frequency used and the favourable distribution of the electric field. Significant radiation losses through the ports would reduce the 'Q' well below the calculated value. However, progressive insertion of a copper wire through the ports had no effect on the power transmitted until the wire protruded beyond the end-plate, when a strong attenuation was observed. It was therefore concluded that radiation losses were negligible with this cavity.

5.5. THE ANCILLARY MICROWAVE EQUIPMENT:

Figure (5.2) shows a block diagram of the complete microwave equipment. About 120 mW of power from an EMI R9559/25204 klystron was transmitted via co-axial line to the E_{010} cavity. A fixed pad co-axial attenuator of about 10 dBs was inserted in the line to decouple the resonant cavity from the rest of the system and prevent frequency pulling. Power transmitted by the resonant cavity was passed via a variable attenuator to the crystal rectifier, after which the signal was amplified and displayed by meter reading on a Saunders VSWR indicator and selective amplifier. The variable attenuator, a Microlab AJ310B co-axial attenuator, consists of a dissipative element which is inserted into a

section of co-axial line and is controlled by a micrometer drive. The author is indebted to Mr. G.W. Parkes, of the Royal Signals and Radar Establishment, for using the computer controlled 8542A automatic net work analyser, to calibrate this instrument, the reflection coefficient of which is 0.1, and to determine the frequency range corresponding to the klystron scale, which was from 2905 to 3245 M.Hz . The modulation was set at 1000 c/s to coincide with the selective frequency of the amplifier.

The system was stabilised within about five minutes of lighting a flame. The method of taking measurements was to adjust the meter reading to give a suitable "null-point" reading with a clean flame and then introduce the additive to the flame. The drop in power transmitted by the cavity, indicated by a decrease in the meter reading, was compensated by reducing the attenuation of the variable attenuator until the original null-point was restored. By this means, the power reaching the crystal at the time of measurement was kept constant and variations in the crystal response had no effect on the result. The attenuation, βdB, was related to the power transmitted, t, by the previously quoted relation:

$$\beta = 20 \log_{10} t^{\frac{1}{2}}$$

5.6. CALIBRATION OF THE RESONANT CAVITY AND THE ATOMISER:

Since the theoretical equation for power loss was not soluble in real conditions, the apparatus had to be calibrated with known electron concentrations. The quantities to be determined for a calibration of the apparatus are the 'cavity factor' and the 'atomiser factor'. The first of these gives the proportionality between $(t^{\frac{1}{2}}-1)$ and the number of electrons

per cc, n_e, and the atomiser factor relates the strength of the salt solution in the atomiser to the amount of additive in the flame.

From equations (5.3) and (5.4) it is seen that

$$g = \frac{\omega L}{Q_1} (t^{\frac{1}{2}} - 1).$$

Of the terms in this equation, 'g' and 'L' can be calculated from the geometry of the cavity and ω, the resonant frequency, and Q_1 can be measured. The conductivity σ, however, requires a knowledge of the collision frequency ω_1, between electrons and gas molecules for its relation to n_e (equation 5.1). Since ω_c, cannot be reliably estimated this procedure was not used, and the cavity factor was obtained from measurements of the equilibrium ionisation of alkali metals which provide a simultaneous determination of the atomiser factor.

Following the study of the equilibrium ionisation of an alkali metal A in section 3.2.a, and using the charge balance equation, $[A^+] = [e^-]$, and the relation that the total amount of metal added $[A]_o = [A] + [A^+]$, equation (3.2) becomes:

$$[e^-]^2 + K_1[e^-] - K_1[A]_o = 0 \qquad (5.14)$$

This quadratic equation gives $[e^-] = [A]_o$ for $[A]_o << K_1$ and $[e^-] = (K_1[A]_o)^2$ for $[A]_o >> K_1$. The value of K_1 can be determined from the Saha equation (3.3) for the ionisation of alkali metals, hence a theroetical plot can be constructed of log $[e^-]$ vs log$[A]_o$, which is a straight line plot of slope 1.0 at low values of $[A]_o$, bending over to a slope of 0.5 at large $[A]_o$. By fitting the experimental plot of log $(t^{\frac{1}{2}}-1)$ vs log M to this theoretical plot, the cavity and atomiser factors may be obtained.

This simple treatment is complicated by the fact that the

ionisation of most of the alkali metals is not equilibrated in the time available, and stable hydroxides are also formed by some of them in the flames, reducing the effective $[A]_o$ value. The ionisation of caesium, however, is known to proceed extremely rapidly[73] and at low levels of addition, where the caesium is virtually fully ionised, the formation of caesium hydroxide is not important. At higher levels of addition hydroxide formation must be taken into account and it is also found that the amount of ionisation is frequently so high that it is beyond the range of the cavity. To overcome this difficulty, the experimental plots from caesium have been combined with those from potassium which, because of its higher ionisation potential, gives manageable ion concentrations in the 'square-root' region of the plot. Hydroxide formation by potassium is negligible in the flames used, but potassium cannot be used on its own for the calibration because its slow rate of ionisation results in ion concentrations below the equilibrium levels in the linear portion of the ionisation plot. The experimental results for the calibration with a flame at 2300°K are shown in Figure (5.3) together with the theoretical plots for caesium and potassium. From this plot the following relations were derived:

$$n_e = 1.38 \times 10^{11} (t^{\frac{1}{2}} - 1) \qquad (5.15)$$

$$1 \text{ unit of } (M) = 1.42 \times 10^{14} \, Cs_o \, cm^{-3} \qquad (5.16)$$

The cavity factor is sensitive to the state of cleanliness of the cavity, and frequent checks were made by observing the electron concentration resulting from the addition of a known amount of caesium to the flame.

Variation in the concentration of electrons in the flame

at different heights, different alkali metals, and different temperatures with different amounts of phosphorus is shown in Figure (5.4).

In many cases the electron concentrations passes through pronounced maxima, occurring at a lower level, and towards lower amounts of phosphorus with increasing the flame temperature, and increasing distance from the burner (lower γ) in accord with equation (3.22). These maxima disappear at relatively higher distances, especially at higher temperatures.

The numerical results (Table 5.1) will be exploited together with those of positive ion measurements and spectroscopie studies, in Chapter 8.

TABLE (5.1)

T(K)		2000			2300			2500		
M	ht Cm	E_m^2	$B_m x10^{-4}$ atm	S_e *	E_m^2	$B_m x10^{-4}$ atm	S_e *	E_m^2	$B_m x10^{-4}$ atm	S_e *
Cs	1	1.31	0.8	4000	1.13	1.66	800	1.45	4.9	300
	2	1.255	0.73	3500	1.09	1.33	700	1.105	4.2	250
	3	1.185	0.6	3000	1.075	1.2	650	1.075	3.6	200
	4	1.095	0.47	2000	1.03	0.66	500	-	-	-
	5	1.015	0.33	500	-	-	-	-	-	-
Rb	1	1.475	1.4	3500	1.12	1.8	700	1.056	2.26	250
	2	1.27	1.06	2500	1.091	1.6	600	1.032	1.66	200
	3	1.2	1	2000	1.08	1.46	550	1.02	1.4	150
	4	1.1	0.8	1200	1.052	1.3	450	-	-	-
	5	-	-	-	-	-	-	-	-	-
K	1				1.06	1.46	400	1.018	1.2	150
	2				1.03	1.04	200	1.011	1.06	100
	3				1.02	1.3	150	-	-	-
	4				1.007	1.26	50	-	-	-
Na	1				1.054	1.86	300	1.02	1.93	100
	2				1.018	1.8	100	1.01	1.66	50
	3				1.008	1.73	50	-	-	-
	4				-	-	-	-	-	-

* S_e is the initial slope of the $\left(\frac{E^2}{E_o}\right)$ graph against $[B_o]$.

Continued...../

Table (5.1) continued

		$(E/E_o)^2$ at different PP of "P"				
$^oT(K)$	ht.cm	2×10^{-4} atm	4×10^{-4} atm	6×10^{-4} atm	8×10^{-4} atm	10×10^{-4} atm
	1	0.92	0.59	0.38	0.26	0.21
	2	0.76	0.49	0.33	0.22	0.17
Cs	3	0.72	0.44	0.275	0.175	0.103
2000	4	0.6	0.345	0.21	0.125	0.092
	5	0.525	0.3	0.175	0.09	0.09
	1	1.12	1.05	0.99	0.94	0.9
	2	1.06	0.975	0.905	0.845	0.8
Cs	3	1.025	0.925	0.83	0.76	0.705
2300	4	0.94	0.835	0.745	0.68	0.63
	5	0.86	0.76	0.68	0.625	0.57
	1	1.06	1.11	1.13	1.125	1.1
	2	1.05	1.1	1.085	1.065	1.05
Cs	3	1.04	1.07	1.05	1.035	1.02
	4	1.00	0.99	0.98	0.97	0.96
	5	0.99	0.98	0.965	0.95	0.925
	1	0.86	2.72	0.34	0.23	0.19
	2	0.80	2.54	0.315	0.22	0.175
Rb	3	0.77	2.47	0.3	0.2	0.155
2000	4	0.7	2.45	0.275	0.18	0.145
	5	0.63	2.61	0.25	0.17	0.14

Continued...../

Table (5.1) continued

M, T(K)°	ht.cm	$(E/E_o)^2$ at different PP of "P"				
		2×10^{-4} atm	4×10^{-4} atm	6×10^{-4} atm	8×10^{-4} atm	10×10^{-4} atm
	1	1.03	1.204	0.85	0.816	0.8
	2	1	1.189	0.84	0.81	0.783
Rb	3	0.98	1.172	0.834	0.801	0.782
2300	4	0.964	1.178	0.827	0.798	0.781
	5	0.944	1.196	0.82	0.794	0.778
	1	1.05	1.12	0.982	0.968	0.958
	2	1.021	1.103	0.964	0.952	0.944
Rb	3	1.001	1.093	0.95	0.939	0.932
2500	4	0.979	1.098	0.937	0.929	0.924
	5	0.963	1.11	0.929	0.92	0.914
	1	1.12	0.948	0.9	0.876	0.86
	2	0.996	0.93	0.89	0.864	0.854
K	3	0.984	0.92	0.88	0.856	0.844
2300	4	0.97	0.91	0.872	0.848	0.839
	5	0.96	0.9	0.864	0.844	0.834
	1	1.03	0.98	0.966	0.96	0.958
	2	0.995	0.973	0.961	0.955	0.955
K	3	0.988	0.968	0.956	0.951	0.951
2500	4	0.976	0.962	0.953	0.949	0.947
	5	0.972	0.956	0.947	0.943	0.942

Continued...../

Table (5.1) continued

		$(E/E_0)^2$ at different PP of "P"				
M, T(K)°	ht.cm	2×10^{-4} atm	4×10^{-4} atm	6×10^{-4} atm	8×10^{-4} atm	10×10^{-4} atm
	1	1.12	0.964	0.89	0.83	0.78
	2	1.05	0.934	0.87	0.818	0.77
Na	3	0.994	0.924	0.862	0.81	0.766
2300	4	0.972	0.91	0.854	0.804	0.76
	5	0.934	0.88	0.828	0.784	0.75
	1	1.03	0.991	0.975	0.964	0.957
	2	1.01	0.981	0.968	0.959	0.953
Na	3	0.992	0.977	0.964	0.956	0.951
2500	4	0.985	0.97	0.959	0.951	0.947
	5	0.979	0.964	0.952	0.944	0.94

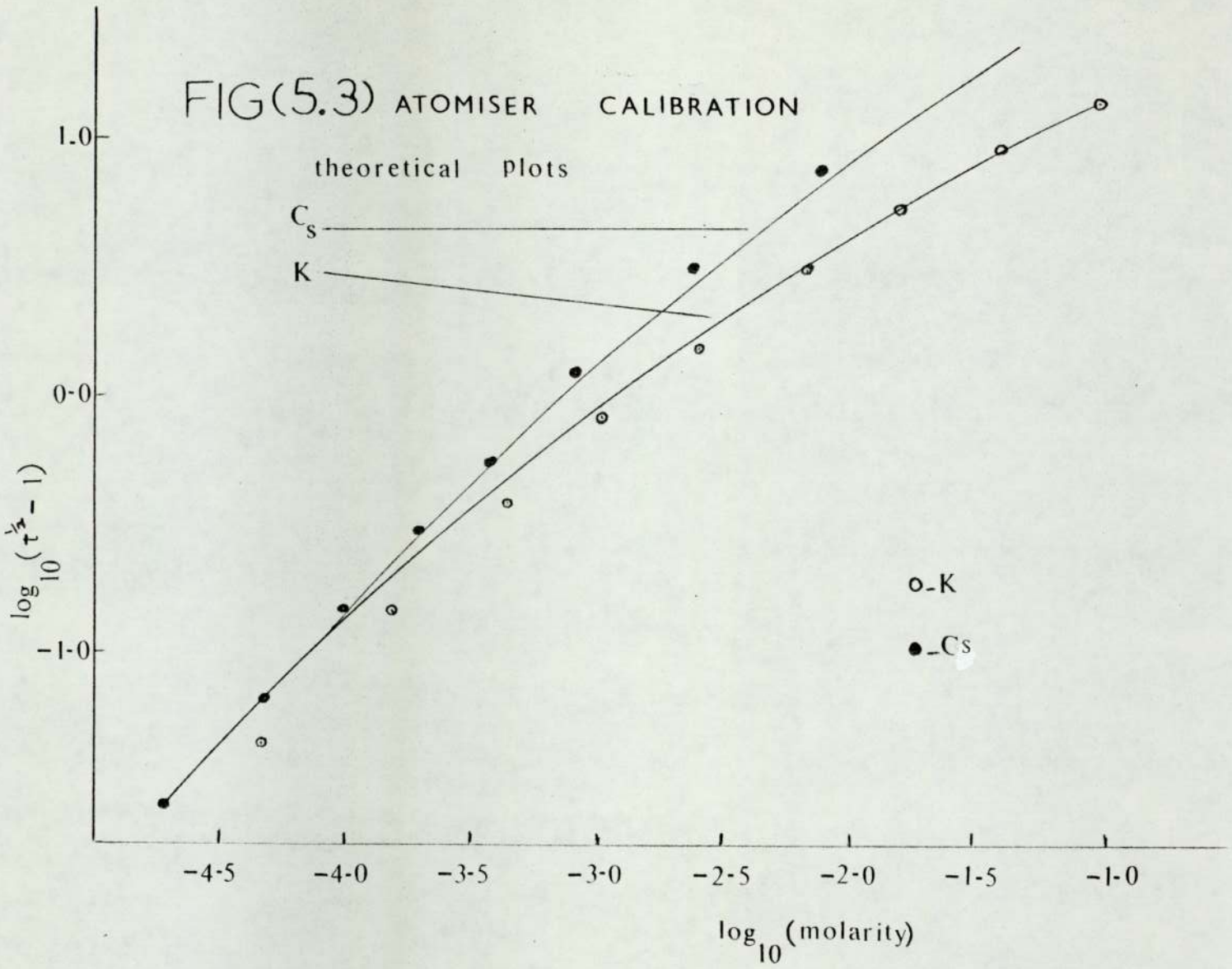
FIG(5.3) ATOMISER CALIBRATION
theoretical plots
C_s
K
1·0
0·0
−1·0
$\log_{10}(\tau^{\frac{1}{3}}-1)$
o-K
●-Cs
−4·5
−4·0
−3·5
−3·0
−2·5
−2·0
−1·5
−1·0
$\log_{10}$(molarity)

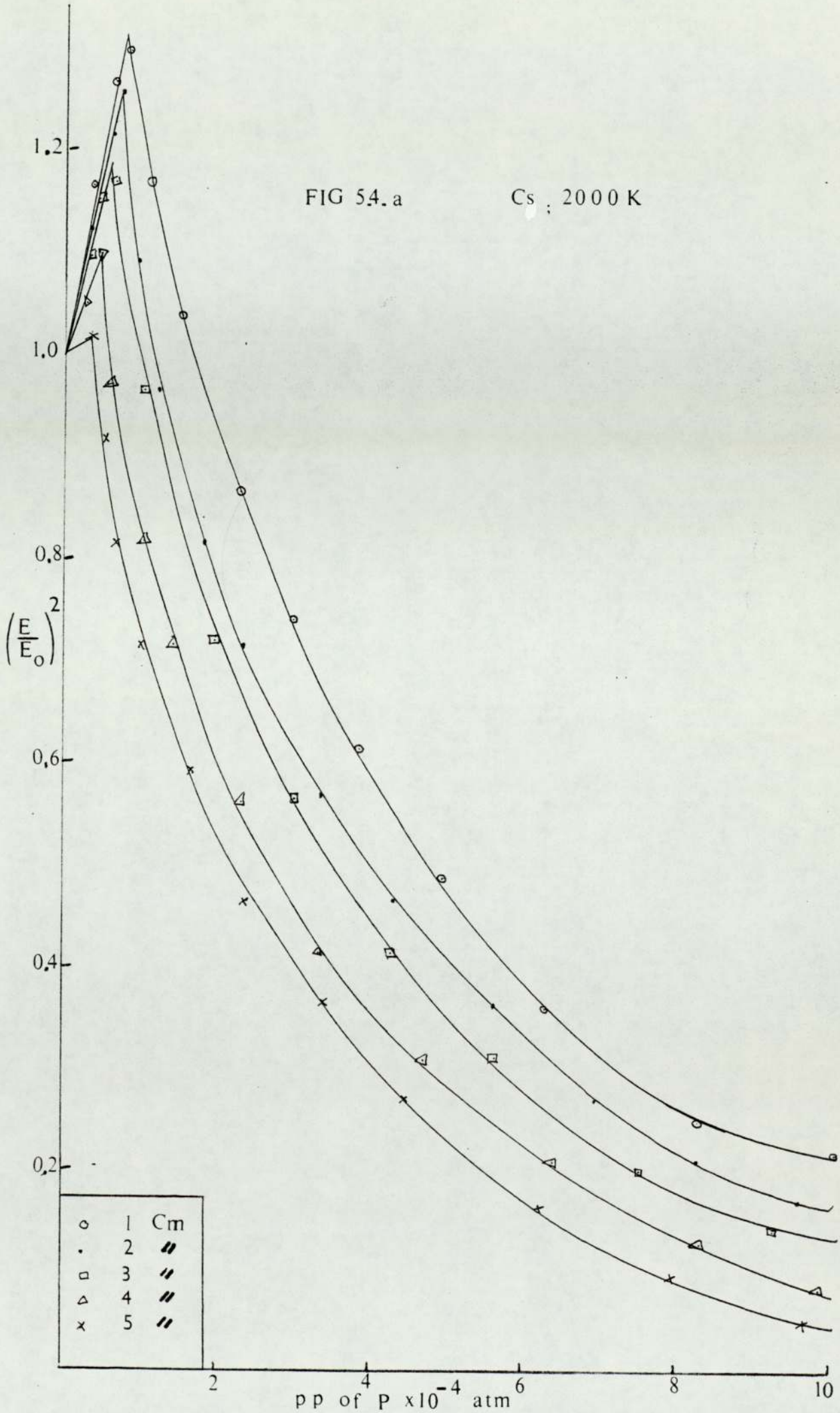

FIG 54.a Cs ; 2000 K

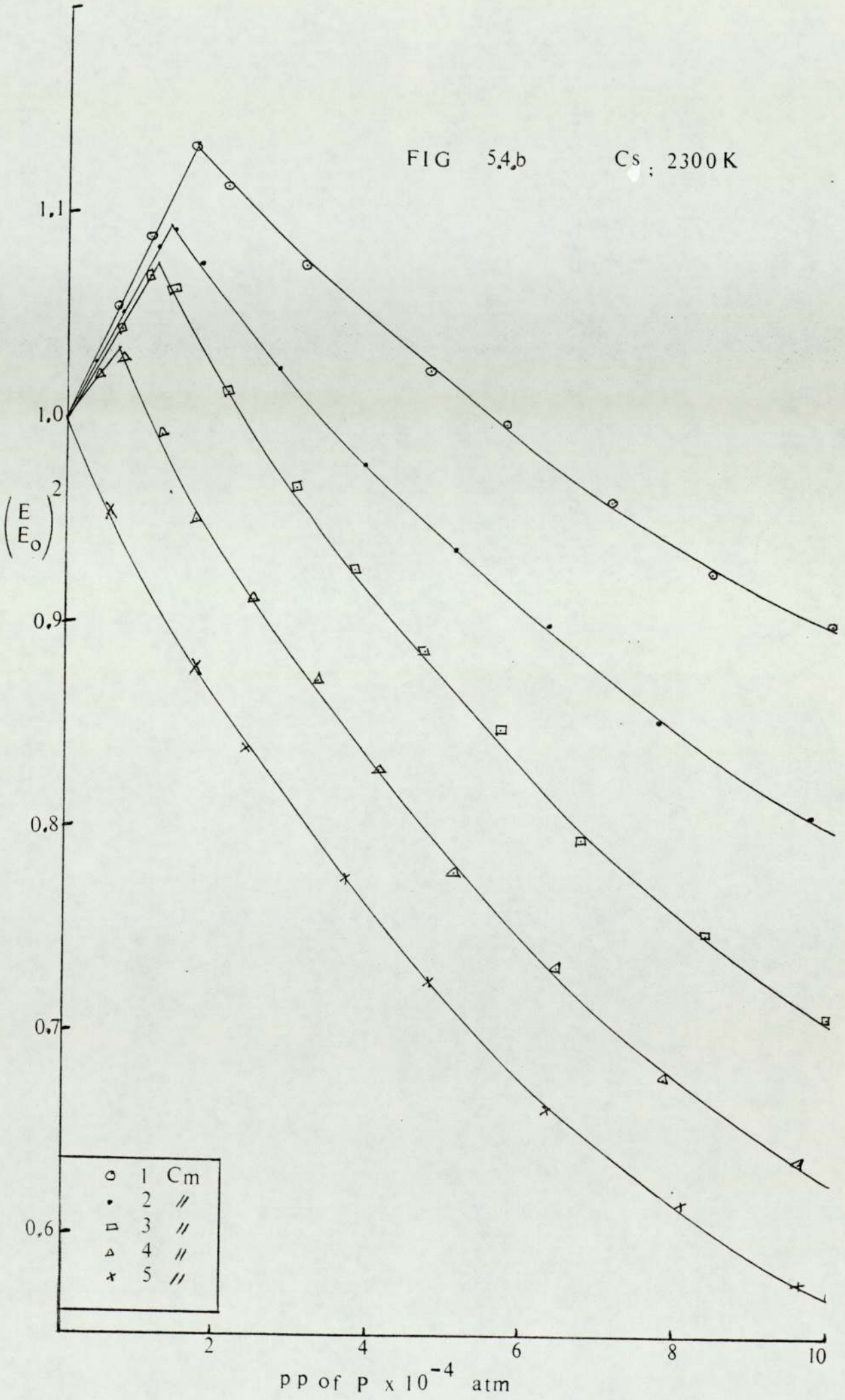
FIG 5.4.b
Cs ; 2300 K
1.1
1.0
0.9
0.8
0.7
0.6
$\left(\frac{E}{E_o}\right)^2$
1 Cm
2 //
3 //
4 //
5 //
2
4
6
8
10
pp of P x 10^{-4} atm

FIG 5.4.c Cs ; 2500 K

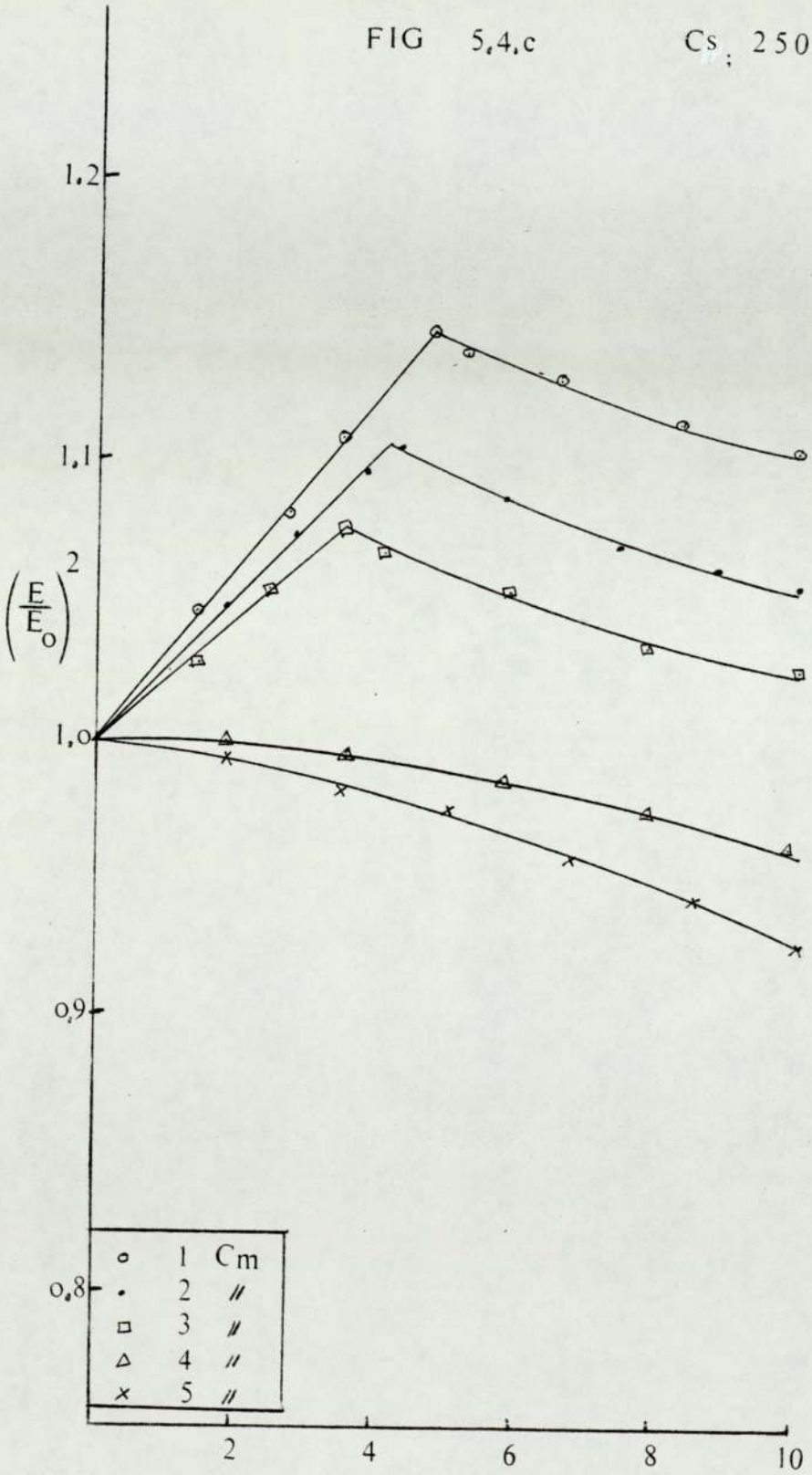

FIG 5.4.d Rb : 2000 K

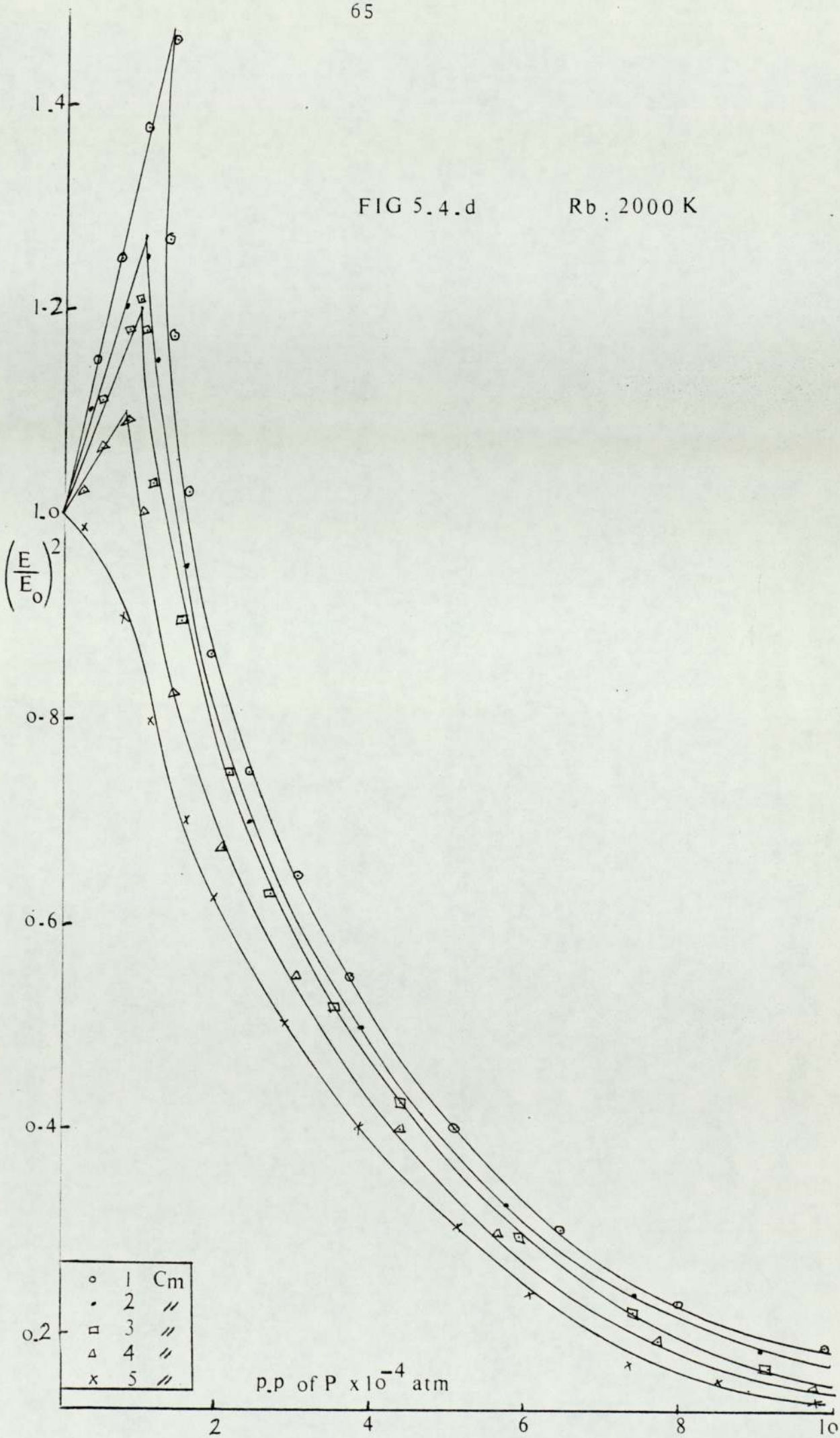

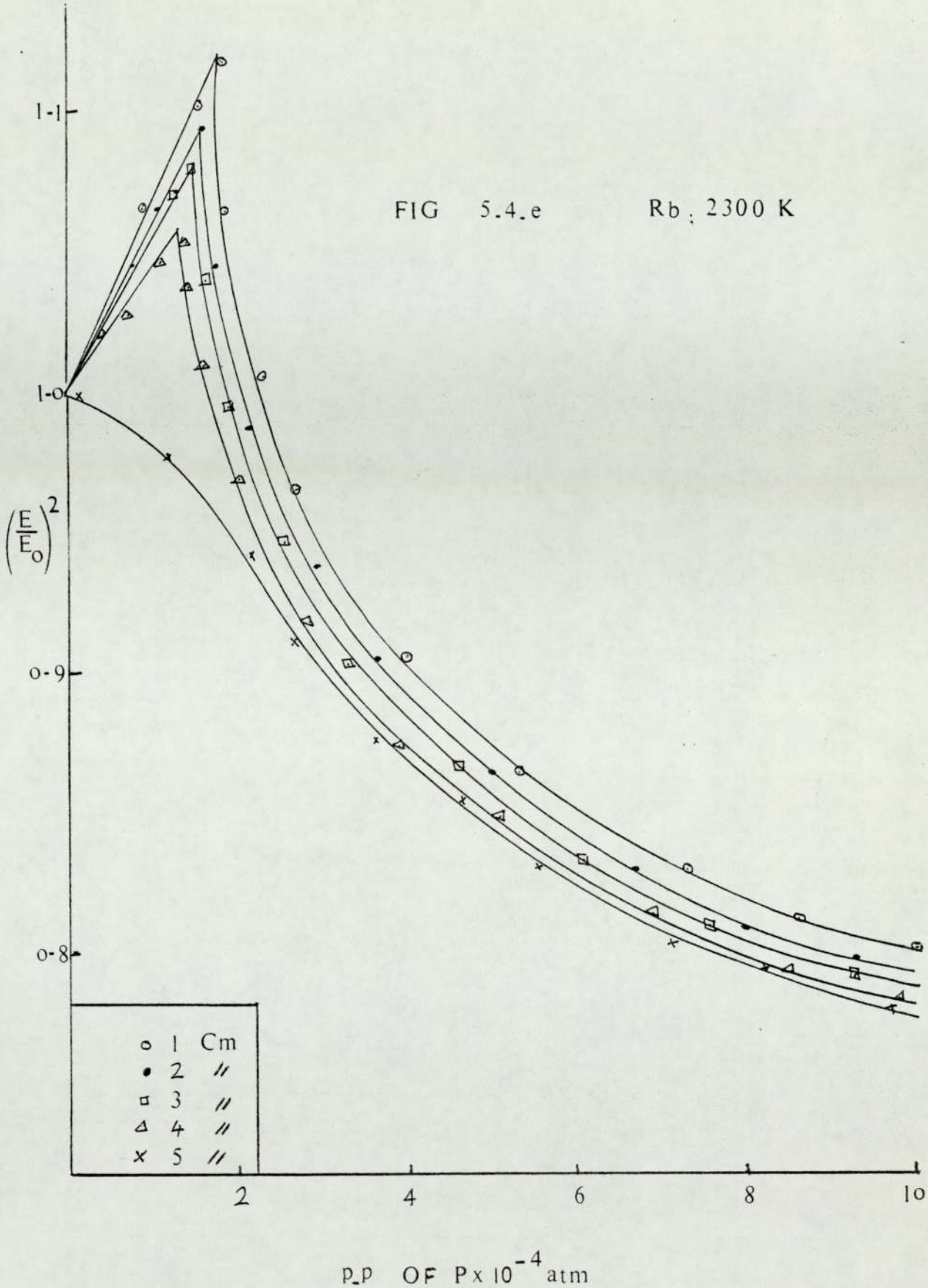

FIG 5.4.e Rb ; 2300 K

FIG 5.4.f Rb : 2500 K

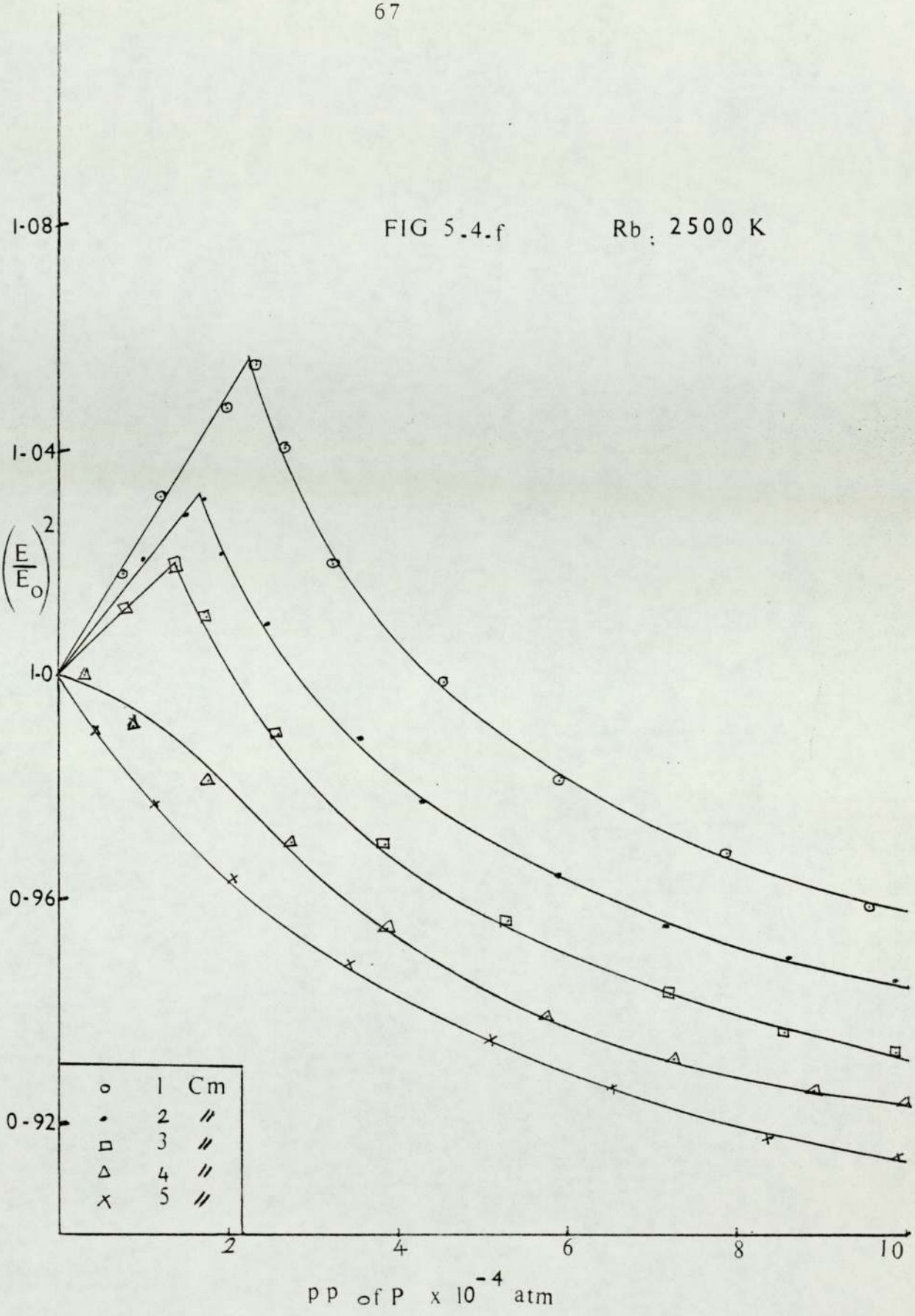

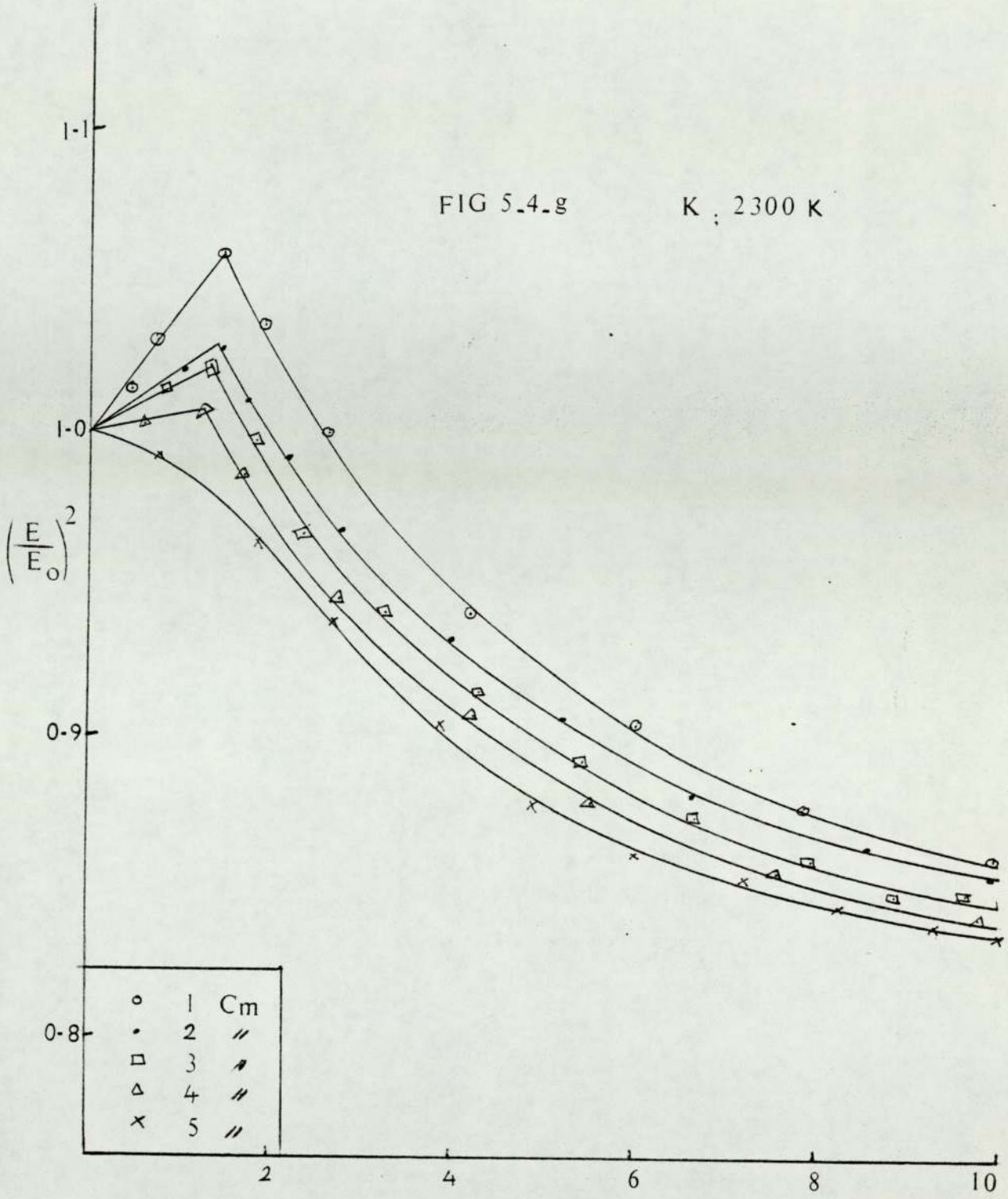

FIG 5.4.g K : 2300 K

FIG 5.4.h K : 2500 K

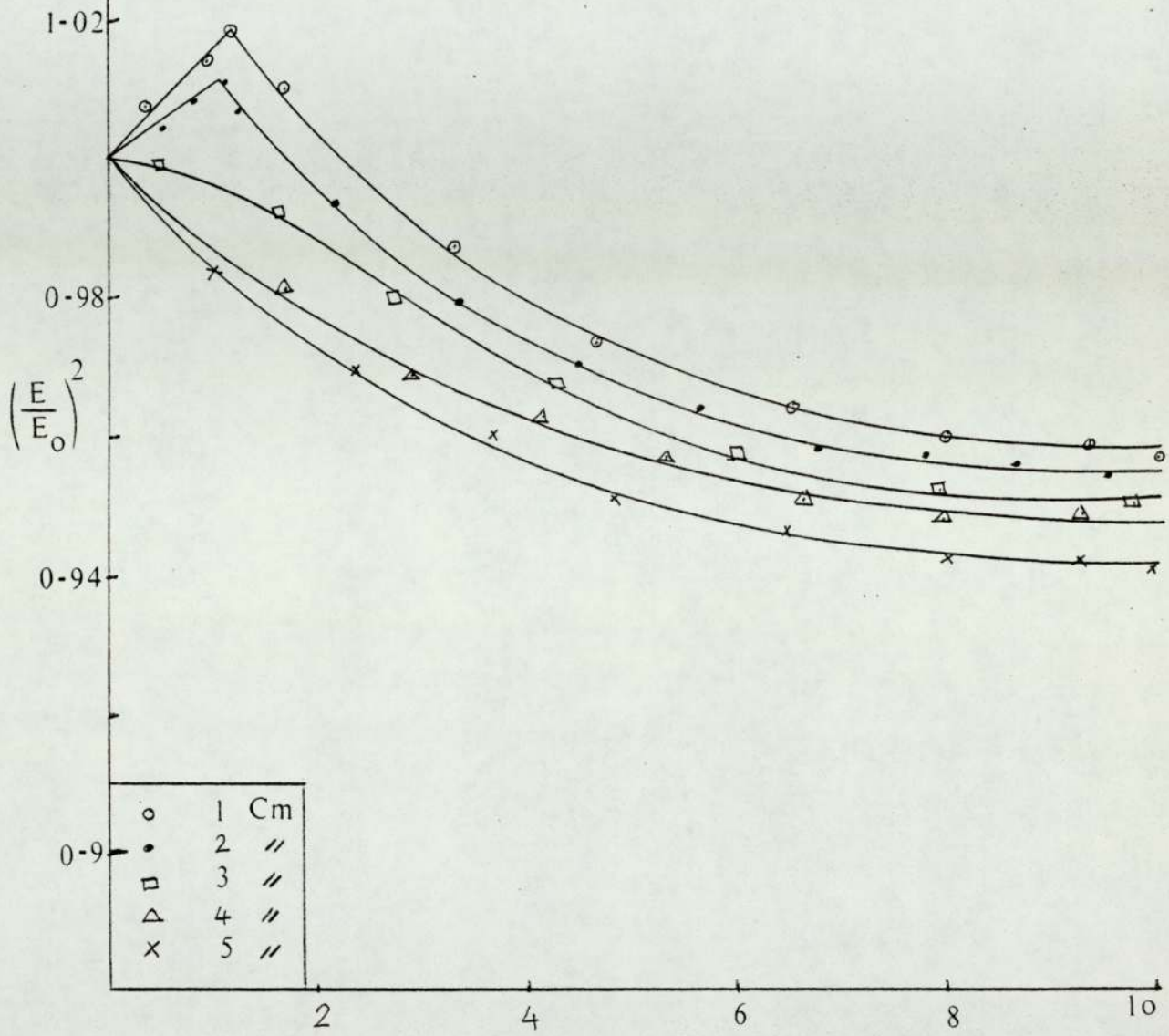

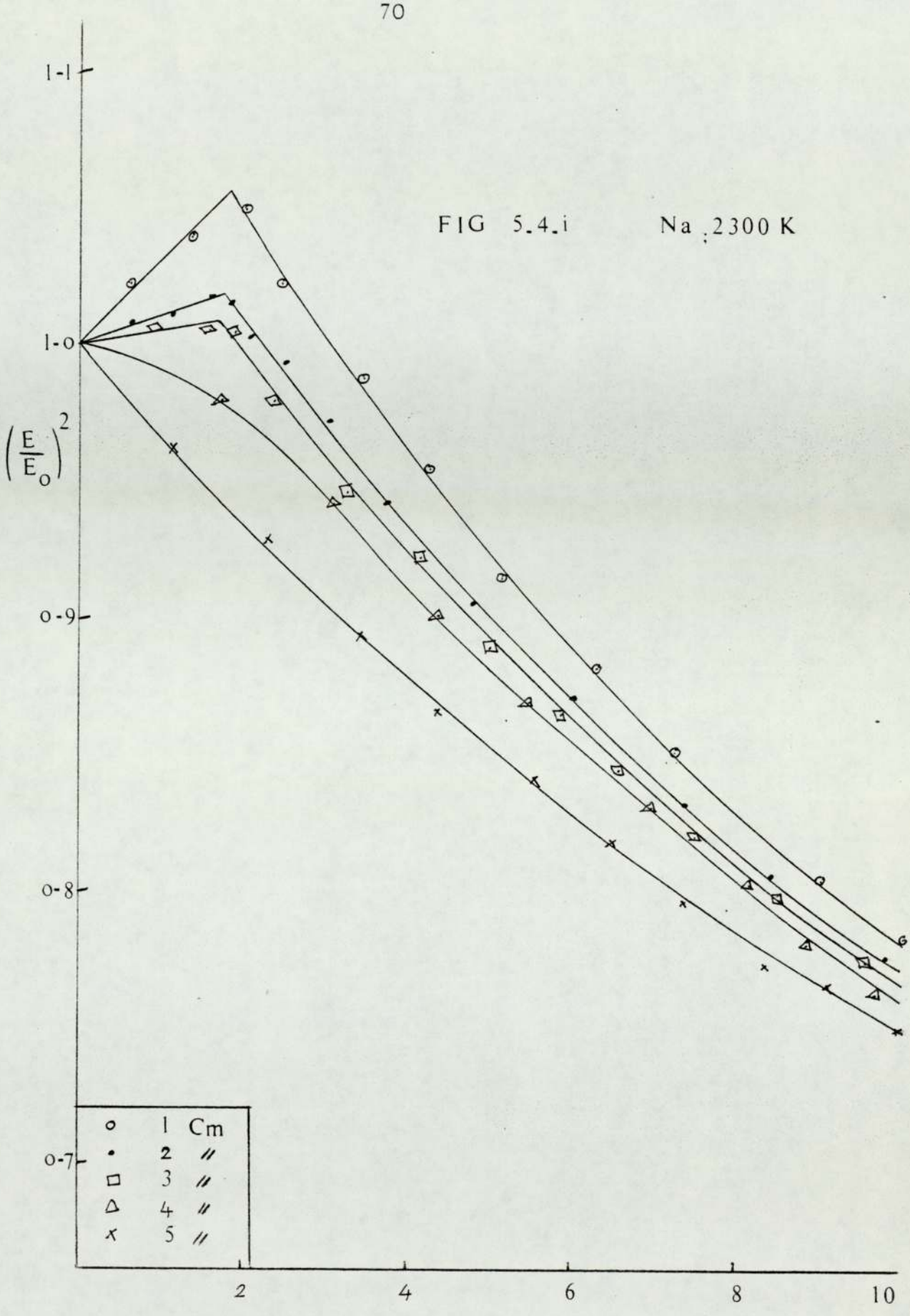

FIG 5.4.i Na ; 2300 K

FIG 5.4.j Na ; 2500 K

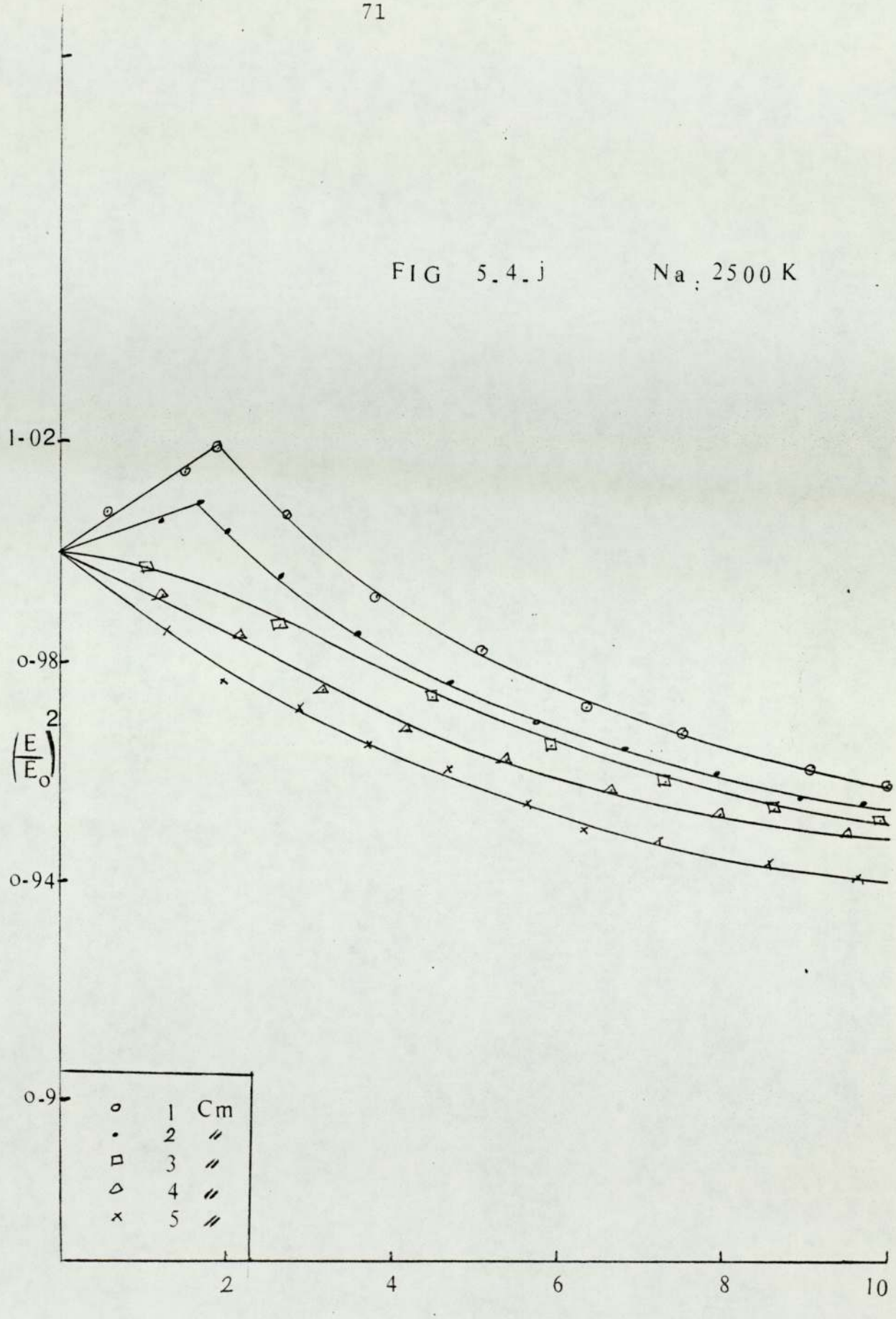

6. ELECTROSTATIC PROBE TECHNIQUES AND MEASUREMENT OF POSITIVE ION CONCENTRATIONS

6.1. INTRODUCTION:

Positive ions, whose temperatures are accepted to be close to those of the flame gases[74,75] have been measured using the electrostatic probe. Some doubt exists about the temperatures of the electrons which Von Engels argues should be significantly higher[76,77], as found by Calcote. Williams[78] has disputed this and points out that leakage currents can cause the same numerical observations as high temperatures. Because of this uncertainty, it has been found better to determine electron concentrations by the resonant cavity method.

An electrostatic probe is an extremely simple device, consisting of a small electrode inserted into the flame. The current drawn by the electrode at various applied potentials is measured, and analysis of the measurements allows the determination of positive ion concentration, and, with suitable precautions, the electron temperature. The outstanding advantage of probes is their ability to make local measurements, which makes them ideally suited for the production of ion profiles in flames. Probes have been used for this purpose by Calcote[79].

Although the device is unfortunately not ion-selective, it enables considerable insight to be gained into the mechanism of ionisation reactions, when it is used in conjunction with mass-spectrometric measurements. In view of the advantage of simplicity and high spatial resolution of electrostatic probes, it was decided to employ the technique for measuring positive ion concentrations in the present work.

The electrostatic probe technique was originally developed as a means of measuring the potential distribution along the positive column of low pressure gas discharge. A probe in the form of a small insulated wire was inserted through the wall of the discharge and allowed to 'float', or assume its own potential relative to the plasma. The potential taken up by the probe was measured with an electrometer. However, the pioneering work of Irving Langmuir showed that very much more information could be obtained about the conditions in the plasma if the probe was not allowed to float, but was subject to an externally applied potential. When operated in this manner a probe enables values to be obtained for the electron and positive ion concentrations, and the electron temperature.

A Langmuir probe usually consists of a small metallic sphere or wire which is inserted into the plasma at the location of interest. It is attached to a power supply capable of biasing it at various voltages positive and negative with respect to the plasma. Measurement of the current drawn by the probe enables a current-voltage characteristic to be constructed, from which the desired plasma parameters may be derived. For probe measurements to provide meaningful information about the plasma, it is an essential requirement that the perturbation of the plasma should be limited to a small region around the probe. The value of electrostatic probes lies in their ability to meet this requirement over a wide range of conditions, because of the shielding properties of plasmas which are able to localise the disturbance created by the probe.

The first theoretical treatment of probe measurements were made by Langmuir[80,81], who concerned himself with low-

pressure plasmas (~ 0.01 mm Hg) where mean free paths are large and collisions may be neglected. For high pressure plasmas some of these assumptions are no longer valid, and in consequence modifications are required. In this discussion the original Langmuir theory will be reviewed first, as it introduces the basic concepts and terminology of probes. It will be followed by a consideration of the refinements necessary for collision dominated plasma.

6.2. THE THEORY OF ELECTROSTATIC PROBES[122]:

6.2.1. Flame Plasmas

An ionised flame is an example of a plasma, which is usually defined as a partially or fully ionised gas containing ions and electrons in approximately equal numbers, the whole assembly possessing overall electrical neutrality. Plasmas demonstrate characteristic behaviour arising from the simple fact that charged particles interact with each other by long-range forces. A charged particle will tend to be surrounded on average by particles of opposite charge, and will interact with many particles simultaneously. This interaction gives rise to collective modes of plasma behaviour which do not exist in ordinary gases, where the molecules interact by short-range forces only. The most important characteristic of the bulk plasma is the Debye length λ_D, which marks the division between single-particle behaviour and collective processes. The significance of this parameter may be obtained from a consideration of a spherical volume of plasma, from which nearly all of the electrons have been removed within a radius a. There will be produced an electrostatic potential $2\pi ne a^2$, where n is the number of electrons per cm^3 and e their charge, and a

potential difference now exists between the centre and the neutral plasma boundary. Additional electrons will only be able to escape if their kinetic energy per degree of freedom kT/2 is given by:

$$k\,T_e/2 = 2\pi\, nea^2e \qquad (6.1)$$

or

$$a = \left(\frac{kT_e}{4\pi ne^2}\right)^{\frac{1}{2}} = \lambda_D \qquad (6.2)$$

where T_e is the electron temperature and k is the Boltzmann's constant.

λ_D thus represents the maximum charge separation that can be achieved by the plasma, and the plasma cannot of itself produce any significant charge separations exceeding the Debye length since the kinetic energies are insufficient. If the distance between two passing particles is appreciably less than λ_D, normal coulombic attraction or repulsion will occur and one can define the encounter as a simple collision, to which the ordinary laws of particle dynamics apply. However, if the minimum distance of approach of two particles is greater than λ_D, the collective motions of the surrounding plasma electrons induced by the passage of the particle will be such as to screen the test particle from feeling the influence of the other particles, or any others beyond the distance λ_D. In the vicinity of a boundary to the plasma such as an electrode, local fields will exist, and a sheath region will be produced containing predominantly particles of one sign. This sheath, which is of the order of a Debye length in thickness, serves to shield the bulk of the plasma from the influence of the perturbing field. A consequence of this sheath formation at plasma boundaries, is that a region

of ionised gas must be many Debye lengths thick in order to deserve the name plasma. It is interesting to consider under what conditions the term plasma may justifiably be applied to laboratory flames, which have typical dimensions of a few centimeters.

For a flame at 2000°K containing 10^8 electrons per cm^3 equation (6.2) gives a Debye length of 0.03 cm, while an electron density of 10^7 per cm^3 raises the Debye length to about 0.1 cm. It is apparent therefore that true plasma properties can only be expected in flames at this temperature which contain a minimum of 10^8 electrons per cm^3.

6.2.2. Langmuir Probes in a Collision Less Low Density Plasma

The best introduction to the operation of probes is a short discussion of the ideas of Langmuir[82] for a single probe in a low pressure plasma, such as a gas discharge. In this simple use the mean free path of the ions and electrons is greater than the Debye length and therefore in calculating the space charge limited currents collected no account need to be taken of the collisions of the ions with other neutral or charged species, while crossing the sheath region. The current drawn by the probe from the plasma at varying probe bias is shown in Figure (6.1). Three regions of the characteristic are readily distinguished, corresponding to the saturation ion current (AB), the retarding field or the transition region (BC) and the saturation electron current (CD).

When the probe is strongly negative relative to the plasma, electrons will be repelled and the current received will be entirely due to positive ions. These will form a space charge sheath over the probe surface, effectively screening the plasma

from the field of the probe. Ions which strike the sheath will do so by virtue of their random thermal velocities, so that the probe will receive the random ion current of the plasma. Under these circumstances a decrease in probe potential will not enable any more ions to be collected, and a space charge-limited or saturated positive ion current is drawn by the probe.

If the probe is made less negative, there comes a point (B) where a few of the high energy electrons can penetrate the positive ion sheath against the retarding potential. This causes a reduction in the nett probe current, which continues to decrease after B until it falls to zero at the point marked V_w, known as the wall or floating potential, where the number of electrons reaching the probe is just equal to the random positive ion current. This will be the potential assumed by any isolated body immersed in the plasma. Potentials more positive than V_w cause a current of opposite sense to be registered, for the electron current to the probe will now exceed that from the positive ions.

Further reduction in the negative potential of the probe brings it to V_s. where the applied voltage is equal to the plasma potential, there are no electric fields to disturb the plasma, which consequently extends right up to the probe surface, the remaining positive ion sheath being destroyed. Both electrons and positive ions may reach the probe, because of the much higher random velocities of electrons than ions very many more electrons are collected per second, and the current is mainly electron current.

If the probe is made increasingly positive relative to V_s, the small positive ion current rapidly disappears and an electron space charge sheath builds up around the probe.

Since the current is essentially a space charge-limited one and the probe is already receiving the full random electron current of the plasma an increase in the positive bias will not be reflected in a corresponding increase in electron current until the applied bias is sufficient to cause breakdown between the probe and the plasma boundaries, i.e. the probe current in the region CD is a saturated electron current collected due to the formation of a negative space charge over the probe surface. A result of this space charge is that the body of the plasma is shielded from the applied voltage.

Quantitative interpretation of the characteristic just described enables values to be deduced for N_e and N_i, the electron and positive ion concentrations, and the electron temperature T_e.

In practice in the regions AB and CD, the characteristic will show a slope, as indicated, due to the increase in space charge sheath dimensions, with increasing applied voltage, and incomplete shielding of the plasma by the space charge.

6.3. THE DETERMINATION OF N_e, N_i and T_e

6.3.1. The Determination of Electron Concentration (N_e)

Electron concentrations are estimated from the saturated electron current. For a gas with N particles/cm^3 which are undergoing their random thermal motions with an average velocity $\bar{c}$, kinetic theory shows that the number of these striking unit area per second from all directions is:

$$n = \tfrac{1}{4} N\bar{c} \qquad (6.3)$$

when these are electrons of charge e, they will constitute a current density per cm^2 per second of:

$$J = \tfrac{1}{4} e N_e \bar{c} \qquad (6.4)$$

Assuming that a Maxwellian distribution of velocity exists

among the electrons, then the average velocity c^- is given by:

$$c^- = \left(\frac{8\ k\ T_e}{\pi\ m_e}\right)^{\frac{1}{2}} \qquad (6.5)$$

where k is Boltzmann's constant, and T_e and m_e are the electron temperature and mass.

Combining (6.5) and (6.4) gives for the current density:

$$J = \tfrac{1}{4}\ e\ N_e\ \left(\frac{8k\ T_e}{\pi\ m_e}\right)^{\frac{1}{2}} = e\ N_e\ \left(\frac{k\ T_e}{2\pi\ m_e}\right)^{\frac{1}{2}} \qquad (6.6)$$

This current density is by definition the result of the random thermal motions of the electrons, and it was shown earlier that along the region CD of the characteristic, that is the saturated electron current region, the probe I_{es} is attributed to just this agency. The description of I_{es} is therefore:

$$I_{es} = JA = e\ N_e\ A\ \left(\frac{k\ T_e}{2\pi\ m_e}\right)^{\frac{1}{2}} \qquad (6.7)$$

The measured values of I_{es}, together with a knowledge of the electron temperatures as determined below, enable the value of N_e to be established.

6.3.2. The Determination of Positive Ion Concentration (N_i)

The random ion current I_{is}, from which N_i is determined, may be expressed by an equation similar in form to (6.7) on replacement of N_e, T_e, and m_e by N_i, T_i, and m_i, so giving:

$$I_{is} = J_{is}\ A = e\ N_i A\ \left(\frac{k\ T_i}{2\pi\ m_i}\right)^{\frac{1}{2}} \qquad (6.8)$$

Unfortunately T_i is unknown and cannot be obtained from a retarding potential experiment as used for the electron temperature, because when the probe is positive with respect to the plasma, the ion current is masked by the very much greater

electron current. However, it is often possible to assume a value for T_i, for reasons which are not applicable to the electron temperature T_e which may be very much greater than the neutral gas species due to the small electronic mass. The electrons in low pressure discharges are continuously supplied with energy from the electric field. In an elastic collision between an electron and a molecule, the electron because of its small mass is able to lose only a very small fraction of its kinetic energy, and as a result it is quite normal for electrons in the discharge to have energies much greater than those of the ions or neutral molecules. A collision between an ion and a molecule is quantitatively very different from the electron-molecule case, because an ion and a molecule have almost exactly the same mass. Consequently, an ion may lose much of its kinetic energy when it strikes a molecule, and ions and molecules in a plasma exchange their kinetic energies in the same way as do the molecules in an unionised gas. Because the energies of ions and molecules are equilibrated in this way, the value of the gas temperature may be used for T_i, allowing N_i to be found from equation (6.8).

6.3.3. The Determination of the Electron Temperature (T_e)

Over the region BC of the probe characteristic, electrons reaching the probe, do so only because their kinetic energy $\frac{1}{2} m V^2 = \frac{3}{2} kT$ is greater than the retarding potential on the probe. The slope of BC is thus a function of the electron energy distribution, which Langmuir assumed to be Maxwellian. Assuming the probe to be a perfect reflector, all electrons which strike it will rebound and the distribution will be undisturbed. Under these conditions the ratio of the electron concentration n^- right at the surface of the probe to that

outside the sheath is given by the Boltzmann equation:

$$\frac{n^-}{n} = \exp\left(-\frac{e\,V}{kT_e}\right) \qquad (6.9)$$

n being the electron concentration just outside the sheath. Now the currents at the probe surface and at the edge of the sheath are given by:

$$J^- = \tfrac{1}{4}\, n^- eV \quad \text{and} \quad J = \tfrac{1}{4}\, n\, eV \qquad (6.10)$$

$$\text{so that } \frac{n^-}{n} = \frac{J^-}{J} = \exp\left(\frac{-eV}{kT_e}\right) \qquad (6.11)$$

J, the electron current at the sheath edge is the random electron current J_{es}, enabling (6.11) to be written logarithmically as:

$$\ln I^- = \ln JA = \ln J_{es} A - \frac{eV}{kT_e} \qquad (6.12)$$

Thus if the electron current to the probe is measured as a function of V over the region BC of the characteristic, a plot of log I^- against V should be linear with slope: $-e/kT_e$, from which T_e, the mean electron temperature may be calculated. These plots are the normal method of estimating the electron temperature, and the linear form is usually obtained serves to confirm the assumption of a Maxwellian distribution of electron energies.

It is important to note that the use of Boltzmann's equation in (6.9) is strictly only valid for a reflecting probe, where as in practice the probe draws a current. An important condition for the above treatment is that the mean free paths of the electrons are large compared with the probe diameter, so that the distribution of the incoming electrons is not disturbed by collisions near the probe. Under these conditions the electrons come from regions so far removed from the probe that the Maxwellian distribution is unaffected.

6.4. EMITTING PROBES:

One of the difficulties of using probes in hot plasmas such as flames or arcs arises from the need to prevent thermionic emission from the probe surface, for emitted electrons will disturb the charge distribution around the probe. Most of the early studies[83] of ionisation in flames using small probes up to the work of Kinbara and Nakamura[84] took no special precautions to avoid this source of error. Calcote et al[79, 85-88] introduced the water cooled probe and Soundy and Williams[73,89] designed the low duty cycle rotating probe which has been the basis for most of the more recent kinetic studies in flames, and it is general practice to employ metals of high work function, e.g. platinum and tungsten, in the construction of the probe. However, there are circumstances in which the probe is designed to emit thermionically, and Langmuir[90] has shown that probes of this type may be used to locate the plasma potential. Emitting probes usually consist of a small wire loop which can be heated by the passage of an electric current. When the probe is sufficiently positive, emitted electrons will be returned to the probe, and the probe will collect the normal electron current from the plasma. On the other hand, when the probe is negative relative to the plasma potential, emitted electrons will be able to escape and contribute an apparent ion current to the probe. The potential at which the hot-probe and cold-probe characteristics begin to diverge therefore locate the plasma potential, as shown in Figure (6.1). For negative potentials, the difference between corresponding ordinates measure the electron current from the probe. A probe of this type will never draw a positive ion saturation current, and hence is not applicable to the

FIG 6.1 CURRENT-VOLTAGE CHARACTERISTIC FOR LANGMUIR PROBE

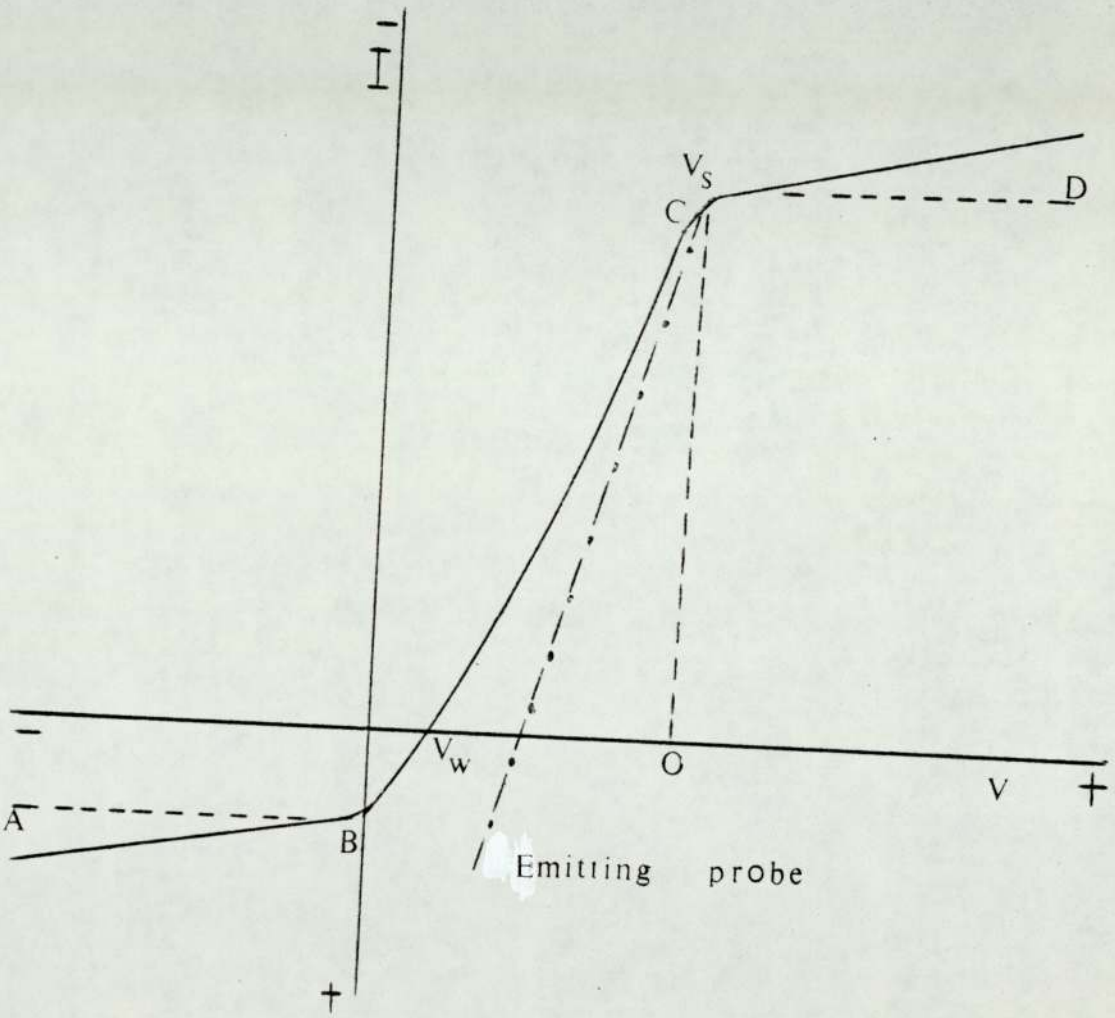

determination of positive ion concentrations. At sufficiently negative potentials the saturation emission current corresponding to the probe temperature will be registered. The technique is thus restricted to the determination of plasma potentials.

6.5. THE DOUBLE-PROBE TECHNIQUE:

It was stated earlier that a criterion of probe operation is that the probe should not disturb the surrounding plasma. With negative probes no problem arises, because the presence of a positive ion sheath shields the plasma from the field of the probe. As a probe approaches plasma potential, however, the electron current drawn from the plasma may become so large that a serious depletion of electrons occurs in the region adjacent to the probe. The plasma potential seen by the probe then becomes a function of probe current. This problem may be overcome by the use of a double probe (Figure 6.2.a), which was first developed by Johnson and Malter for decaying plasmas, where the problem of depletion is particularly serious since carriers removed by the probe cannot be replaced.

The behaviour of a double probe is governed by the following:

(i) The probes are introduced into the plasma with a potential applied between them and the system as a whole is made to float, in this case Kirchhoff's law must be obeyed such that the net total current drawn by the probes is zero, i.e. the total number of electrons flowing to the probes must equal the total number of ions.

(ii) The electron current to each probe is governed by the Boltzman Law.

As a consequence of the first requirement the electron

FIG 6·2 THE DOUBLE FLOATING PROBE

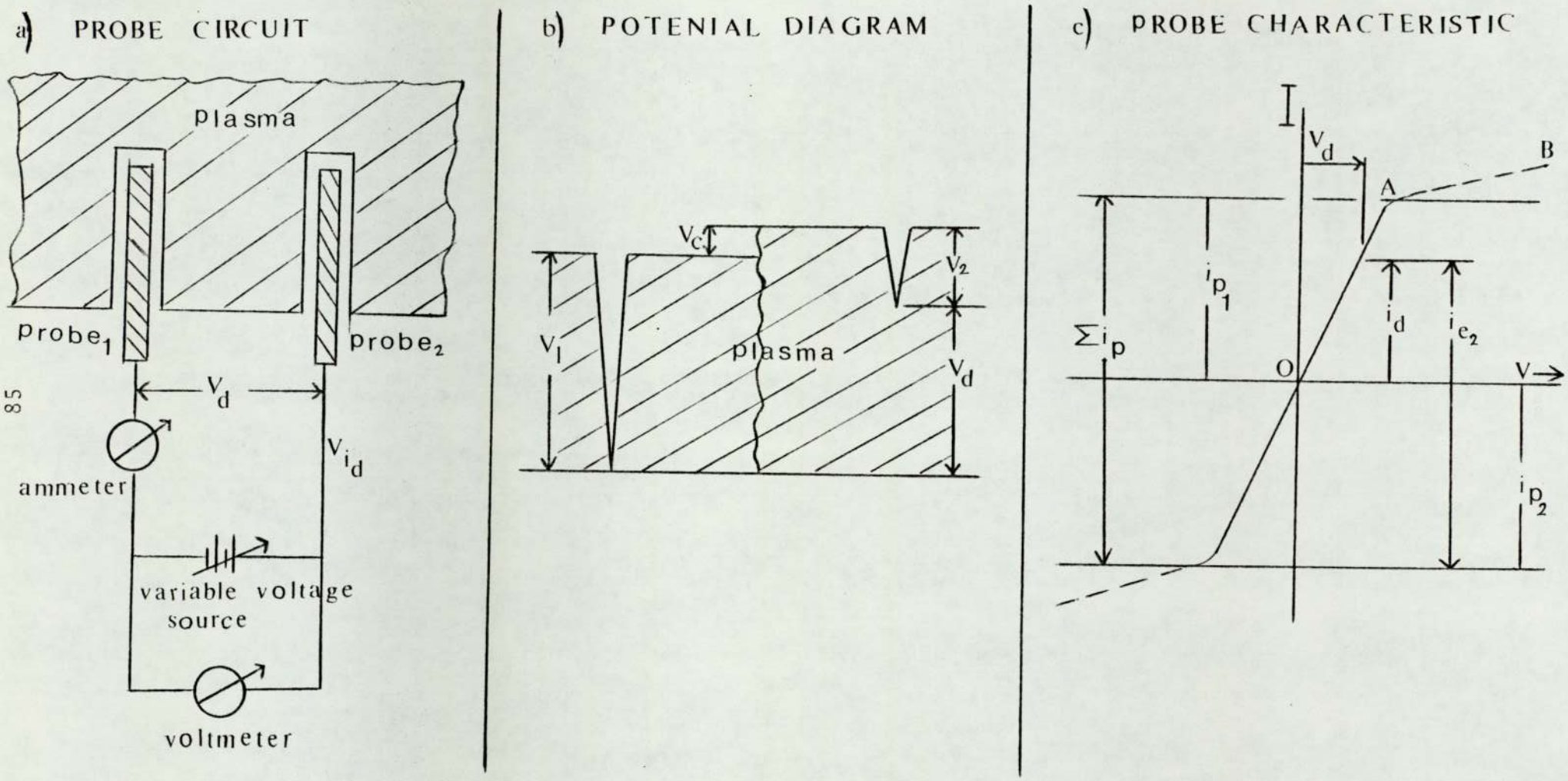

current to the probes is governed by the total positive ion current to both probes. This is several orders of magnitude lower than that collected by a single probe. Thus the main advantage that the disturbance to the plasma is minimised. With no voltage applied (V_d = 0), both probes are at the same floating potential. If a potential difference is applied between the probes they will act in concert to fulfil the requirement of zero current. This can be seen from the potential diagram of Figure (6.2.b), where, as a consequence of the applied negative potential, probe 1 has moved away from plasma potential and probe 2 has moved up towards plasma potential. The increased electron current into probe 2 flows round the circuit to compensate for the deficiency at probe 1. Thus i_d is the excess of electron current over positive ion current for probe 2. Further increase in V_d enables the portion of the characteristic OAB in Figure (6.2.c) to be obtained, and reversal of the whole procedure traces out the lower limb of the characteristic.

The important point to be recognised is that the saturation of the current to probe 2 is not a true electron current saturation, but is a limitation imposed by the saturation ion current to probe 1. Here in lies the great value of the double probe technique, that the total current to the system can never exceed the saturation ion current, since any electron current to the probe must be balanced by an equal ion current. Thus the disturbance of the plasma is minimised. The characteristic provides values for the saturation ion current to each probe, and the electron temperature may be obtained from the transition region of the characteristic by the analysis set out below.

The equality of current to the probes sets:

$$i_{p_1} + i_{p_2} = \sum i_p = i_{e_1} + i_{e_2} \qquad (6.13)$$

The values of i_{e_1} and i_{e_2} are given by the Boltzmann relations:

$$i_{e_1} + i_{e_2} = \sum i_p = A_1 j_{o1} \exp - \phi v_1 + A_2 j_{o2} \exp - \phi v_2 \qquad (6.14)$$

where $\phi = e/kT_e$ and j_{o1} and j_{o2} are the random electron currents in the plasma.

The diagram of potentials shows:

$$V_1 = V_2 + V_d - V_c \qquad (6.15)$$

Where V_c allows for any small difference in plasma potential between the regions surrounding the porbes, plus the total contact potentials acting on the system.

Substitution of (6.15) into (6.14) yields on re-arrangement

$$\ln \left(\frac{\sum i_p}{i_{e_2}} - 1\right) = \phi V_d + \phi V_c + \ln \left(\frac{A_1 j_{o1}}{A_2 j_{o2}}\right) \qquad (6.16)$$

A plot of $\ln (\sum i_p/i_{e_2} - 1)$ against the applied voltage V_d will thus have a slope of ϕ, since V_o is a constant, which provides a value for the electron temperature T_e. Equation (6.16) shows that the slope of the log plot is independent of errors in probe areas, electron random current densities, differences in local plasma potentials between the two probes, and contact potentials. The values of i_p used for the plot are obtained from the points at which the curve in Figure (6.2.c.) breaks away from the saturated regions. Johnson and Malter[91] have shown that any uncertainty in the choice of these break points has very little effect on the slope of the log plot, since any change in the selected values of the i_p's introduces a change (in the same direction) in the estimated values of

i_{e_2}. However, the real merit of the double probe is the one already emphasised, that excessive disturbance of the plasma is avoided because of the limit on electron current set by the positive ion current. This principle of double probe operation means that only the high energy tail of the electron energy distribution is sampled, and the technique has been criticised on this account. This criticism can hardly be regarded as justification for the single probe method, in which the benefit of sampling the whole electron energy distribution is lost because of the errors caused by plasma depletion.

The characteristic in Figure (6.2.c) is applicable to a symmetrical floating probe for which the area A_1 and A_2 are equal. When $A_1 > A_2$, the smaller probe 2 will be able to receive a larger electron current before probe 1 is saturated with respect to positive ions. In the limit, when $A_1 >> A_2$, probe 2 will be able to reach plasma potential and draw a saturation electron current, and an unsymmetrical probe characteristic will be obtained having the same form as the single probe characteristic discussed earlier.

Travers and Williams[89] pointed out that the double probe is relevant to flame measurements. They explained that a single probe biased positive so as to collect electrons was in fact acting as an asymmetrical limiting case of a double probe when the latter consists of two probes of greatly differing areas, since the electron current was limited by the flow of positive ions to the boundary of the plasma, typically the burner top. This may in fact lead to errors in the interpretation of the results with regard to electron temperatures and electron concentrations.

6.6. TIME DEPENDENT PHENOMENA:

In many applications it is found necessary to vary V_p with time, or to investigate plasmas where V_s, N_i and N_e are time dependent. In these situations it is important to know how quickly the probe current will follow changes in V_s, V_p and N_i, N_e, i.e. the response time of the plasma.

For a probe in the electron saturation region, when biased further positive, the sheath must expand to include a volume of space charge and momentarily allow a greater flux of electrons to reach the probe. This overshoot in electrons has been observed by Bills et al[92] and is of the order of 1μs. The effect is not observed at high pressure since collisions within the sheath will prevent any sharp rise in I_e. For the probe in the ion saturation region, the sheath thickness will again increase as V_p increases, the electrons now included in this region are pushed away rapidly. The ion density, however, in this region must be reduced giving rise to a transient ion current.

In general, if in order to adjust to a new situation, the sheath dimensions change so as to balance the transport of ions to the sheath boundary with the space charge-limited flow to the probe. The time response is controlled by the time taken for the ions to move to new positions with their random thermal velocities or mobility controlled motions. An additional displacement current may be seen which can be attributed to the capacitance of the sheath for both negative and positive probes. This is considered to be negligible compared with the overshoot for the positive case but Oskam et al[93] found a large overshoot lasting 0.4 μs for the negative case, which he attributed to a displacement current of this kind.

Although no universally applicable theory is available at this time, it would appear that, at least for low pressure situations, response times of the order of microseconds are to be expected.

6.7. ELECTROSTATIC PROBES AS DIAGNOSTIC TOOLS IN FLAME PLASMAS[123]:

6.7.1. Reliability of Probe Measurements in Flames

Single electrostatic probes have been used at various times for the determination of electron concentrations, ion concentrations and electron temperatures in flames, but it is now recognised that the range of applicability of the probe technique is more restricted in flames than is the case in glow discharge. The probe in flames differs from its counterpart in discharges in three principal respects.

Firstly, the probe is exposed to a much higher gas temperature in flames, which raises practical problems of electrical and thermal insulation of the probe, and so affects the operation of the probe in that the use of small probes is rendered very difficult.

Secondly, the probe operates at pressures up to atmospheric, so that ions or electrons on their way to the probe will make collisions with neutral gas molecules. Under these circumstances the application of the simple Langmuir low-pressure theory to the measurements is not possible. The theoretical treatments applicable to positive ion collection in a collision-dominated plasma are considered in section (6.7.2).

Thirdly, there is no fixed reference of potential in the system, and it follows that the probe must be floating. In flame studies it is customary to place a large wire grid in the flame gases to define a reference of potential, and probe

measurements are made relative to the grid. It is apparent that the arrangement is essentially a double probe, and that electron concentrations can only be measured by the single probe method when the area of the grid is sufficiently large to prevent its saturation by positive ions. Furthermore, reliable values for electron temperature will only be obtained if no depletion effects occur as the probe nears plasma potential.

In spite of these difficulties, a number of flame studies employing single probes have been reported. Ion and electron concentrations and electron temperatures were measured by Calcote[79, 86, 94], in detailed investigations of the ionisation in hydrocarbon flames. Experiments were carried out at a range of pressures, and a number of different probe designs were employed with the object of achieving the necessary asymmetry conditions for single-probe action, and of minimising errors from leakage currents. Two surprising observations were made in the course of this work, firstly that positive ion concentrations exceeded electron concentrations, in some cases by a factor as high as 30, and secondly that very high electron temperatures existed in flames. In some hydrocarbon flames, Calcote recorded electron temperatures exceeding the adiabatic gas temperature by $8000^{o}K$[86]. The observations are difficult to interpret. Calcote attributed the deficiency of electrons in the flame to the presence of negative ions. However, this is in conflict with mass spectrometric evidence. The OH^{-} ion, which by virtue of the abundance and high electron affinity of the OH radical is the most likely negative ion to be present, has been shown to occur in very small concentrations, and then only in the cool outer regions of the flame[95].

Moreover, Padley[96], considering equilibrium attachment of electrons to OH radicals using the Saha equation, has pointed out that for OH^- to explain the discrepancy between positive ion concentration and electron concentration at low pressures, an unreasonably high concentration of OH radicals in the flame would be required. The persistence of enhanced electron temperatures beyond the reaction zone is also open to question, since the redistribution of excess energies of electrons produced in the reaction zone would be expected to be quite rapid.

The difficulties of using single probes in flames have been discussed at length in an incisive article by Travers and Williams[89]. These workers examined the effect of an alteration in probe length on the saturation ion and electron currents to a single probe, at different heights above the burner. It was found that, for positive ion collection anywhere in the flame, an increase in probe length produced an increase in ion current in accordance with the increased collection area of the probe. On the other hand, the saturation electron current to a positive probe situated in a region of high ionisation was independent of probe length, a clear indication that saturation of the reference electrode was occurring. Variation in probe length gives a much more sensitive indication of current limitation than does the variation in grid size used previously[86], and it must be concluded that earlier measurements of electron concentration were low.

It is very difficult to overcome the limitations of the single probe technique. The problem stems from the very nature of an ionised flame, which in the absence of additives

is a plasma decaying rapidly with distance above the reaction zone. A grid situated high in the burned gases thus requires an enormous collecting area if current limitation at this electrode is to be avoided. The use of very small probes, which would assist in the achievement of the necessary assymetry in electrode sizes, is hindered by the difficulties of thermally and electrically insulating such probes in high temperature flame gases. In general therefore, single probes are not applicable to the determination of electron concentration in flames.

Returning to the question of electron temperature in flames, Travers and Williams determined this parameter in low pressure ethylene and acetylene flames using a symmetrical double probe. They found in all cases that the electron temperature was essentially the same as the gas temperature. Because of its safeguards against plasma depletion, a double probe is inherently more suitable for the determination of electron temperatures than is the single probe. The anomalously high values of electron temperature obtained in the early work are therefore probably in error, and it would appear that the use of the single probe for the determination of electron temperature is best avoided. The only area in which a single probe can be employed with confidence is in the estimation of positive ion concentrations.

6.7.2. The Collection of Positive Ions in a Collision Dominated High Density Plasmas

Under conditions of relatively high pressure, the basic assumption of Langmuir's original concept, that the mean free paths of the species concerned are very much greater than the Debye length and the probe dimensions, are now violated; then

density gradients are created, which cause ions to diffuse from the plasma to the sheath region and allow the probe's electric field to penetrate the plasma beyond the sheath edge. The presence of the probe therefore causes a perturbation of both the plasma density and potential in its vicinity. In this case the plasma parameters determined from the probe characteristic are not the same as those of the undisturbed plasma, and the straight forward application of equation (6.8) cannot now be made and descriptions of the current collected by the probe must take account of the diffusive and mobility controlled motions of the species approaching and passing through the space charge region.

The first of the more successful attempts to evaluate probe behaviour under these conditions came from the work of Shultz and Brown[97] for the case of positive ion collection on a cylindrical probe. They determined the probe current by considering cases in which varying numbers of collisions would take place, corresponding to a range of plasma pressures, in the passage of ions through the sheath. Some account was taken of the return to the plasma of ions by collisions with the sheath. Transport to the sheath boundary was assumed to be via normal diffusive motion. Their theory and experimental results agreed for flames up to 10 mmHg pressure. Microwave measurements of electron concentrations showed extremely good agreement with their theoretical predictions. Travers and Williams[89] used the approach of Shultz and Brown for the case of positive ion collection by single and double probes in a flame operating at a few torr pressure.

There have been many other treatments of positive ion collection in a high pressure (> 1 mmHg) gas. Bohm, Burhop

and Massey[98] treated the case of a probe at plasma potential, assuming that under these conditions no electric field exist. For a spherical probe in a high pressure plasma whose ions have a mean free path λ, ions reaching the probe originate from collisions occurring at an average distance λ from the probe, i.e. within the spherical volume of radius λ no collisions will occur. The disturbance caused by the probe at a point p, distance λ from the surface, will be due to the obstruction offered by the probe to ions which would normally pass through the volume occupied by the probe to reach p. The probe will increase the density of ions at p in the ratio of the fraction of all the solid angle subtended by the probe at p, which is $r_p^2/4\lambda^2$, where r_p is the radius of the probe. When r_e/λ is small, the simple Langmuir equation (6.8) will be valid, and when r_e/λ is appreciable this factor may be used to correct the experimental value of N_i. The relationship between positive ion saturation current and ion density for a spherical probe is thus given by:

$$I_{is} = eN_i A\left(\frac{k\,T_i}{2\pi\,m_i}\right) r_p/\lambda \qquad (6.17)$$

Calcote[21,79,94] has used the approach of Bohm, Burhop and Massey for a high pressure plasma, with the probe at plasma potential to study the ionisations in various hydrocarbon flames. The results especially concerning electron temperature measurements have been criticised by Travers and Williams[89], in the context of single probes acting as asymmetric double probes previously mentioned in section (6.5). A development of this approach has been presented by Jensen and Kurzius[99] in which the mass flow effects of a high velocity plasma are dealt with.

Calcote and King[124, 94], who found experimental values of N_i obtained by means of equation (6.8) for flames containing alkali metals to be below the theoretically predicted values by a factor of 200-400, adopted the work of the above authors. Using equation (6.9), they obtained ion densities which were essentially independent of probe size and in good agreement with theory. This procedure has been employed subsequently in other investigations, but the correction factor is rather large as is obtained from the incorrect assumption that no fields disturb the plasma when the probe is at the plasma potential.

A number of theoretical treatments specific to the positive ion saturation regions in high pressure plasmas have been produced. Boyd[100] considered the problem of a spherical probe at pressures greater than 1 mmHg. He divided the plasma around the probe into four regions, commencing at the probe surface with a space charge sheath in which high fields were sustained, and moving outwards through regions of weaker field to the undisturbed quasi-neutral region. By considering these regions in turn and matching the solutions at each boundary, he was able to derive a relationship for the ion currents to the probe. Apart from the rather ad hoc approach to the problem, a major drawback to this treatment is the necessity for an independent determination of the thickness of the probe sheath. This may be measured with difficulty in a glow discharge, but is impossible to obtain in flames, a result which precluded the application of the theory to these systems.

The most rigorous mathemetical treatment on the collection of positive ions by a negative probe in a collision dominated plasma, that of Su and Lam[101] has found the widest application.

They make no assumption regarding presence of a boundary layer sheath and use the continuity equations for ions and electrons and Poisson's equations to determine the potential distribution around a spherical probe. Su and Lam start from these fundamentals and develop from them the relation between probe current and potential. In the course of the analysis a model is constructed of the plasma surrounding the negatively biased probe, and it is shown that in general this is divided into four distinct regions. Far removed from the probe, there is a quasi-neutral region, where positive and negative charges are present in equal numbers. On moving nearer to the probe, this gives way to a transition region where some effect of the negative probe bias is seen and the electron concentration decreases. Next, there lies a sheath region in which no electrons are present, i.e. there is a positive space charge. Finally, a diffusion layer was envisaged to be adjacent to the probe surface. A further important point in the model is that the field from the probe potential and consequently the space charge region decays asymptotically with distance from the probe. This model of the plasma around the probe is shown diagrammatically in Figure (6.3.a), after Su and Lam. Here the ion and electron densities are shown at various values of x^-, a dimensionless parameter inversely related to the radial distance from the probe surface. Figure (6.3.b) shows the distribution of charge around a probe at a strongly negative potential.

A similar theory was deduced by Cohen[102]; however, this does not consider the highly negative potentials, thus the above theory of Su and Lam is more applicable to experiments working with flame plasmas.

FIG 6-3-a ION DENSITY n AND ELECTRON DENSITY n_e IN THE VICINITY OF THE PROBE

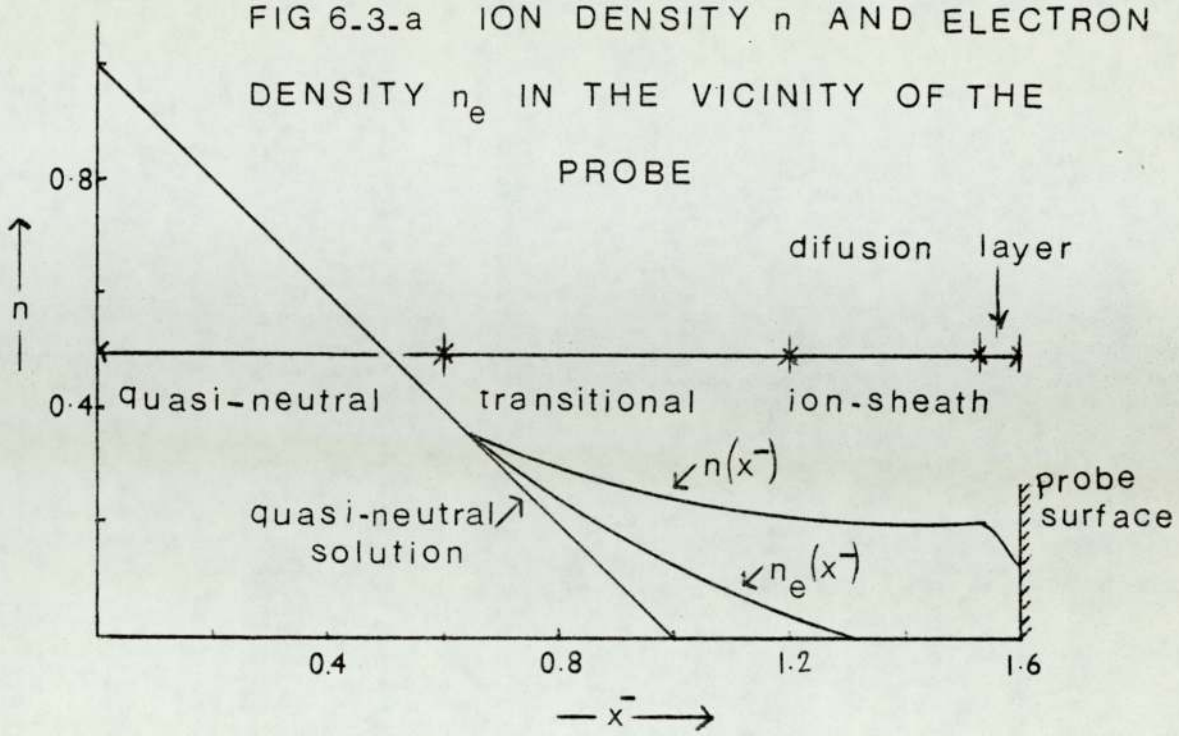

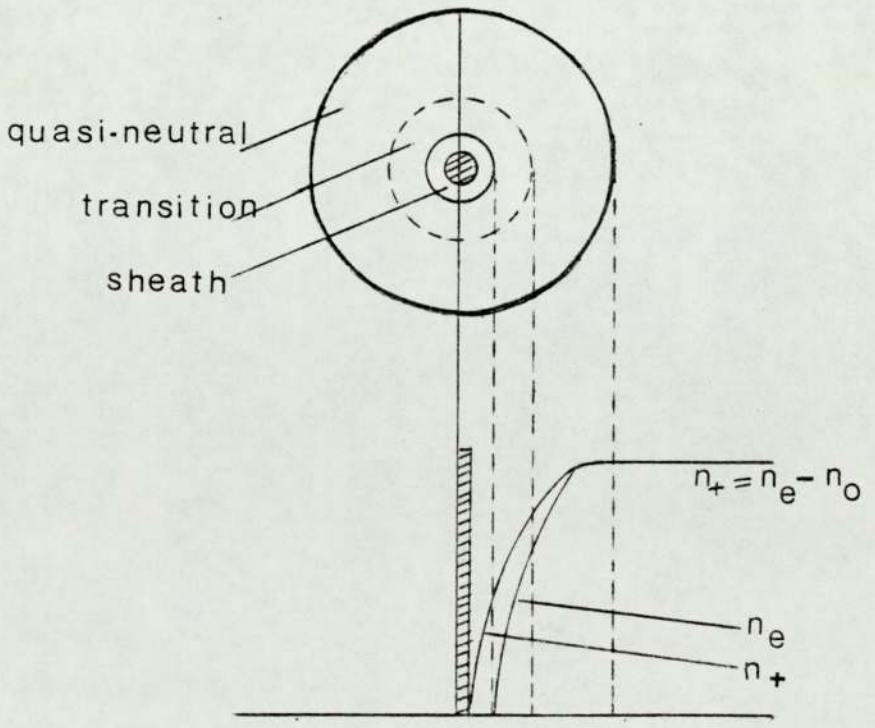

FIG 6-3-b DISTRIBUTION OF CHARGE ROUND A NEGATIVE PROBE.

The first experimental investigation, for the particular case of a large probe biased to a high negative potential, using the Su and Lam theory was by Soundy and Williams[74] who transformed their equation into practical units relating the saturated positive ion current I_i to the probe bias:

$$N_i = \frac{1}{4\pi k\, T_i (4a\, \mu_i^2)^{2/3}} \left(\frac{I_i^2}{\phi_p}\right)^{2/3} \qquad (6.18)$$

where μ_i is the mobility of the ion species, a is the probe radius and ϕ_p the probe potential. The other symbols have their usual meanings.

The assumptions made in the derivation of this relationship are tabulated below:

(i) Only singly charged species are present,

(ii) The probe potential ϕ_p is so large as to make the current collected very much greater than collected when the probe is at the plasma potential,

(iii) The probe radius is large compared with the Debye length, i.e. there is a thin sheath condition,

(iv) The electron temperature is equal to the mean gas and ion temperature.

These conditions are easily met in atmospheric flames. The limited energy available in flames makes the presence of a multiply charged ion very unlikely. The second condition is fulfilled if the probe is operated at a sufficiently high negative potential, which for the present work was -90 volts. The third point can be satisfied by suitable choice of probe size. For the hottest flames used in the present work, around 2500°K, the lowest ion densities employed were 10^9 cm^{-3}. Debye length in such flames equals 10^{-1} mm according to the

equation

$$\lambda_D = 6.9 \left(\frac{T_e}{n_e}\right)^{\frac{1}{2}} \qquad (6.19)$$

The probe used in the work was 2 mm in diameter, and this would therefore be expected to satisfy the third condition so long as the ion density did not fall below 10^9 cm^{-3}.

Soundy and Williams[74] demonstrated that the dependence of N_i and I was as predicted by equation (6.18), and subsequently confirmed the dependence of N_i on $r_p^{-2/3}$ and $\phi_p^{-2/3}$. However, for a flame burning at atmosphere, they found the expression to be in error on absolute magnitude. The positive saturation current predicted for a flame of known temperature and ion density was lower by two orders of magnitude than the experimental value. This requires that the response of a probe used to measure absolute ionisation levels, must be calibrated in a flame containing a known amount of ions. The above workers used the C_s^+ ion as a standard since in these flames caesium will reach its equilibrium level as calculated from Saha equation. Since the only unknown in their calculation was the ion mobility, μ_i, which was assumed to be 1 $cm^2 volt^{-1}$ sec^{-1}, the results cast some doubt on the accuracy of the commonly accepted value for the mobility of ions in flames. However, although mobility measurements date back to very early work in flames[103], and were often made using crude experimental technique, it is difficult to accept that the values could be in error to the extent suggested by the Su and Lam equation. Therefore, the favourable operating characteristics of negative probes in flames are supported by a rigorous theoretical treatment, which closely correlates with experimental observations.

6.8. EFFECTS OF FLOW VELOCITY UPON ION CURRENT IN COLLISION DOMINATED PLASMAS:

Clements and Smy[104,105] have developed the theory of Lam[106] for a probe in a flowing plasma or flame, for both thick and thin sheath situations. The basic idea is that for plasmas with convective velocities of $1ms^{-1}$ or greater flowing relative to a negative probe, convective transport of ions travelling with the plasma velocity v_F is more important than diffusive transport. The probe then sweeps out a section of the flame and leaves a depleted volume of plasma in its wake. The two cases are shown diagrammatically in Figure (6.4).

The conditions of Lam's theory are as follows:

(i) $\alpha = \lambda_D/L << 1$, where λ_D is the Debye length, and L a length characteristic of probe dimensions, typically 2a, the probe diameter,

(ii) $x = \frac{eV_p}{k T_e} >> 1$, where T_e is assumed to equal T_i,

(iii) R, the electric Reynolds number, is given by:

$$R = \frac{v_F L}{U_i (kT_e/e)} > 1$$

Essentially $R = \frac{v_F}{V_d}$, where V_d is the upward diffusive velocity of ions for the stationary plasma case. For large values of V_p or small electrodes, and with $R\alpha^2 x^2 > 1$, when $x >> 1$, the current I_i per unit length of probe, is related to the charge number density n_e, for positive ion saturation, by:

$$I_i = \frac{2(\pi \mu_i E_o)^{1/3} (n_e e v_F V_p)^{2/3}}{\log (I_i/2n_e e v_F a)^{2/3}} \qquad \text{(MKS)} \qquad (6.20)$$

FIG 6.4 SHEATH CONDITIONS

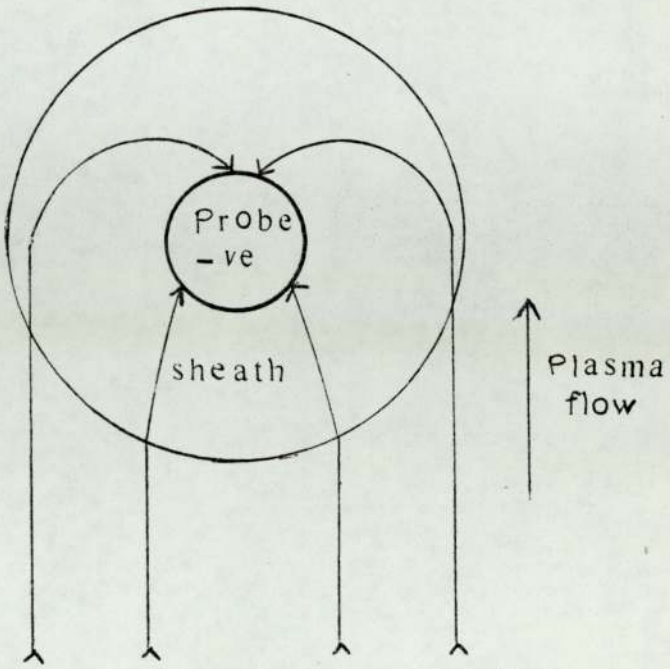

THICK SHEATH

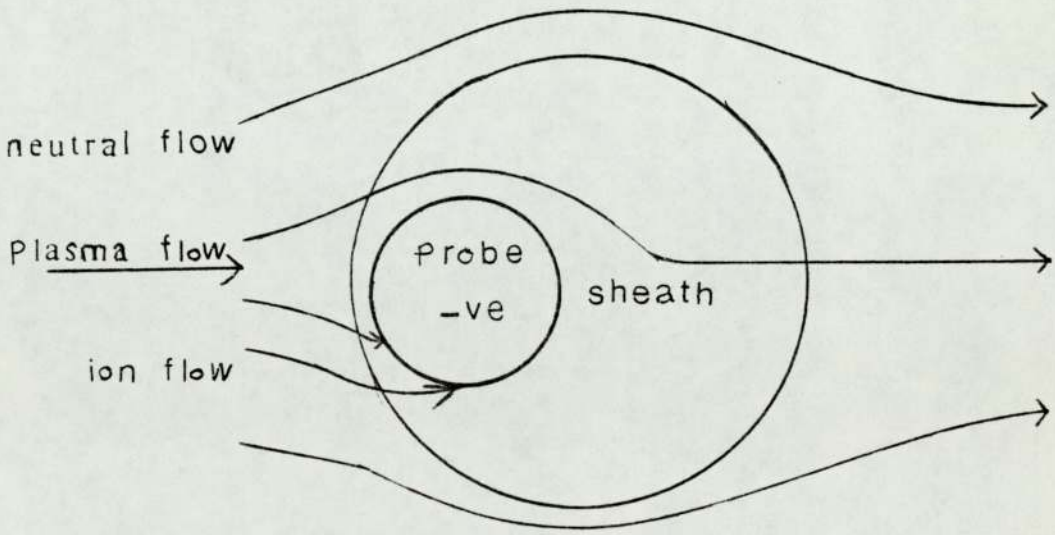

THIN SHEATH

for the thick sheath situation, E_o, being the permittivity of free space.

The equation derived for the thick sheath condition is:

$$I_i = 5.3\, E_o^{\frac{1}{4}}\, e^{\frac{3}{4}}\, \mu_i^{\frac{1}{4}}\, a^{\frac{1}{4}}\, \nu_F^{\frac{3}{4}}\, n_e^{\frac{3}{4}}\, V_p^{\frac{1}{2}} \quad \text{(MKS)} \qquad (6.21)$$

which is of the same form as equation (6.18) derived from the work of Su and Lam except for its inclusion of a dependence on plasma velocity.

Using these relationships Smy and Clements have been able to predict currents drawn by a negative probe in flame plasmas with velocities of 5 $m\,sec^{-1}$ and above, to within 20% of the experimentally measured values.

6.9. INFLUENCE OF PROBE TEMPERATURE UPON CURRENT COLLECTION

Generally electrostatic probes immersed in plasmas such as flame gases are maintained cooler than their surroundings by either rotating the probe through the flame or by water cooling. This is contrary to the continuum theory conditions where it is assumed that the probe and surrounding gases are maintained at the same temperature. The presence of a probe at a temperature lower than the flame gases produces a temperature gradient. Since charged particle number density and ion and electron diffusion coefficients are temperature dependent Thomas[107] considered this to be a possible explanation for the discrepancy between plasma densities determined experimentally and by the Su and Lam expression.

The ion diffusion-mobility equations where modified to include the effects of a temperature gradient and were solved in a similar manner to that used by Su and Lam.

It was concluded that the cooled boundary layer around the probe behaved as a series resistor lowering the probe

current by only a negligible amount.

6.10 EFFECT OF PROBE SIZE ON ION CONCENTRATION:

Sometime ago[85], it was pointed out that when known concentrations of salts were introduced into a flame, the measured ion concentration was lower than the theoretical value by a factor of some 200 to 400, depending upon the salt used. This was attributed to the cooling effect of the probe, that is, the probe cooled the gas in its immediate vicinity and thus lowered the amount of thermal ionisation in this region.

However, a more detailed investigation has shown that the measured value of positive-ion concentration, N_+, is dependent on the size of the measuring probe - the larger the probe, the lower the measured value of ion concentration. This means the measured value of ion concentration must be corrected for probe size in order to obtain a true value in the undisturbed plasma. The amount of this correction can be shown to depend on the size of the probe and the length of the mean free path:

$$N_+ \text{ (corrected)} = (r/\ell)\, N_+ \text{ (exptl)}$$

where r is the radius of the probe and (ℓ) is the mean free path.

For low pressure flames[44], if the probe dimensions (i.e. diameters) are small compared with the mean free paths of electrons and ions, then the following simple expression is valid:

$$J_+ = \frac{I_+}{A_p} = \frac{n_+ e\nu}{4} = \frac{n_+ e}{4}\sqrt{\frac{2k\,T}{m_+}} \qquad (6.22)$$

where J_+ is the random ion current density (amp m^{-2}),

I_+ is the random ion current (amp), as indicated in Figure (6.1), (taken at the inflection of the curves),

A_p is the area of the probe (m^2),

m_+ is the mass of the positive ion (kg),

n_+ is the ion density,

e is the electronic charge 1.6×10^{-19} couloumb,

ν is the mean velocity of the ions (m/sec),

k is the boltzmann constant 1.38×10^{-23} joule/^{o}k

6.11. APPARATUS USED FOR PROBE MEASUREMENTS:

A severe materials problem is encountered when probes are to be used in high temperature flames, in that there are no materials of sufficiently high melting point and non-violable nature which may be immersed in a flame without protection. A further limitation arises from the essential requirement that thermionic emission from the probe surface must be negligible. There are two principle methods of overcoming these problems, water-cooling of the probe and the use of a rotating probe which is allowed time to cool down in between each pass through the flame. Water cooled probes have been reported[86], but have the disadvantage that the presence of a cooling tube extending nearly to the probe tip may distort the ion sheath on the probe. In the work to be described, therefore, a platinum probe was rotated by a synchronous motor and swept through the flame (48 R.P.M.), the residence time in the flame being about 20 milliseconds. This ensured that the probe never reached such a temperature that thermionic emission became important. However, it has been announced recently[108] that the thermionic emission of a platinum (or nickel) probe swept in the plasma is very small at high temperatures, suggesting no appreciable decrease of work function in this case.

The burner, gas delivery system, and flame characteristics, have been previously described in Chapter 4. The probe itself,

shown in Figure (6.5), together with its external circuit, was a platinum sphere, 2 mm in diameter, formed at the end of 33 s.w.g. platinum wire. Thermal and electrical insulation of the probe wire, except for the spherical collecting area of the probe, was achieved by supporting the wire in a rod of boron nitride. This material retains its excellent insulating properties at high temperatures. A short length of wire between the spherical probe and the boron nitride insulator ensured that disturbance of the probe sheath was minimised. The probe was biased 90 volts negative to the burner top, which was held at ground potential. The current collected by the probe was measured on a SOLARTRON CD513 oscilloscope. A small magnet mounted on the probe armature operating a reed switch as it rotated was used to trigger the oscilloscope as the probe passed into the flame region. The height of the pulse on the oscilloscope was related to the positive ion concentration and was measured visually against the graticule.

Mains pick-up was found to be a problem in these measurements, and to eliminate this, screened cable was used for all of the electrical leads, and the battery and other circuit components wereplaced in grounded metal boxes. Also, because of the probe use for prolonged runs in flames containing alkali metals, the probe current tended to fall off because of contamination of the probe surface. Periodically therefore, the probe was cleaned by heating after treatment with hydrochloric acid, and by this means the sensitivity of the probe could be restored.

6.12. THE USE OF THE ELECTROSTATIC PROBE IN FLAMES

In section (6.7.2), mention was made of the success of the

FIG 6.5 THE PROBE ASSEMBLY

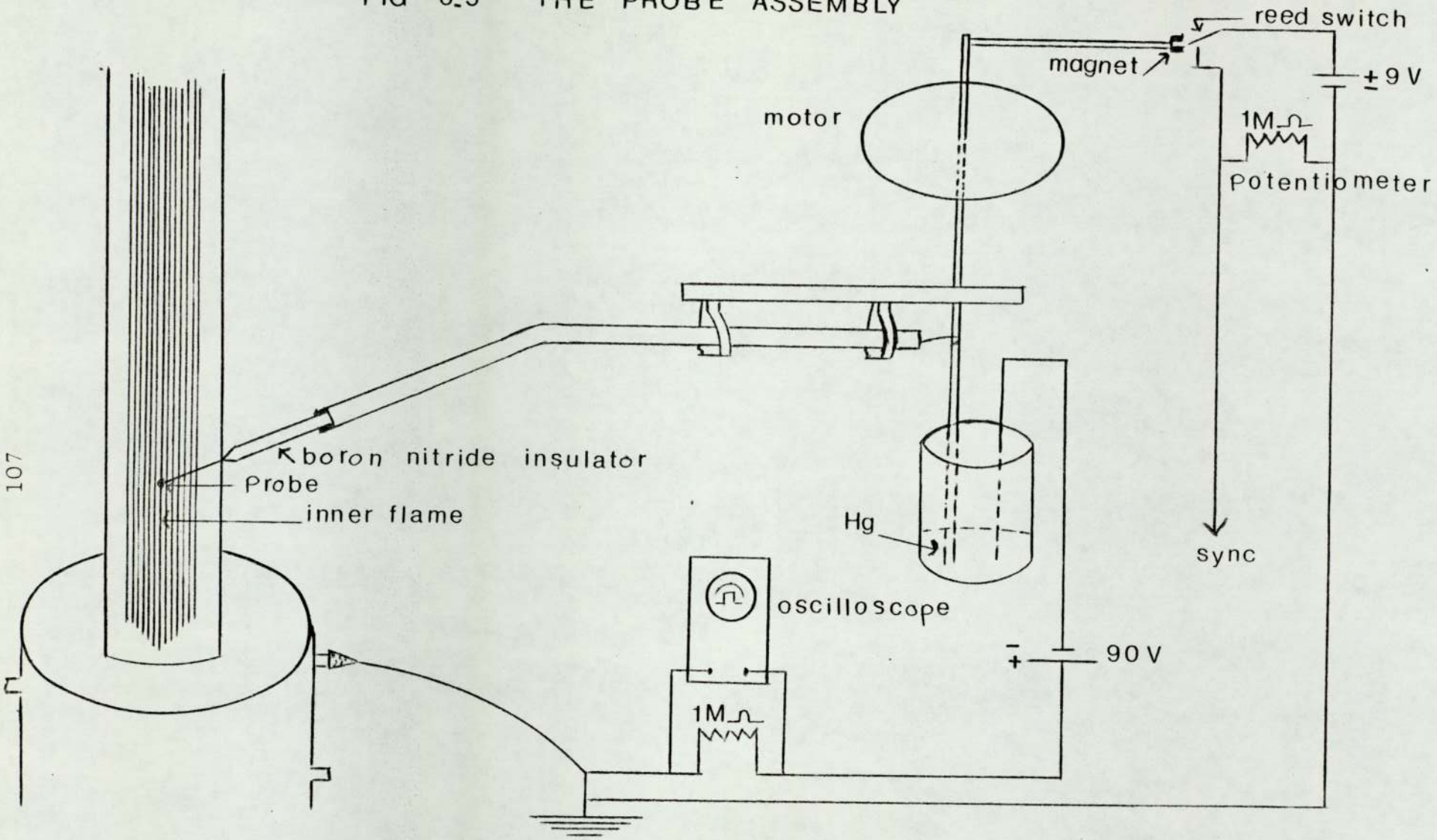

Su and Lam theory in predicting the observed dependence of N_i on $r_p^{-2/3}$, $Q_p^{-2/3}$ and $I^{4/3}$, but of its failure with regard to the absolute magnitude of ion current. This weakness prevented the treatment of probe currents as absolute values from which ion concentrations can be calculated, and it was therefore necessary to calibrate the probe.

6.12.1. Calibration of the Probe and Atomiser

6.12.1.a. Theoretical Considerations

For positive ions, the only occurrence which needs to be considered is hydroxide formation, which will reduce the number of neutral atoms and hence the ion concentration in the flame. Hydroxides are formed to varying degrees by the alkali metals, the effect being negligible for sodium and most marked for lithium. Caesium, which was used in the calibration of the probe, has been shown by Jensen and Padley[73] to form hydroxide in significant amounts even at temperatures as high as 2600°K. Accordingly its effect on the ionisation equilibrium needs to be taken into account.

Under conditions when part of the alkali metal added to the flame takes part in the reaction:

$$A + H_2O \rightleftarrows AOH + H \qquad (6.23)$$

then the mass-balance equation becomes:

$$[A]_o = [A^+] + [A] + [AOH] \qquad (6.24)$$

using $\phi = \frac{[AOH]}{[A]}$ (3.13) this may be written:

$$[A] = \frac{[A]_o - [A^+]}{1 + \phi} \qquad (6.25)$$

which on substitution into equation (3.4) ($K = \frac{[A^+]^2}{[A]}$ assuming that the only ions present are A^+ and e^-) yields

$$K = \frac{[A^+]^2 (1 + \phi)}{[A]_o - [A^+]} \tag{6.26}$$

$$\text{or } [A^+]^2 + \frac{K}{1+\phi} [A^+] - \frac{K}{1+\phi} [A]_o = 0 \tag{6.27}$$

This may be written:

$$[A^+]^2 + K_1 [A^+] - K_1 [A]_o = 0 \tag{6.28}$$

where $K_1 = K(1+\phi)^{-1}$ is the equlibrium constant for the ionisation reaction corrected for hydroxide formation.

Equation (6.28) gives $A^+ = (K_1[A]_o)^{\frac{1}{2}}$ for $A_o >> K_1$ and $[A^+] = [A]_o$ for $A_o << K_1$. A plot of log $[A^+]$ against log $[A]_o$ should therefore be a straight line of slope 0.5 at large $[A]_o$, turning over to a slope of unity at small $[A]_o$. The construction of this curve requires a knowledge of ϕ, which was obtained from the work of Jensen and Padley. If K_ϕ is the equilibrium constant for (6.23):

$$K_\phi = \frac{[AOH][H]}{[A][H_2O]} = \phi \frac{[H]}{[H_2O]} \tag{6.29}$$

ϕ was calculated from this equation using the reported values of K_ϕ for Caesium. It was assumed that a few cm above the reaction zone the concentrations of H and H_2O would be equilibrated, and theoretical values for these concentrations were used in the calculation. Substitution of the value for ϕ into equation (6.27) enabled a plot of log $[A^+]$ against log $[A]_o$ to be made for caesium at 2300°K. The resulting curve, for the theoretical ionisation of caesium at this temperature is shown in Figure (6.6).

6.12.1.b. Calibration procedure

The rotating probe was used to measure the ion concentrations of a flame at 2300°K supplied in turn with a range of caesium chloride solutions from 10^{-1} to 10^{-4} molar. By this means the pulse height (θ) on the oscilloscope was determined as a function of solution molarity (M). Since for the probe, ion concentration is proportional to $\theta^{4/3}$, and the caesium concentration in the flame is proportional to the caesium chloride molarity in the atomiser, a plot of log $\theta^{4/3}$ against log (M) exhibits the same form as the theoretical one of log (Cs^+) against log $(Cs)_o$. By plotting the experimental log $\theta^{4/3}$ - log (M) curve on translucent graph paper, it was possible to fit this curve to the theoretical curve, so locating the two vertical axes and the two horizontal axes with respect to one another. In Figure (6.6) the experimental points are shown fitted to the theoretical curve. This procedure simultaneously calibrates $\theta^{4/3}$ in terms of (Cs^+) and (M) in terms of $(Cs)_o$. The calibration factors so obtained were:

$$1 \text{ unit of } \theta^{4/3} = 1.72 \times 10^{11} \quad Cs^+ \text{ cm}^{-1}$$

$$1 \text{ unit of (M)} = 1.13 \times 10^{14} \quad Cs_o \text{ cm}^{-3}$$

The relationship between N_i and $\theta^{4/3}$ given by Su and Lam's equation (6.18), is dependent on ion mobility, and this precludes the general application of the caesium calibration to any ion. It is therefore necessary to include a mobility correction factor in order to enable the calibration to be transferred to other ions. It is well known, that for ions in the same gas, the term controlling the mobility is[121] $(1 + \frac{m_g}{m_i})^{\frac{1}{2}}$, where m_g is the mass of the neutral gas molecules and m_i is the mass of the ion. From inspection of equation

FIG 6-6 CALIBRATION OF THE PROBE AND ATOMISER.

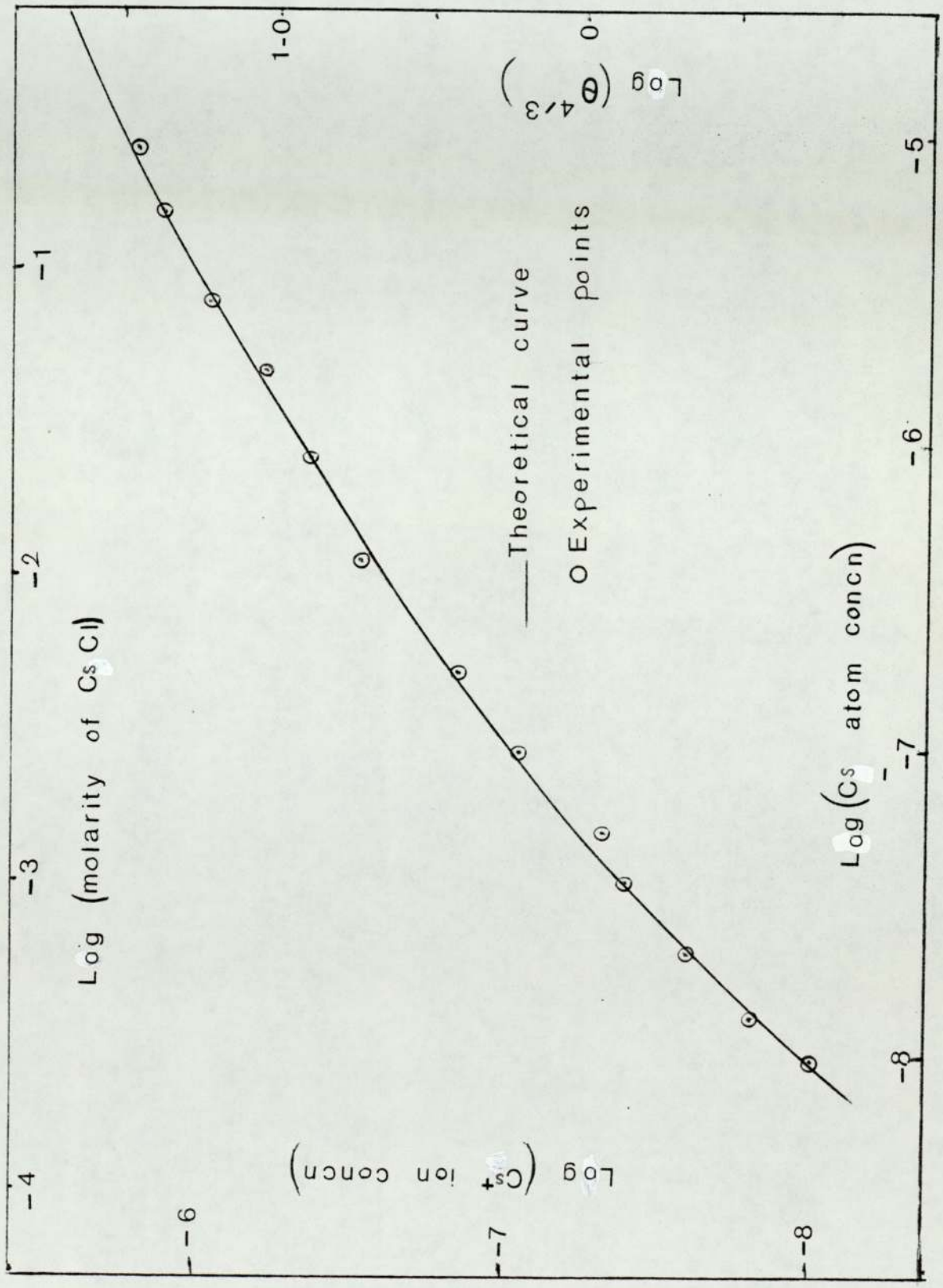

(6.18):

$$N_i = \frac{1}{4\pi kT} \cdot \frac{1}{(4r_p \mu_i^2)^{2/3}} \cdot \left(\frac{I^2}{\phi_p}\right)^{2/3} \qquad (6.18)$$

it can be seen that the mobility correction factor will be of the form:

$$\left(\frac{1 + m_g/m_{c_s}^+}{1 + m_g/m_i}\right)^{2/3} \qquad (6.30)$$

where $m_{c_s}^+$ is the mass of the caesium ion (133). The general equation for ion collection by the probe, in the flame in question, thus becomes:

$$N_i = 1.72 \times 10^{11} \left(\frac{1 + m_g/m_{c_s}^+}{1 + m_g/m_i}\right)^{2/3} \theta^{4/3} \qquad (6.31)$$

It can be seen from equation (6.31) that the mobility correction factor will be most important for light ions ($m_i < m_g$), while for heavy ions, ($m_i > m_g$), the deviation from the caesium calibration will be quite small. For a hydrogen-oxygen-nitrogen flame, m_g for these purposes may be taken as 23, the mean of the masses of H_2O (18) and N_2 (28), since these are the predominant neutral gas molecules in the flame.

5.13. THE RESPONSE OF THE PROBE IN FLAMES CONTAINING DIMETHYLPHOSPHITE AND ALKALI METALS:

Following the calibration of the probe, exploratory investigations of the positive ion concentration in flames containing dimethylphosphite and alkali metals were commenced. Graphs for flames with different alkali metals at different temperatures and at different heights above the burner, in presence of dimethylphosphite, are shown in Figure (6.7).

It was found that the effect was specific to every alkali metal at certain temperatures and at certain heights above the

burner. The results are shown in Tables (6.1). The survey showed that the addition of phosphorus produced a uniform increase in the positive ion concentration, and as shown in all cases that the initial slope decreases first and subsequently increases. These surprising results could be explained in making a comparison between phosphorus and sulphur.

In a study paralleling their work on phosphorus[24], Fenimore and Jones[32] examined with a mass spectrometer the burnt gases of oxyhydrogen flames containing sulphur. In rich as well as in lean flames, they found that added sulphur appeared mostly as sulphur dioxide owing to the effect of atomic hydrogen in promoting the reaction:

$$H_2S + 2H_2O + 2H \longrightarrow SO_2 + 4H_2$$

This reaction is admittedly exothermic by 2eV. However, the H_2S and SO_2 accounted for only 75% of the added sulphur in rich flames. They expected S_2 on the basis of the SH + S reaction but could not detect it except by its emission in the reaction zone. Neither could they detect SH. They believed that the recombination of H + H and H + OH in rich flames is catalysed by SO_2 via the intermediate molecule HSO_2.

These conclusions about sulphur give an indication that it could be the case about phosphorus either by forming very slowly compounds which oppose the reaction or by forming very rapidly compounds in the flame.

Chapter 8 will include more discussion, relating these experimental results with those of electron concentrations and spectroscopic studies.

Table (6.1)

M	ht.cm	S_p^{*}(2000°K)	S_p^{*}(2300°K)	S_p^{*}(2500°K)
Cs	1	10000	1350	450
	2	9000	1250	400
	3	8000	1150	350
	4	8500	1200	380
	5	9500	1300	420
Rb	1	9000	1250	400
	2	8000	1150	350
	3	7000	1050	280
	4	7500	1100	300
	5	8500	1200	320
K	1		950	300
	2		850	250
	3		750	180
	4		800	200
	5		900	220
Na	1		850	250
	2		750	200
	3		650	130
	4		700	150
	5		800	170

*S_p is the initial slope of the $\left(\frac{P}{P_o}\right)^2$ graph against $[B_o]$.

Continued Table (6.1)

M/T(°K)	ht cm	$(P/P_q)^2$ at different P.P. of "P"				
		2×10^{-4} atm	4×10^{-4} atm	6×10^{-4} atm	8×10^{-4} atm	10×10^{-4} atm
	1	2.475	3.07	3.37	3.5	3.565
	2	2.35	2.97	3.25	3.395	3.445
Cs	3	2.25	2.87	3.13	3.28	3.315
2000	4	2.3	2.92	3.18	3.32	3.365
	5	2.42	3.03	3.31	3.455	3.51
	1	1.184	1.226	1.242	1.25	1.252
	2	1.174	1.22	1.236	1.243	1.245
Cs	3	1.164	1.214	1.23	1.236	1.238
2300	4	1.167	1.217	1.234	1.241	1.243
	5	1.179	1.223	1.24	1.247	1.249
	1	1.078	1.131	1.172	1.202	1.22
	2	1.07	1.119	1.159	1.189	1.209
Cs	3	1.062	1.117	1.144	1.174	1.194
2500	4	1.067	1.114	1.152	1.182	1.203
	5	1.074	1.124	1.165	1.195	1.214
	1	2.31	2.72	2.93	3.07	3.16
	2	2.14	2.54	2.75	2.88	2.96
Rb	3	2.01	2.47	2.61	2.73	2.79
2000	4	2.06	2.45	2.66	2.78	2.85
	5	2.2	2.61	2.82	2.96	3.04
	1	1.16	1.204	1.229	1.245	1.257
	2	1.149	1.189	1.213	1.228	1.236
Rb	3	1.135	1.172	1.193	1.207	1.216
2300	4	1.14	1.178	1.2	1.214	1.221
	5	1.155	1.196	1.222	1.237	1.247

Continued Table (6.1)

M, T(K)°	ht.cm.	$(p/p_o)^2$ at different P.P. of "P"				
		2×10^{-4} atm	4×10^{-4} atm	6×10^{-4} atm	8×10^{-4} atm	10×10^{-4} atm
	1	1.07	1.12	1.16	1.189	1.207
	2	1.058	1.103	1.139	1.168	1.188
Rb	3	1.052	1.093	1.126	1.154	1.175
2500	4	1.055	1.098	1.133	1.162	1.182
	5	1.063	1.11	1.147	1.177	1.196
	1	1.141	1.206	1.242	1.262	1.268
	2	1.13	1.193	1.232	1.254	1.261
K	3	1.118	1.181	1.218	1.239	1.245
2300	4	1.124	1.187	1.224	1.243	1.248
	5	1.134	1.199	1.237	1.258	1.264
	1	1.055	1.097	1.132	1.158	1.174
	2	1.041	1.075	1.102	1.126	1.142
K	3	1.034	1.062	1.085	1.106	1.121
2500	4	1.037	1.068	1.094	1.116	1.132
	5	1.047	1.084	1.115	1.14	1.157
	1	1.13	1.195	1.232	1.252	1.258
	2	1.119	1.181	1.22	1.242	1.25
Na	3	1.105	1.166	1.207	1.232	1.243
2300	4	1.112	1.175	1.215	1.238	1.247
	5	1.124	1.188	1.226	1.247	1.254
	1	1.046	1.083	1.114	1.14	1.157
	2	1.032	1.058	1.081	1.1	1.117
Na	3	1.024	1.046	1.063	1.071	1.091
2500	4	1.028	1.052	1.073	1.09	1.105
	5	1.037	1.067	1.093	1.115	1.132

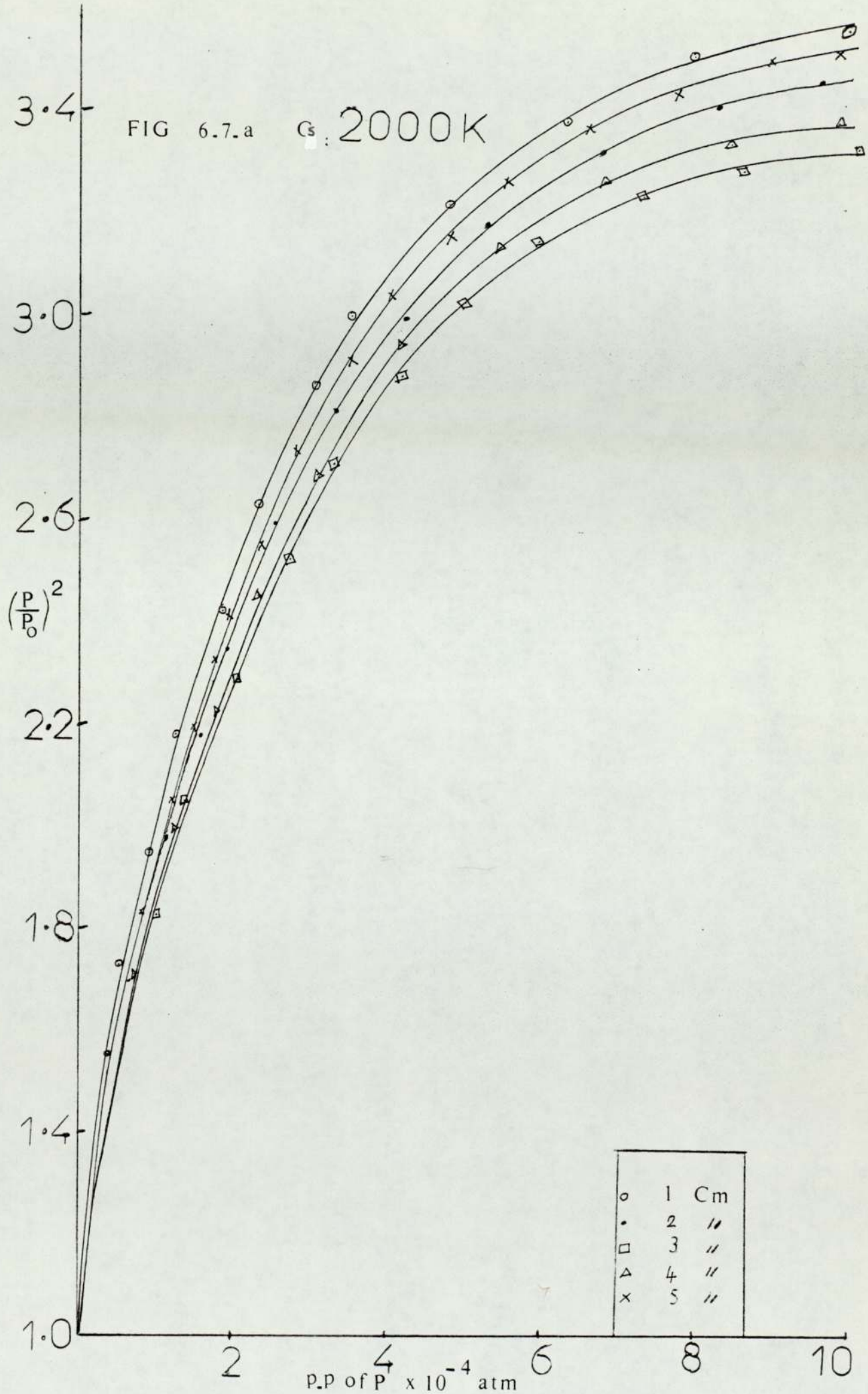
FIG 6.7.a Gs : 2000K
3·4
3·0
2·6
2·2
1·8
1·4
1·0
$(\frac{P}{P_0})^2$
2
4
6
8
10
p.p of P x 10^{-4} atm
1 Cm
2 //
3 //
4 //
5 //

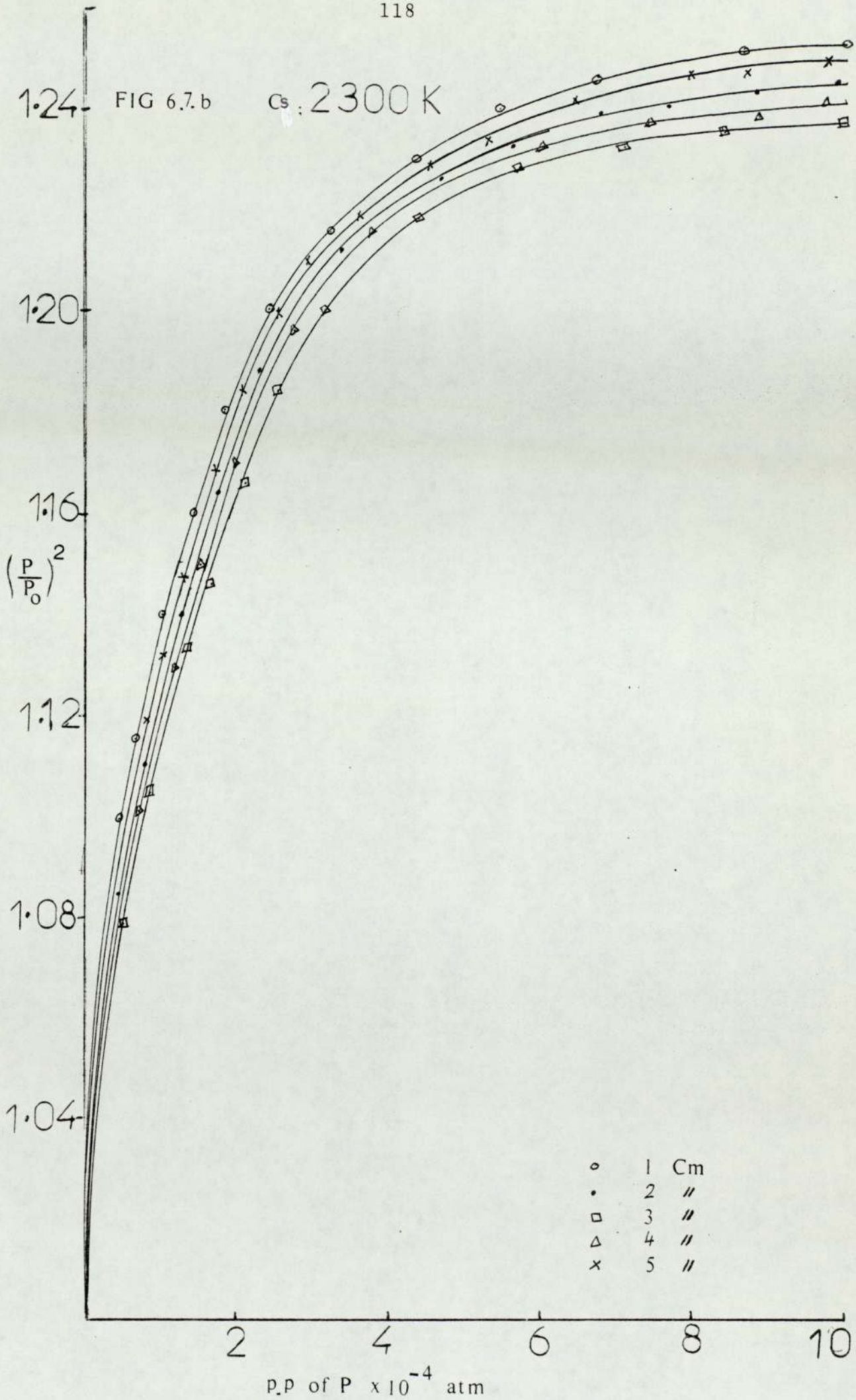
FIG 6.7.b
Cs : 2300 K
1·24
1·20
1·16
1·12
1·08
1·04
$\left(\frac{P}{P_o}\right)^2$
2
4
6
8
10
p.p of P x 10^{-4} atm
1 Cm
2 //
3 //
4 //
5 //

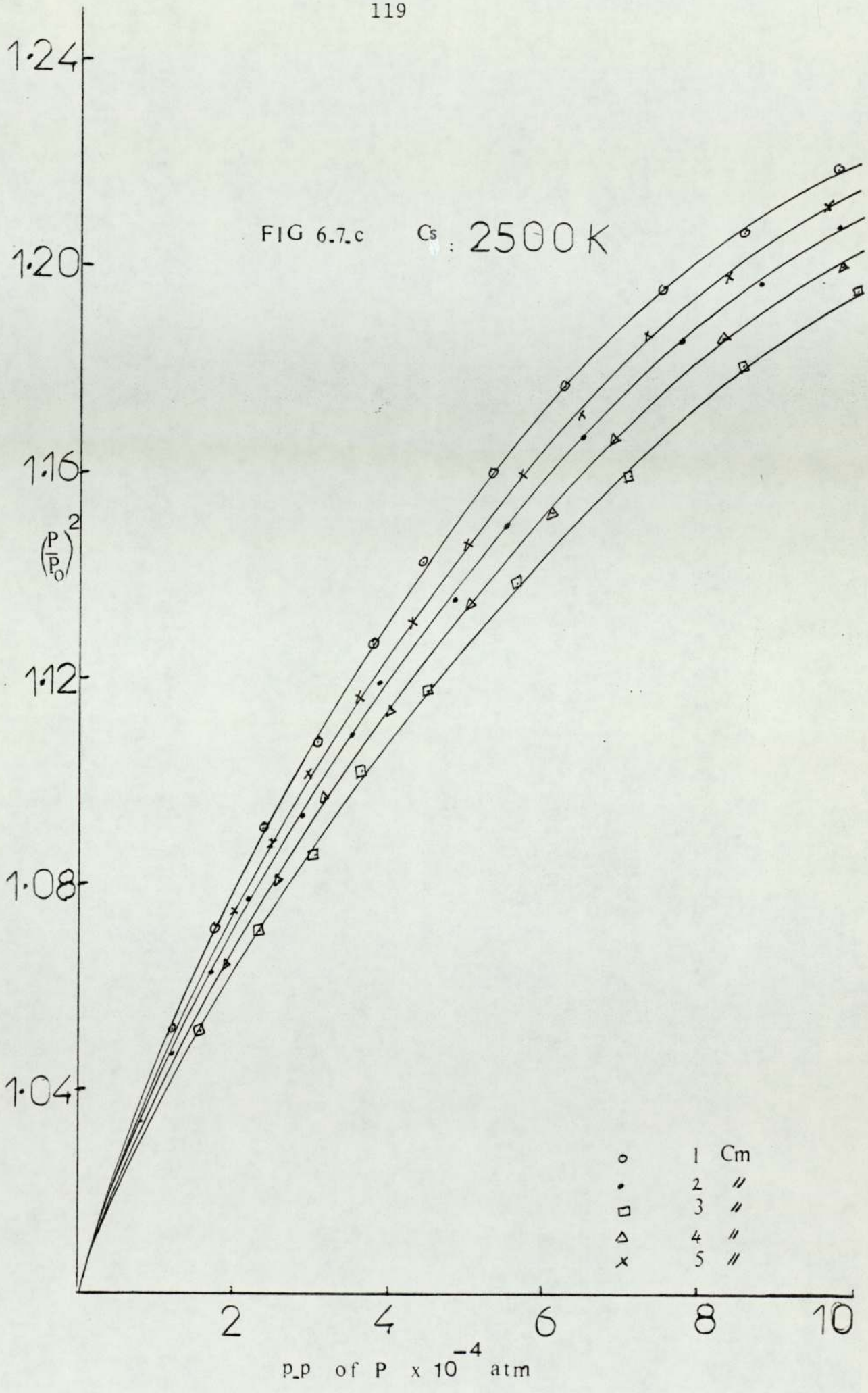

FIG 6.7.c Cs : 2500 K

FIG 6.7.d Rb : 2000 K

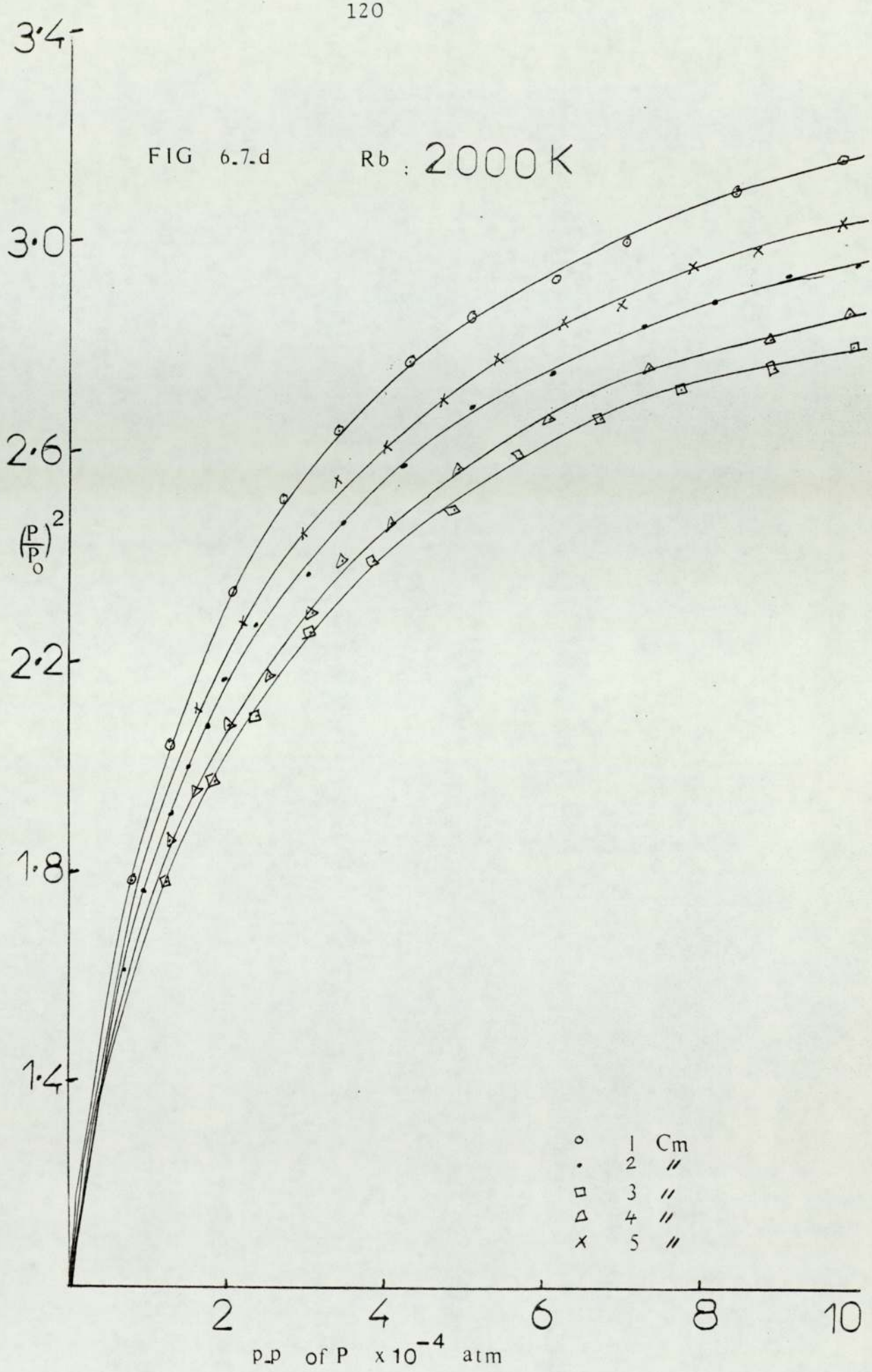

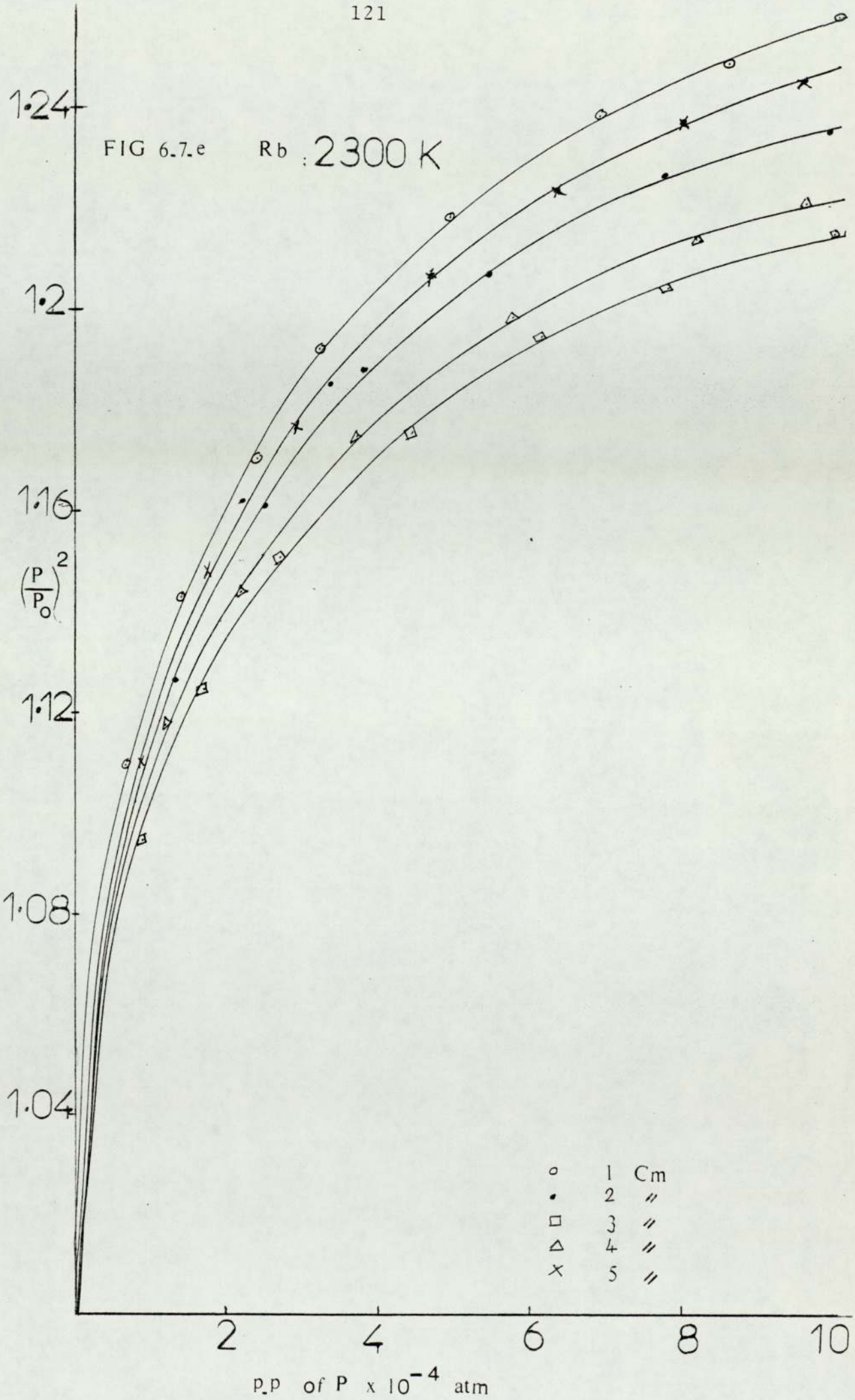

FIG 6.7.e Rb : 2300 K

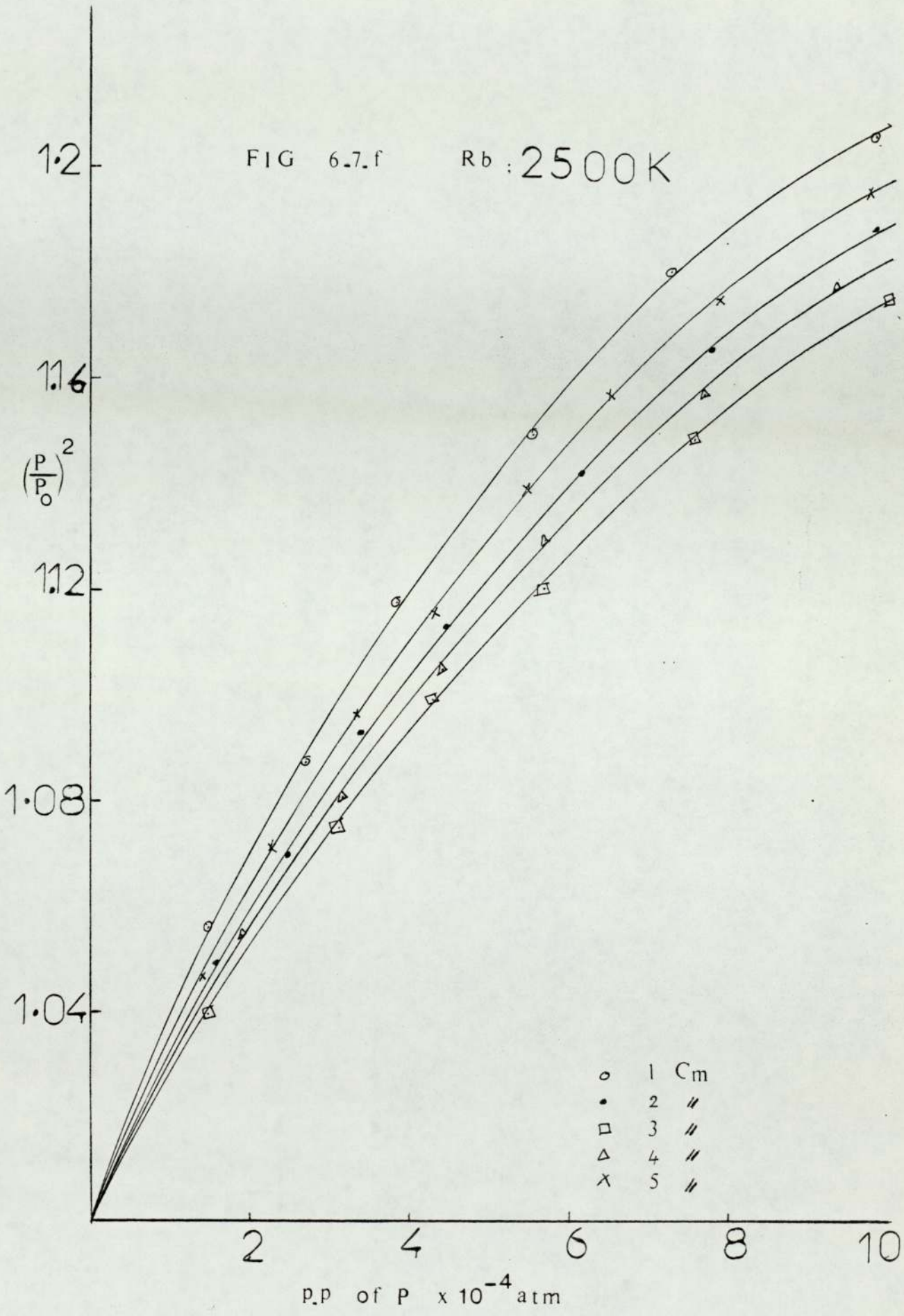
FIG 6.7.f
Rb : 2500K
1·2
1·16
1·12
1·08
1·04
$\left(\frac{P}{P_o}\right)^2$
2
4
6
8
10
p.p of P x 10^{-4} atm
1 Cm
2 //
3 //
4 //
5 //

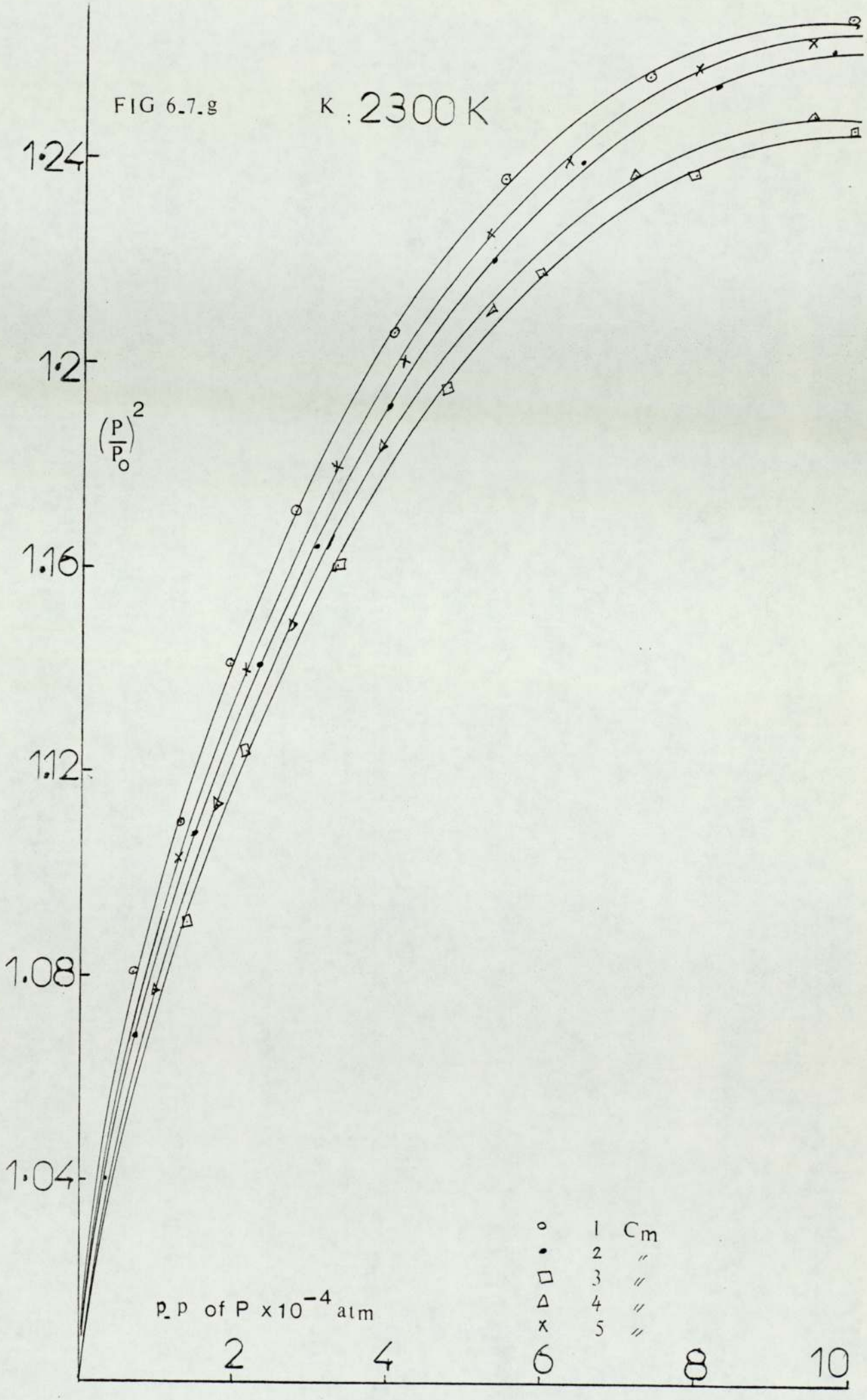
FIG 6.7.g
K : 2300 K
1·24
1·2
1·16
1·12
1·08
1·04
$\left(\frac{P}{P_o}\right)^2$
p p of P x 10^{-4} atm
2
4
6
8
10
1 Cm
2 //
3 //
4 //
5 //

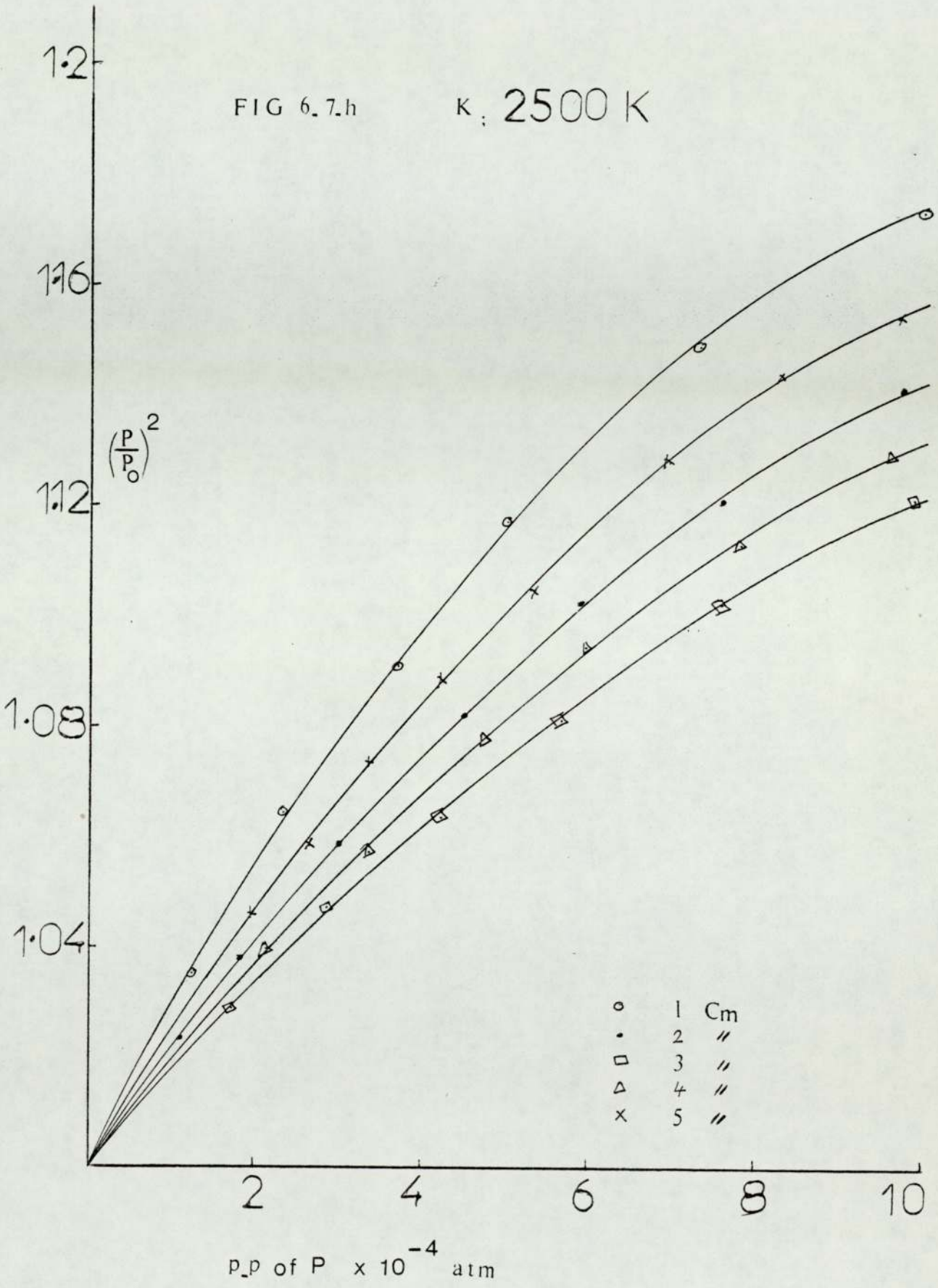
FIG 6.7.h
K : 2500 K
1·2
1·16
1·12
1·08
1·04
$\left(\frac{P}{P_o}\right)^2$
2
4
6
8
10
p.p of P x 10^{-4} atm
1 Cm
2 //
3 //
4 //
5 //

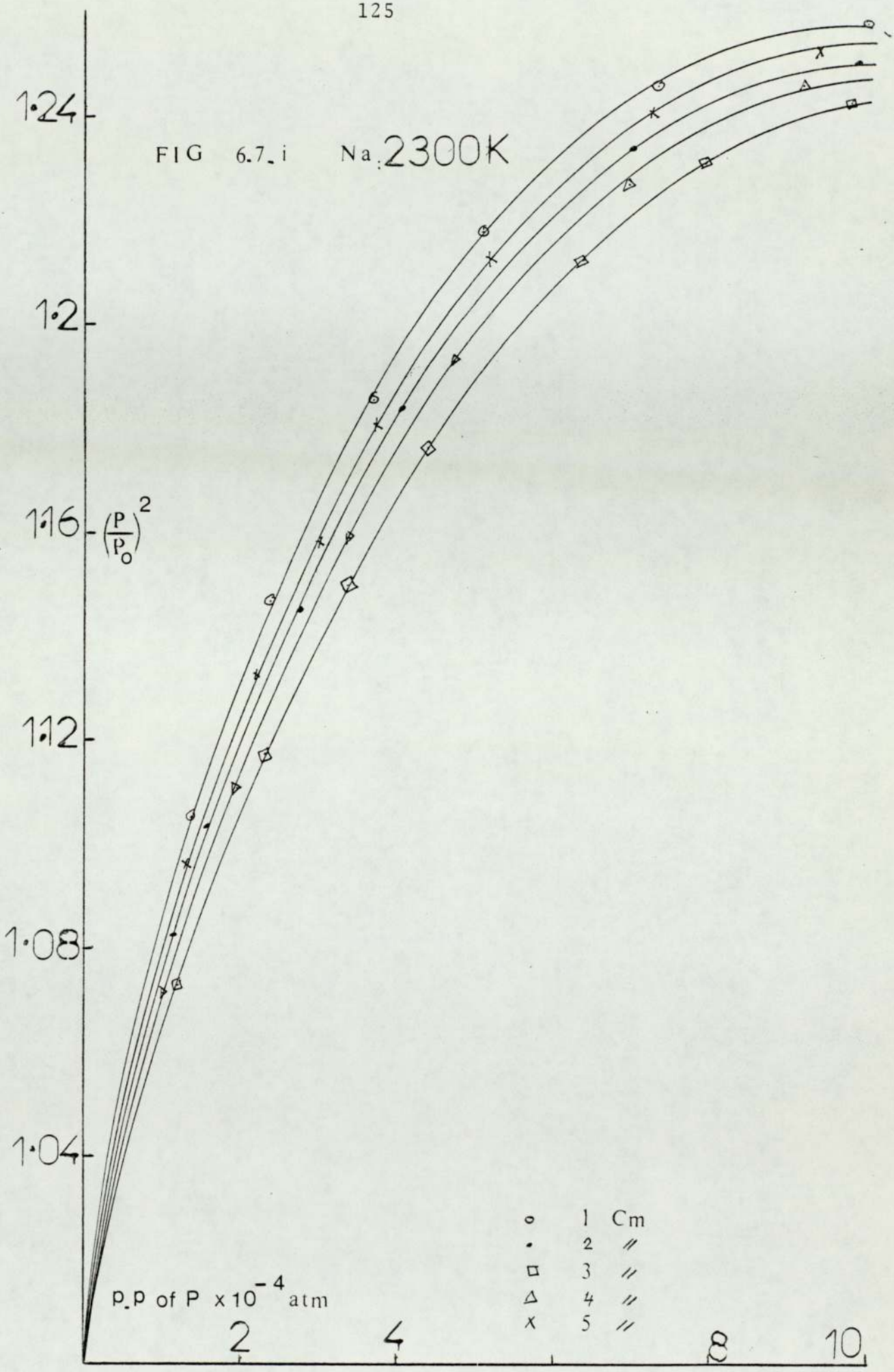

FIG 6.7.i Na. 2300K

FIG 6.7.j Na : 2500 K

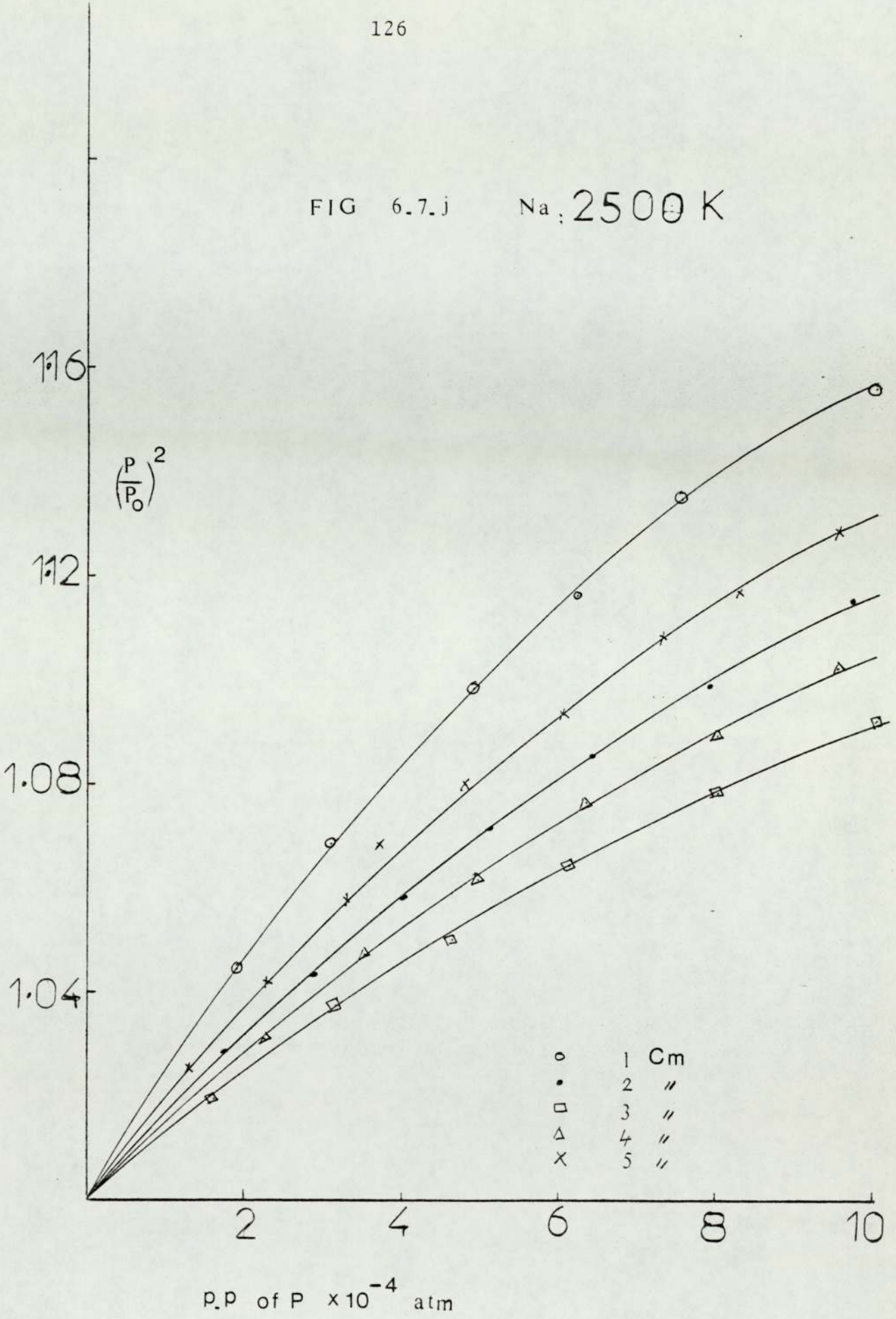

7. SPECTROSCOPIC STUDIES

7.1. HYDROGEN ATOM CONCENTRATION[4]:

It was suggested by Arthur[109] that premixed flames at atmospheric pressure might have concentrations of radicals, particularly of hydrogen atoms, which were in excess of those calculated on the basis of full thermodynamic equilibrium at the temperature of the flame. The work of Bulewicz, James and Sugden[110] showed this suggestion to be correct, and demonstrated the pattern of such excess concentration. At high temperatures, the measured concentrations were indistinguishable from the calculated values, but at progressively lower temperatures the two deviated more and more, temperature having little effect on the actual H atom concentration below 2000°K.

The measurement of the concentration of the minor species in the burnt gases - H atoms, OH radicals, etc. - can be achieved in several ways. The majority of the studies of flame kinetics have been carried out in flames for which the minor constituent composition has been determined by a photometric technique, and the first and most important of these is the Sodium/Lithium comparison technique of Bulewicz, James and Sugden[110] which depends on the establishment of the rapid, balanced reaction:

$$Li + H_2O \rightleftharpoons LiOH + H$$

In another method a solution of a sodium salt in hydrochloric acid is used, based on the equilibrium in the flame of the reaction:

$$Na + HCl \rightleftharpoons Na\,Cl + H$$

Neither the Na/Li nor the Na/Cl techniques are very easy

to apply: particularly in the study of kinetics in flames, the formation of hydrides in the flame has been employed.[114] Typical example is provided by the COPPER FLAME BAND METHOD developed by Bulewicz and Sugden. They showed that the intensity of the band system around 428 nm, due to CuH ($A^1\Sigma^+ - X^1\Sigma^+$) and the broad system in the green, ascribed by them to CuOH[111], depends upon height in the flame in the same way as the concentration of H atoms; however, the intensity of the Cu resonance doublet at 325 nm was not affected by the composition of the flame. Sugden[113] had demonstrated mathematically that if a compound AB can be balanced against free A by the two processes:

$$A + HB \rightleftharpoons AB + H$$

$$A + B + M \rightleftharpoons AB + M$$

where M is the third body, the first process would be followed if the A-B bond energy were greater than 300 kJ mol^{-1}, but the second if the bond energy were less. LiOH and NaCl follow the former process. CuOH and CuH, with low bond energies, follow the latter so that the equilibrium constants may be written down:

$$\frac{[CuH]}{[Cu][H]} = K_H \qquad \frac{[CuOH]}{[Cu][OH]} = K_{OH}$$

If the temperature in a given flame is sensibly uniform, and no dilution occurs through diffusion, or entrainment of air, the concentration of copper atoms, which represent the major form of copper in the flame, will be constant, so that:

$$[CuH] = K_H [Cu][H] \qquad [CuOH] = K_{OH} [Cu][OH]$$

or:

$$I_{CuH} = \alpha[H] \qquad I_{CuOH} = \beta[OH]$$

The relative intensities of the CuH or CuOH bands are therefore a direct measure of the relative concentration of

H or OH respectively at the points of measurement within any one flame.

The H atom concentration in a flame decreases markedly with height, as shown in Figure (7.3), through the recombination process:

$$H + H + M \longrightarrow H_2 + M \qquad (7.1)$$

The first detailed study of recombination was due to Bulewicz and Sugden[114] who used the CuH method to determine [H] at various heights in a series of flames in the temperature range 1600-2400°K.

The use of these measurements[110] to study the kinetics of reaction (7.1) is discussed below.

It is believed that the pairs of reactions

$$H_2O + H \rightleftharpoons H_2 + OH \qquad K_\alpha \qquad (7.2)$$

$$OH + H \rightleftharpoons H_2 + O \qquad K_\beta \qquad (7.3)$$

are close to equilibrium, the known data suggesting that they should be in balance after 1μs. It is therefore possible, at all times of significance, to write:

$$[OH] = K_\alpha [H_2O][H]/[H_2] \qquad (7.4)$$

$$[O] = K_\beta [OH][H]/[H_2] \qquad (7.5)$$

$$= K_\alpha K_\beta [H_2O][H]^2/[H_2]$$

In all but the most extreme flames, H_2O and H_2 will be major constituents of the flame gases, whose ratio will not depend to any significant extent on whether or not the radicals are equilibrated, though it will depend on the fuel/oxidant ratio. Determination of the local H atom concentration in a premixed flame therefore also determines the OH and O concentrations where the concentrations of the radicals [H], [OH] and [O] are interrelated by the above equations (7.2-7.5)

as in any one flame they rise or fall together since the concentrations of the bulk constituents $[H_2]$ and $[H_2O]$ do not alter; conversely, the dependence of any effect on the H atom concentration is indistinguishable from a dependence on the OH concentration, unless a comparison can be made between flames of different composition.

7.2. THE SPECTROPHOTOMETER:

There is the great advantage that spectroscopic studies do not interfere with the flame processes.

The spectra were studied photometrically by the copper flame band method using a Hilger Medium Quartz spectrograph, with an IP28 photomultiplier scanning unit. The signal currents from the photomultiplier in response to the incident radiation is directed into the Brookdeal 9503 precision Lock-in Amplifier whose meter reading is an indication of the signal response of the photomultiplier against position of the scanning slit. The radiation from the flame was chopped by a rotating sectored disc, in synchrony with that from a pea lamp to a photocell, to prevent excessive build-up of the emission from the flame. Both signals were fed into the phase sensitive detector of the 9503, this being a standard method in such systems of improving the signal to noise ratio.

In this photoelectric method, the second slit covering the photomultiplier should have the same length and width because the optimum adjustment for this second slit is so that it just takes in the image of the first slit. The light intensity is then determined by the amount of light reaching the photo-multiplier surface, that is by the product of the brightness, slit-width and slit-length[35].

A condensing lens has been employed to throw an image of

the flame onto the slit of the spectrograph. With a lens of focal length f, the flame must be at 4f away from the slit for an image to be formed.

The flame and condensing lens must, of course, be carefully lined up on the axis of the spectrograph.

The greatest limitation of the photo-electric method is the need to keep the flame absolutely steady and constant while the spectrum is scanned through. Any flickering may produce spurious structure, any drift in mixture composition or change due to warming up of the burner may upset the relative intensities. The photoelectric method is one-dimensional, so that if the spectrum of a flame is required at different heights in the flame, it is necessary to scan through separately at each height. The general layout is shown in Figure (7.1).

Using the photographic technique, resolution of the order of a few angstroms was possible but, with the scanning unit, the need for intensity required the resolution to be much less than this. Adjustment of both the spectrograph slit and that covering the spectomultiplier was used to obtain optimum conditions, and these conditions were maintained strictly constant throughout any series of measurements. The principle errors involved in the spectral measurements, were emission from air borne impurities drawn into the shield flame, and some variations in flame temperature, caused by fluctuations in the gas flow rates to the flame. No error was attributed to possible variations in the purity of the gases obtained from the British Oxygen Company. Initially, a great deal of interference was detected from a multitude of atomic lines produced by the laboratory discharge lighting, and this was lessened by

FIG 7.1 SPECTROGRAPH

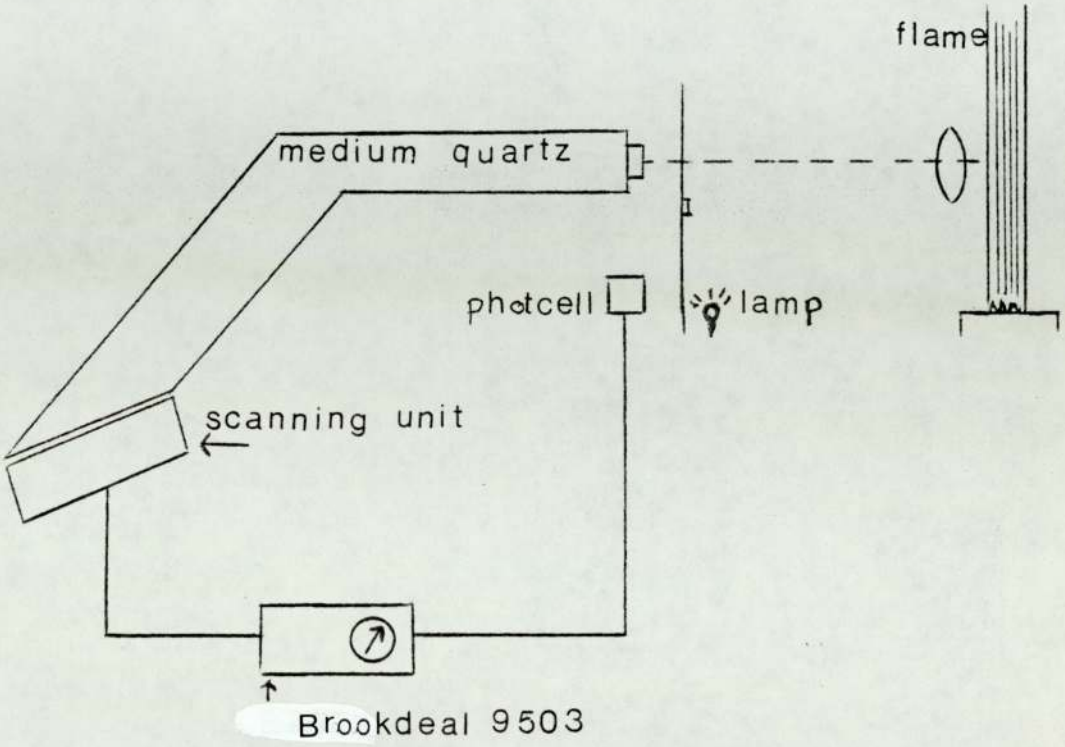

placing a charcoal covered board around the flame.

The mean error in the intensity measurements was estimated from the results to be 10% or less, a quite acceptable level for the purposes of the second law estimations.

To relate relative intensity measurements to absolute concentrations by comparison with the emission from a known amount of sodium in the flame as an internal standard, it was necessary to calibrate[123] the response of the photomultiplier over the range of wavelength involved. This was achieved by comparing the response of the spectrophotometer to that from a tungsten filament lamp at a known temperature and at various wavelengths. The temperature of the lamp was measured as before using an optical pyrometer, and the final calibration of the response was taken as the mean of the results of three calibrations, corresponding to the three different brightness temperatures of the lamp used, 2000°K, 2300°K and 2500°K. From the brightness temperatures of the lamp and the emissivity of tungsten at the pyrometer operating wavelength, the radiant temperature of the tungsten filament was found. The measured response from the spectrophotometer at each wavelength in arbitrary units was divided by the calculated intensity to give a relative scale of response factors at each wavelength. Figure (7.2) shows the calibration.

Wavelengths were indicated on the instrument by a mechanical counter coupled to the drive of the scanning unit. The calibration supplied by the manufacturers was checked against standard atomic line sources and found to be sufficiently accurate for the purposes of the investigation. Using this device, any spectral feature could be positioned to better than ± 20°, subject to the limitations of the slit

FIG 7.2 PHOTOMULTIPLIER CALIBRATION

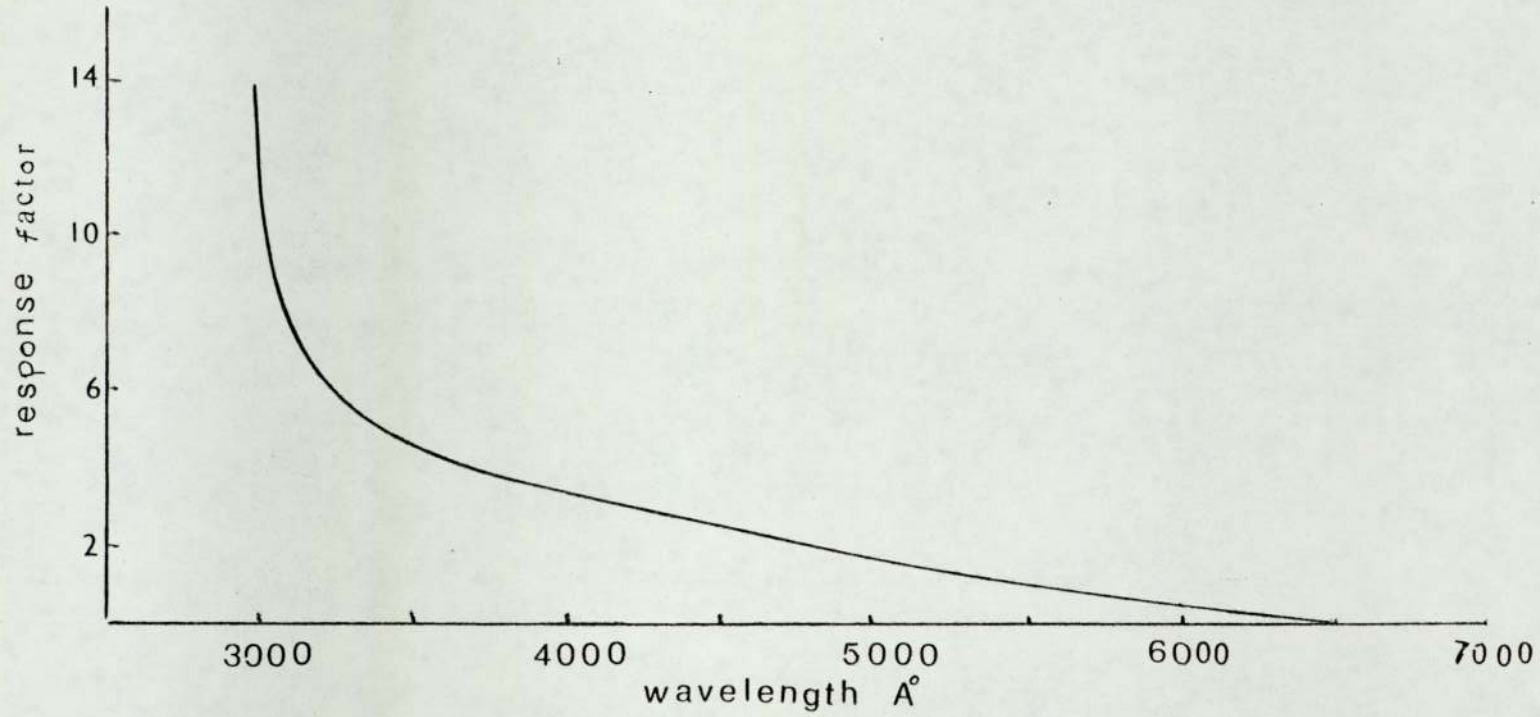

width used.

The sensitivity of emission lines depends to a large extent upon the position of the flame in relation to the optical axis of the instrument. Also, the ratio of the combustible gas to oxygen (or air) is important, partly because of the effect of the components of the partially burned flame gases, upon the equilibria between metal atoms, metal hydroxides and oxides, and other metal salts, and partly because the height of the inner cone will vary from rather short, with lean flames, to an abnormally high cone with fuel-rich flames. In general, the most suitable portion of the flame for measurement purposes commences at the upper edge of the interconal gases and extends a further 10 mm upward. However, observations made in a higher position in the flame mantle would tend to minimise emissions from elements difficult to excite.

A plot of the relative concentration of CuH against height above the burner, Figure (7.3), shows that the alkali metal does not affect the Cu line intensity in the flame. The curve is reproducible with and without alkali metal in absence of phosphorus, experiments have been made adding Na and Cs alternatively.

It has been found experimentally that the addition of phosphorus drops the alkali metal resonance line, and this drop is the same, whether the alkali metal is Na or Cs.

Measuring the Cu line intensity along the flame axes without phosphorus or with a fixed amount, no measureable change has been noticed. This indicates that the flame temperature change along the axes is not sufficient to affect the population of Cu atoms which are responsible for the line intensity.

FIG 7.3.a

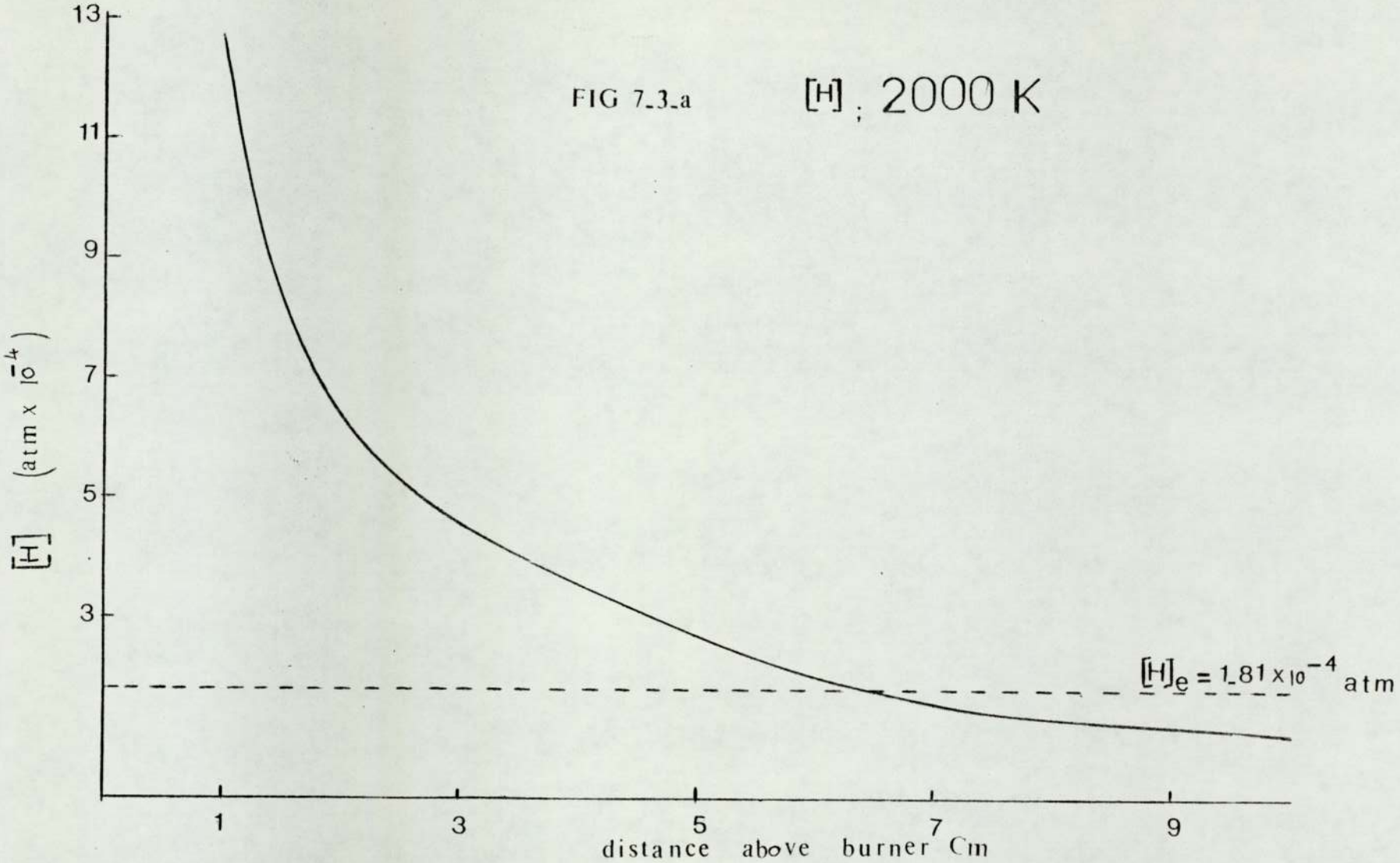
[H] ; 2000 K
[H] (atm x 10⁻⁴)
13
11
9
7
5
3
[H]e = 1.81 x 10⁻⁴ atm
1
3
5
7
9
distance above burner Cm

FIG 7.3.b [H] ; 2300 K

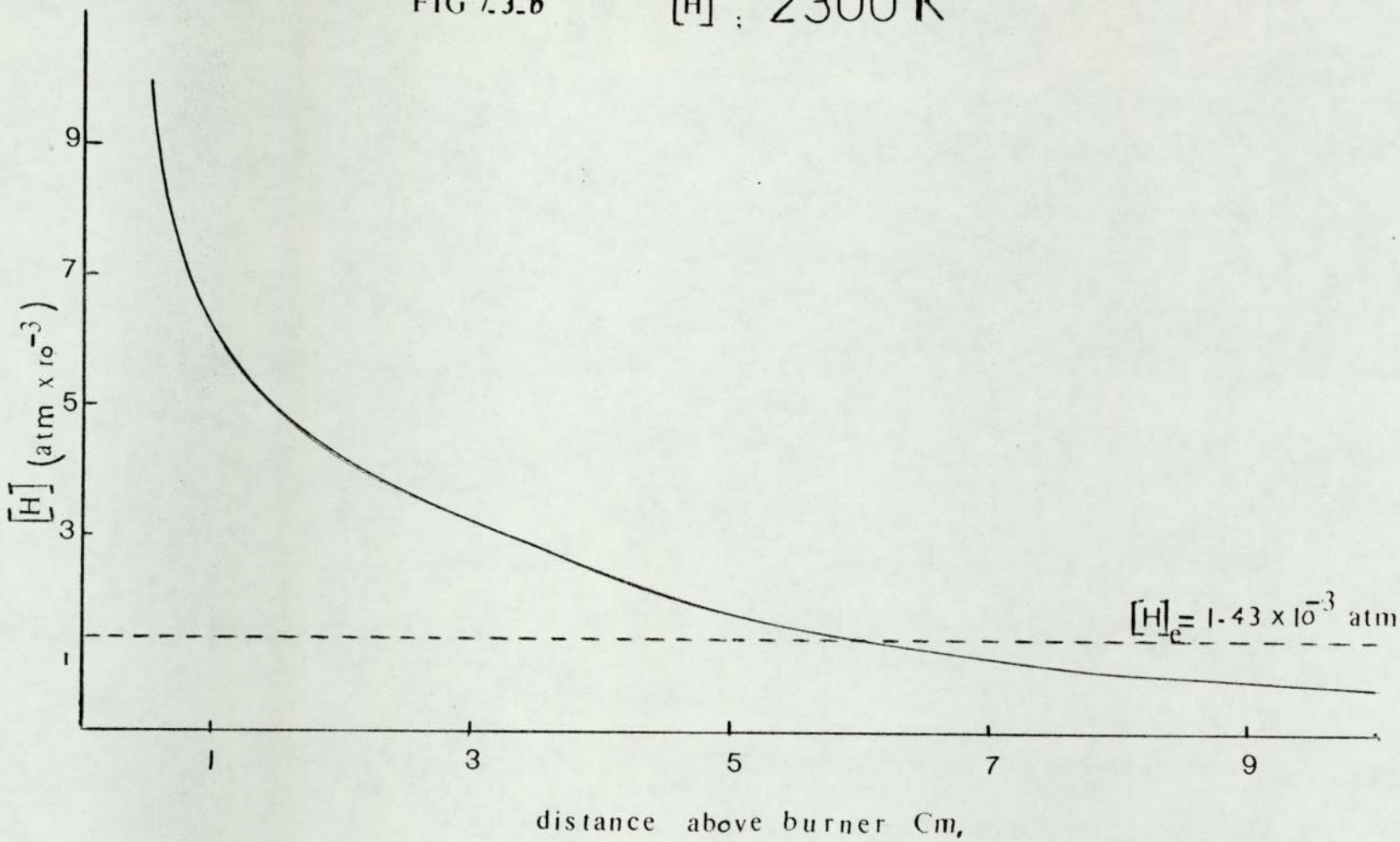

FIG 7.3.c [H] ; 2500 K

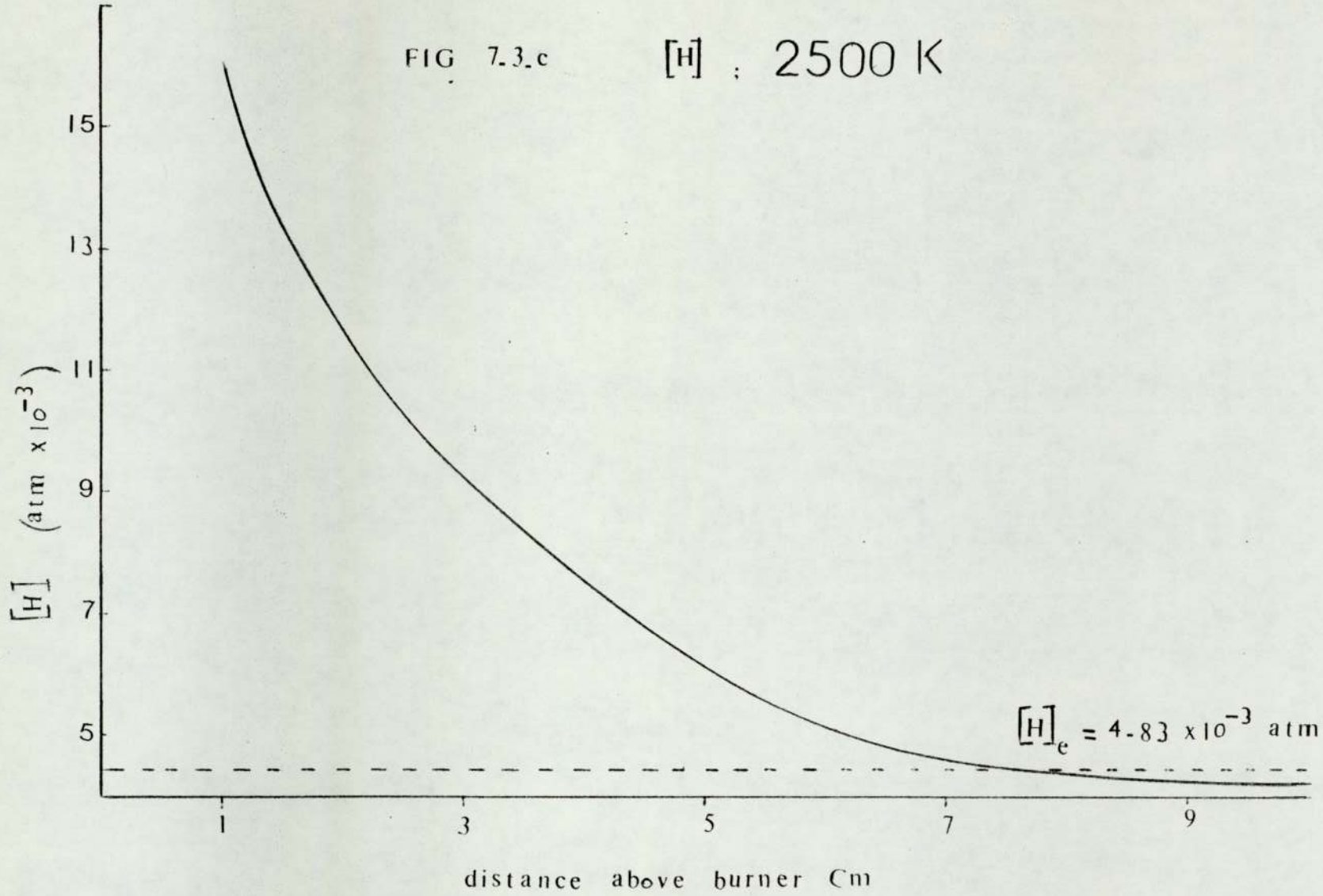

Studying the effect of temperature, Figure (7.4) shows that as the temperature increases, the relative intensity at the resonance lines of alkali metals decrease, that is as was expected, since both the flame volume and the amount of water vapour in the flame increase with increasing the flame temperature. (Tables 7.1 and 7.2).

These spectroscopic studies together with those of both electron concentrations and positive ion concentrations, will be the base of discussion and conclusions next chapter.

Table (7.1)

P.P. OF "P" x 10^{-4} atm	Relative intensite at resonance line					
	Cs			Na		
	2000°K	2300°K	2500°K	2000°K	2300°K	2500°K
2	0.29	0.27	0.26	0.2	0.19	0.185
4	0.27	0.25	0.25	0.19	0.185	0.18
6	0.25	0.24	0.23	0.185	0.18	0.175
8	0.24	0.23	0.23	0.18	0.174	0.17
10	0.23	0.22	0.21	0.175	0.17	0.168

Table (7.2)

Straight lines slopes

T/K°	Cs	Na
2000	1030	840
2300	970	770
2500	940	710

FIG 7_4

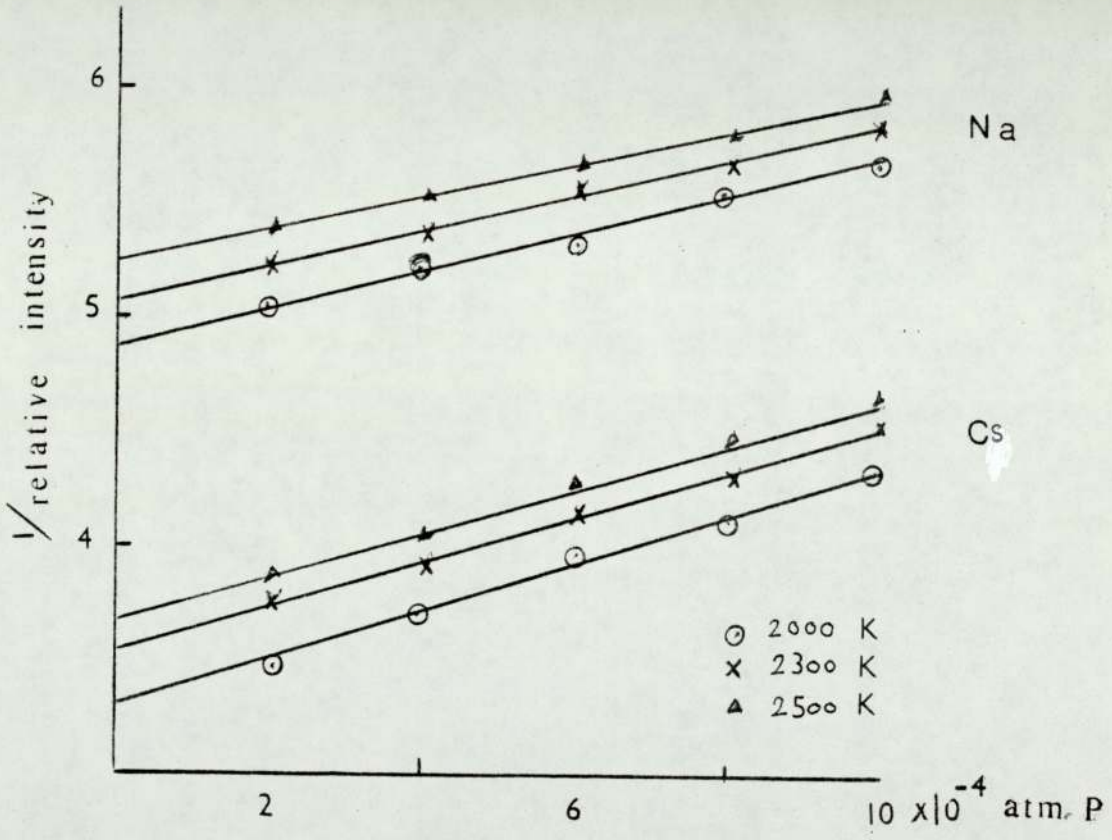

The Effect of Temperature on the Relative Intensity for Cs and Na.

8. DISCUSSION AND CONCLUSIONS

A powerful method for studying chemical phenomena, which can be applied to systems of any complexity, is that of thermodynamics.

The thermodynamic function which is perhaps of great utility in flame studies is the enthalpy, defined by:

$$H = E + PV$$

For use in flame studies, it is generally sufficient to consider only the thermodynamics of ideal gases, ideal in the sense that they obey the gas law:

$$PV = nRT$$

and that the enthalpy is a function only of temperature, so that:

$$\left(\frac{\partial H}{\partial P}\right)_T = \left(\frac{\partial H}{\partial V}\right)_T = 0$$

This restriction is valid for the relatively low pressures (1 atm or less).

On the other hand, the two broad phases of chemical kinetic studies may be considered to be, first, the determination of the mechanism by which a given reaction takes place, i.e. the fundamental steps or elementary reactions which actually occur during the overall chemical change, and second, the determination of the rate constants (and their temperature dependence) for these elementary reactions.

From the absolute values of the equilibrium constants or from the variation of their relative values with temperature, the corresponding thermal changes in the reactions may be deduced. For formed compounds in the flame, since the amounts of the free radicals in the flame gases which enter into the

steady state equations are often very different from their final equilibrium amounts, the steady state is not a full equilibrium one.

The chosen flames throughout the work have been extensively characterised as to their radical and bulk gas composition. The pertinent data (i.e. that needed for the calculation of various equilibrium constants) are given in Table (8.1).

Table (8.1)

Properties of Chosen Flame Gases

Composition $H_2:O_2:N_2$ (Unburnt volumes)	2.9/1/5.18	2.9/1/3.2	3/1/2.25
Temp (^oK)	2000	2300	2500
$[H_2O]$ (atm)	2.47×10^{-1}	3.22×10^{-1}	3.69×10^{-1}
$[H_2]$ (atm)	1.12×10^{-1}	1.49×10^{-1}	1.85×10^{-1}
$[H]_e$ (atm)	1.81×10^{-1}	1.43×10^{-3}	4.63×10^{-3}
$[OH]_e$ (atm)	1.21×10^{-4}	1.31×10^{-3}	4.38×10^{-3}
γ (1 cm)	7	4.19	3.4
γ (2 cm)	3.3	2.8	2.48
γ (3 cm)	2.5	2.3	2

Using equations (3.18), (3.19), (3.20) and (3.21) we can derive important relations to get some needed parameters:

$$E^2 = \frac{(1 + X\,[B_o])\,(1 + \phi)}{(1 + X\,[B_o]\,\gamma^{-2})\,(1 + \phi + \xi)(1 + \eta)} \qquad (3.18)$$

$$P^2 = \frac{(1 + X\,[B_o])\,(1 + \phi)\,(1 + \eta)}{(1 + X\,[B_o]\,\gamma^{-2})\,(1 + \phi + \xi)} \qquad (3.19)$$

$$S_e = \left[\frac{dE^2}{d\,[B_o]}\right]_{[B_o] = 0} = \frac{R_2(\gamma^2-1) - \gamma^2(1+\phi)(1 + K\eta/K_\xi)}{K_\eta\gamma^2(1 + \theta)} \qquad (3.20)$$

$$S_p = \left[\frac{dP^2}{d[B_o]}\right]_{[B_o] = 0} = \frac{R_2(\gamma^2-1) + \gamma^2(1+\theta)(1-K\eta/K_\xi)}{K\eta\gamma^2(1 + \theta)} \qquad (3.21)$$

Division of equation (3.19) by equation (3.18) gives:

$$P^2/E^2 = (1 + \eta)^2 \qquad (8.1)$$

Addition of equations (3.20) and (3.21) gives:

$$S_e + S_p = \frac{2R_2(\gamma^2 - 1)}{K_\eta\gamma^2\,(1+\theta)} - \frac{2}{K_\xi}, \qquad (8.2)$$

and subtraction of equation (3.20) from equation (3.21):

$$S_p - S_e = \frac{2}{K\eta}, \qquad (8.3)$$

Therefore, we can get K_η from both equation (8.1) and equation (8.3), and we can get K_ξ from equation (8.2) by plotting $(S_p + S_e)\,\frac{\gamma^2}{\gamma^2-1}$ against $\frac{\gamma^2}{\gamma^2-1}$ as shown in figures (8.2 - 8.7).

Table (8.2)

Temp. ^{o}K	Metal	Average K_{η}, the $(S_p - S_e)$ method	Average K_{η}, the (P^2/E^2) method
2000	Cs	3.2×10^{-4}	3.42×10^{-4}
	Rb	3.6×10^{-4}	2.96×10^{-4}
2300	Cs	3.5×10^{-3}	3.2×10^{-3}
	Rb	3.73×10^{-3}	3.03×10^{-3}
	K	3.25×10^{-3}	3.52×10^{-3}
	Na	3.3×10^{-3}	3.48×10^{-3}
2500	Cs	1.3×10^{-2}	1.31×10^{-3}
	Rb	1.54×10^{-2}	7.44×10^{-3}
	K	1.3×10^{-2}	3.76×10^{-3}
	Na	1.3×10^{-2}	1.12×10^{-2}

Table (8.3)

T/K^{o}	K_{ξ}		$\log_{10} K_{\xi}$	
	Cs	Rb	Cs	Rb
2000	2.79×10^{-4}	1.7×10^{-4}	- 3.55	- 3.7
2300	6.1×10^{-3}	3.8×10^{-3}	- 2.2	- 2.4
2500	4.9×10^{-3}	2.9×10^{-3}	- 2.3	- 2.5

Table (8.4)

T/K^{o}	Average K_{η}	$\log_{10} K_{\eta}$
2000	3.295×10^{-4}	- 3.48
2300	3.38×10^{-3}	- 2.47
2500	1.186×10^{-2}	- 1.93

K_η (Table 8.2) and K_ξ (Table 8.3) have been obtained at different heights above the burner at different temperatures (2000/2300/2500 °K), K_η has been obtained by both the $(S_p - S_e)$ method and the (P^2/E^2) method with quite good agreement between them as shown in Table (8.2).

The results show, within the experimental error, that K_η is independent of both the alkali metal and height above the burner.

Since K_η is the equilibrium constant of $PO_2 + e \longrightarrow PO_2^-$ we may use Saha's equation in the form:

$$\log K = -\frac{5050V}{T} + 5/2 \log T - 5.9,$$

from this equation V has a constant value, 2.3, 2.26, and 2.24 respectively at 2000°K/2300°K, and 2500°K respectively, then we can conclude that it is simple equilibrium.

Plotting $\log K_\eta$ as average between the $(S_p - S_e)$ method, and the P^2/E^2 method (Table 8.4) against $\frac{1}{T}$ as shown in Figure (8.1), the electron affinity of PO_2^- has been calculated as 3.1 eV.

The constant in Saha's equation for ionisation equilibrium in a monatomic gas (which is a function of fundamental constants and of the statistical weights) is 6.4.

For PO_2 and PO_2^-, neither the statistical weight nor the electronic structure is known, and PO_2 is not monatomic. Then the rotational and vibrational entropies have to be taken into account. It could be guessed that PO_2^- will have a smaller angle and higher frequency of vibration than PO_2, so it will have a smaller moment of inertia. This will mean that both entropies will act to make the constant less negative and might produce the factor of 40 needed to

FIG 8.1

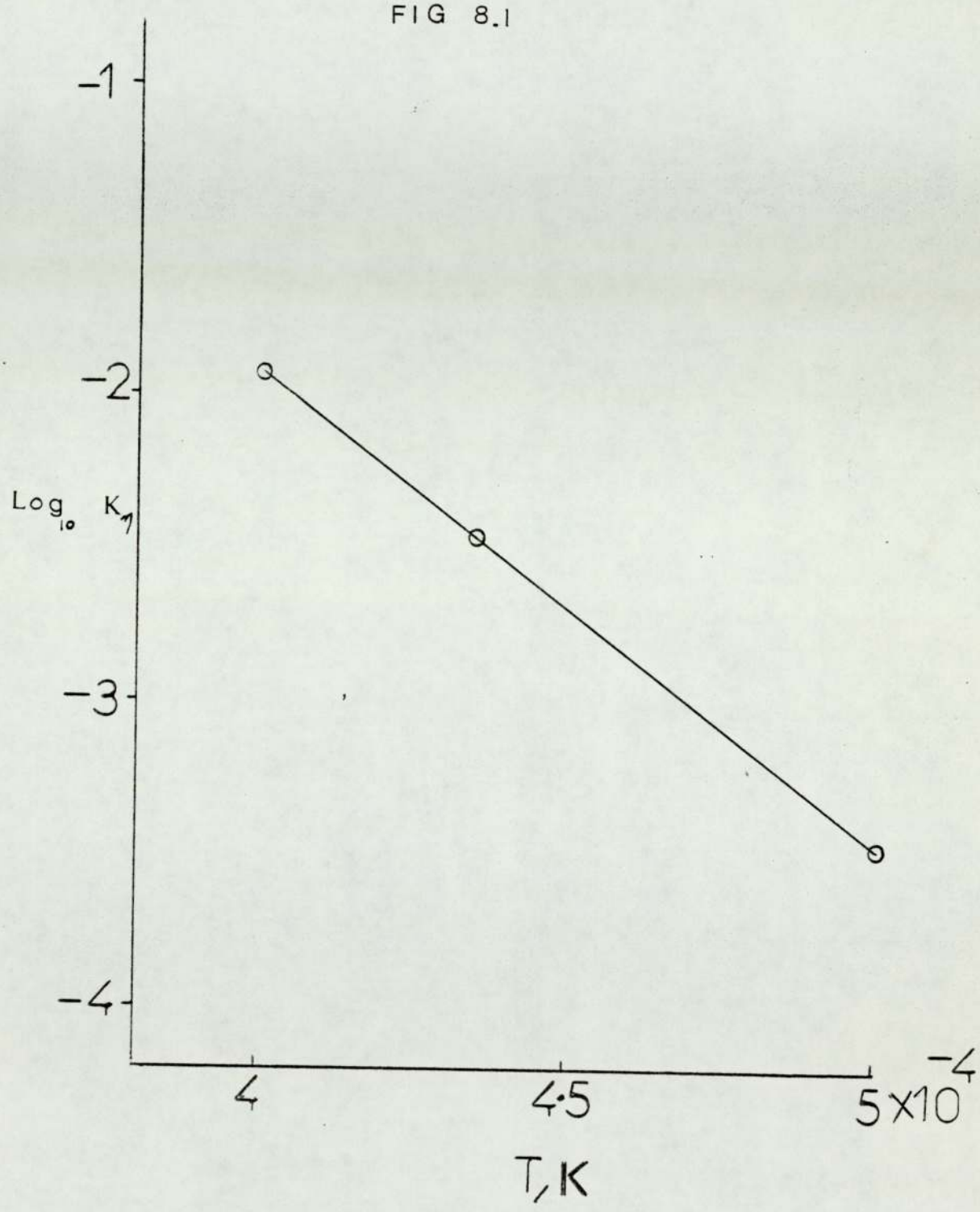

Graphical estimation of the Electron Affinity of PO_2^-

account for the discrepancy (o.7 eV) between 3.1 eV obtained from the K_η plot and the corresponding value obtained from Saha's equation.

Similarly, plotting log K_ξ against $\frac{1}{T}$, it was found that, as can be seen from Figure (8.8), a deviation from linearity does occur when flames of final temperature greater than about 2300K are used. Part of this deviation is caused by formation of A^+ ions and part result from formation of AOH molecules.

The sharp curvature or scatter of the graphs of Figure (8.8) indicates that no useful information can be obtained from this approach.

If AB = A + B is a true equilibrium, then the enthalpy required to break the A-B bond is 90 Kcal in the case of Cs and as 109 Kcal in the case of Rb. These values (Cs<Rb) reverse the expected order and reinforce the conclusion that the data will not bear analysing to this extent.

$K_\xi(1+\theta)$ may, however, be obtained directly from the flame photometric measurements as follows:

The total alkali metal added into the flame could be found in the form:

$$A_o = A + A^* + A^+ + AB + AOH$$

Since $A^* = A_e^{-h\nu/kT}$, and neglecting A^* and A^+ because of their relative small values, therefore:

$$A_o = A\left(1 + \frac{AB}{A} + \frac{AOH}{A}\right)$$

$$\frac{A_o}{A^*} \; e^{h\nu/kT} = 1 + \frac{AB}{A} + \frac{AOH}{A}$$

hence:

FIG 8.2

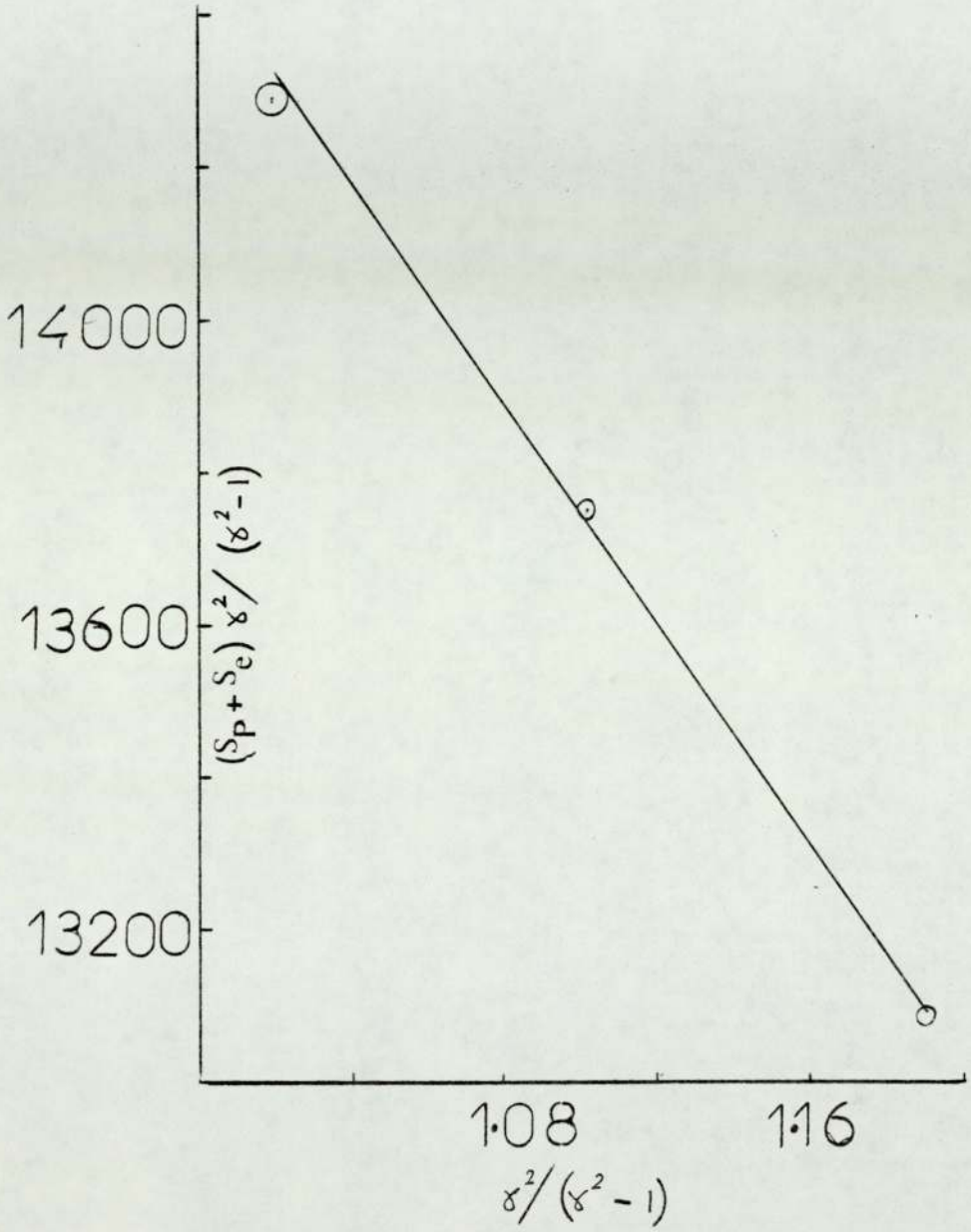

Determination of K_ξ for Cs at 2000 ^{o}K

FIG 8·3

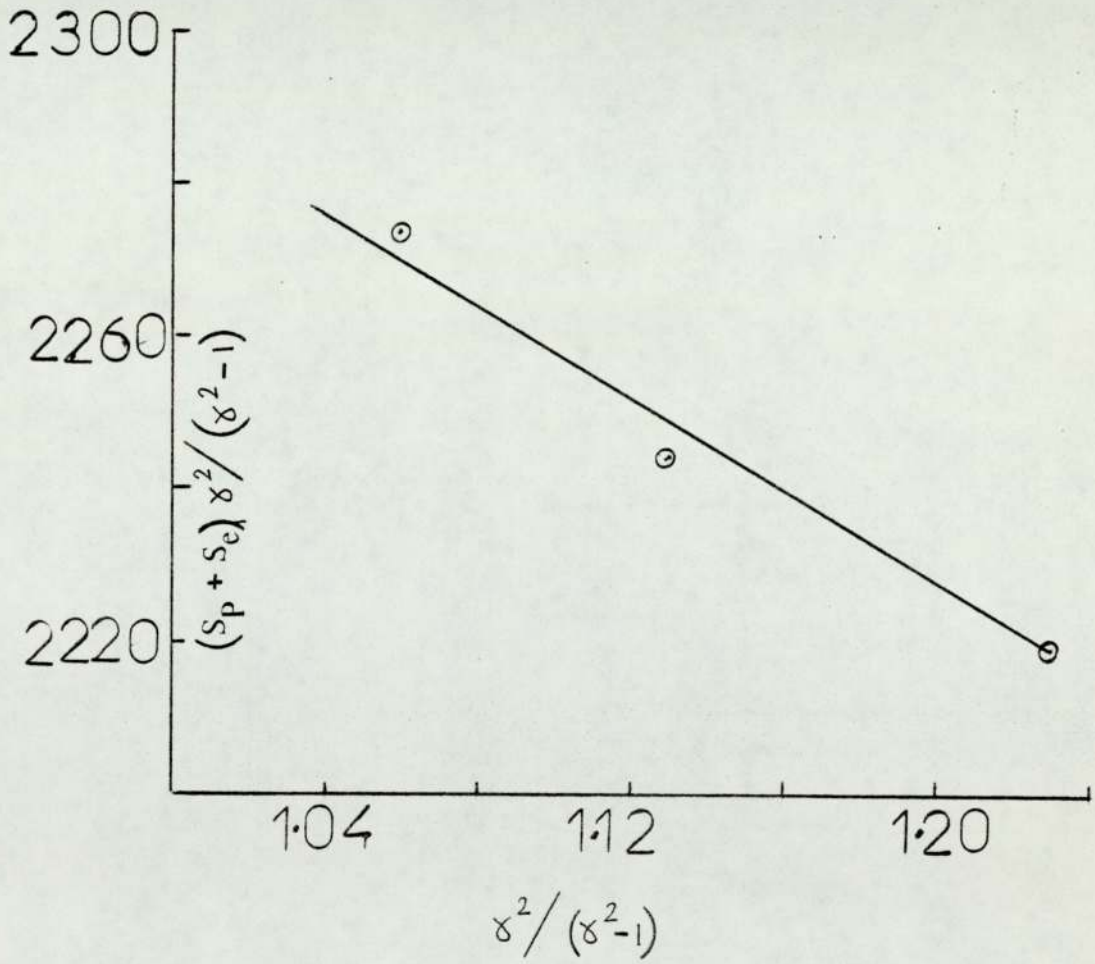

Determination of K_ξ for Cs at 2300 ^{o}K

FIG 8-4

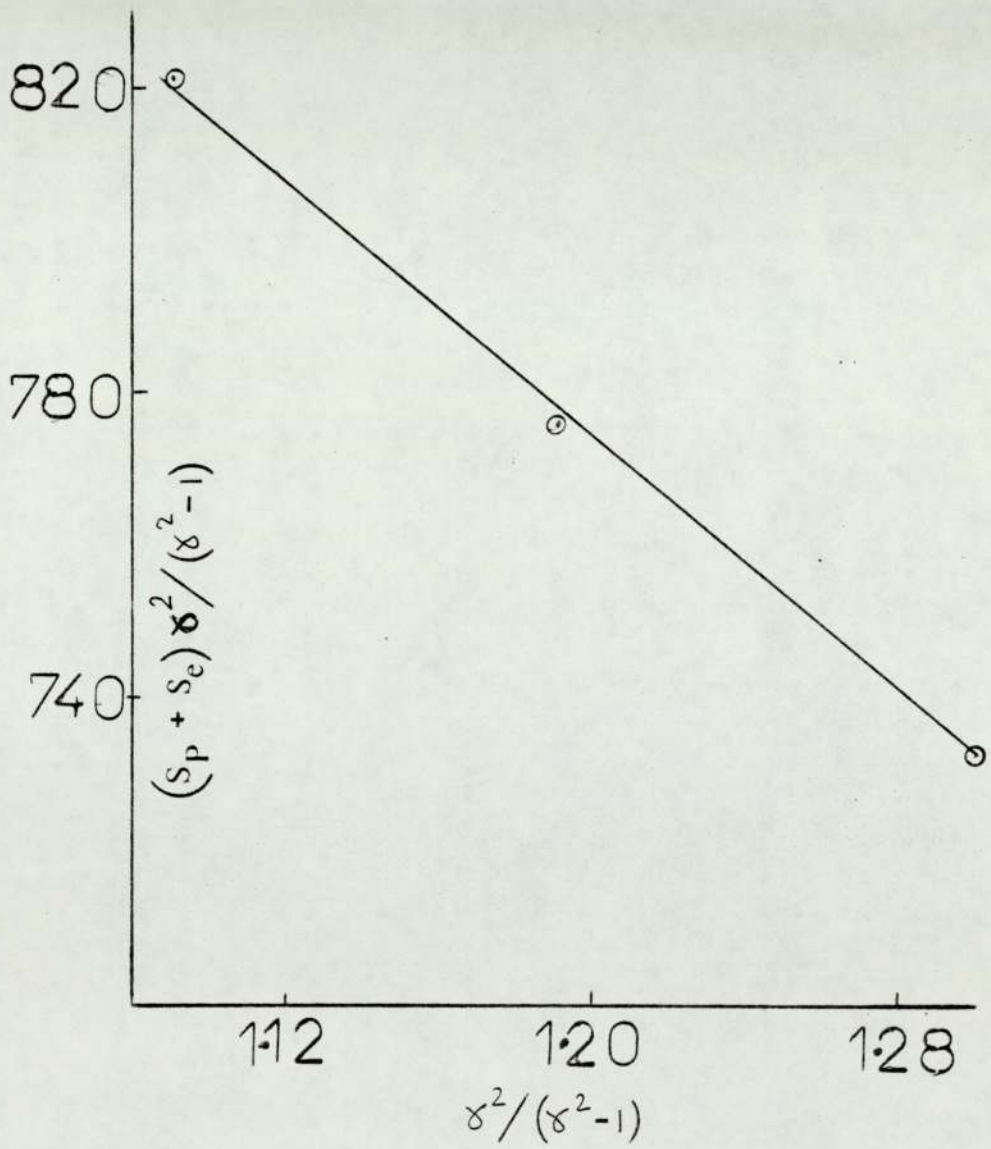

Determination of K_ξ for Cs at 2500 $^{\circ}$K

FIG 8-5

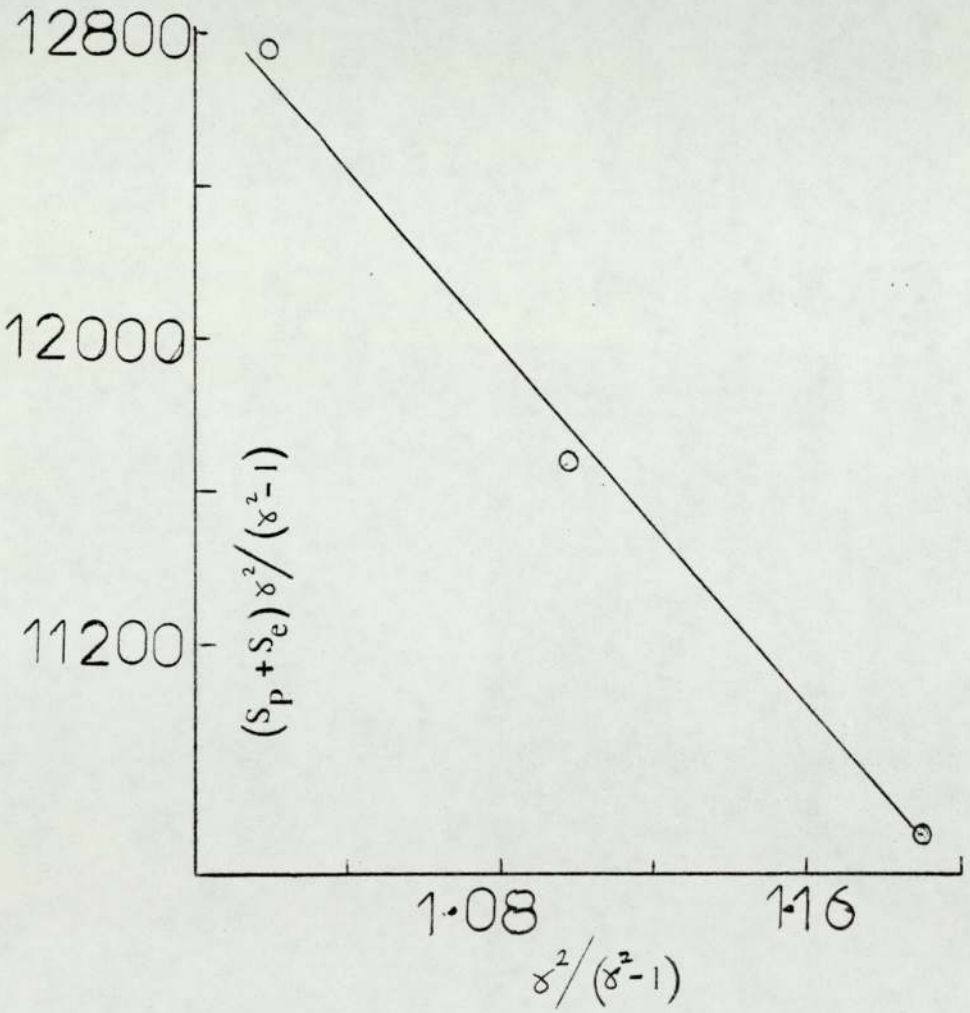

Determination of K_ξ for Rb at 2000 ^{o}K

FIG 8·6

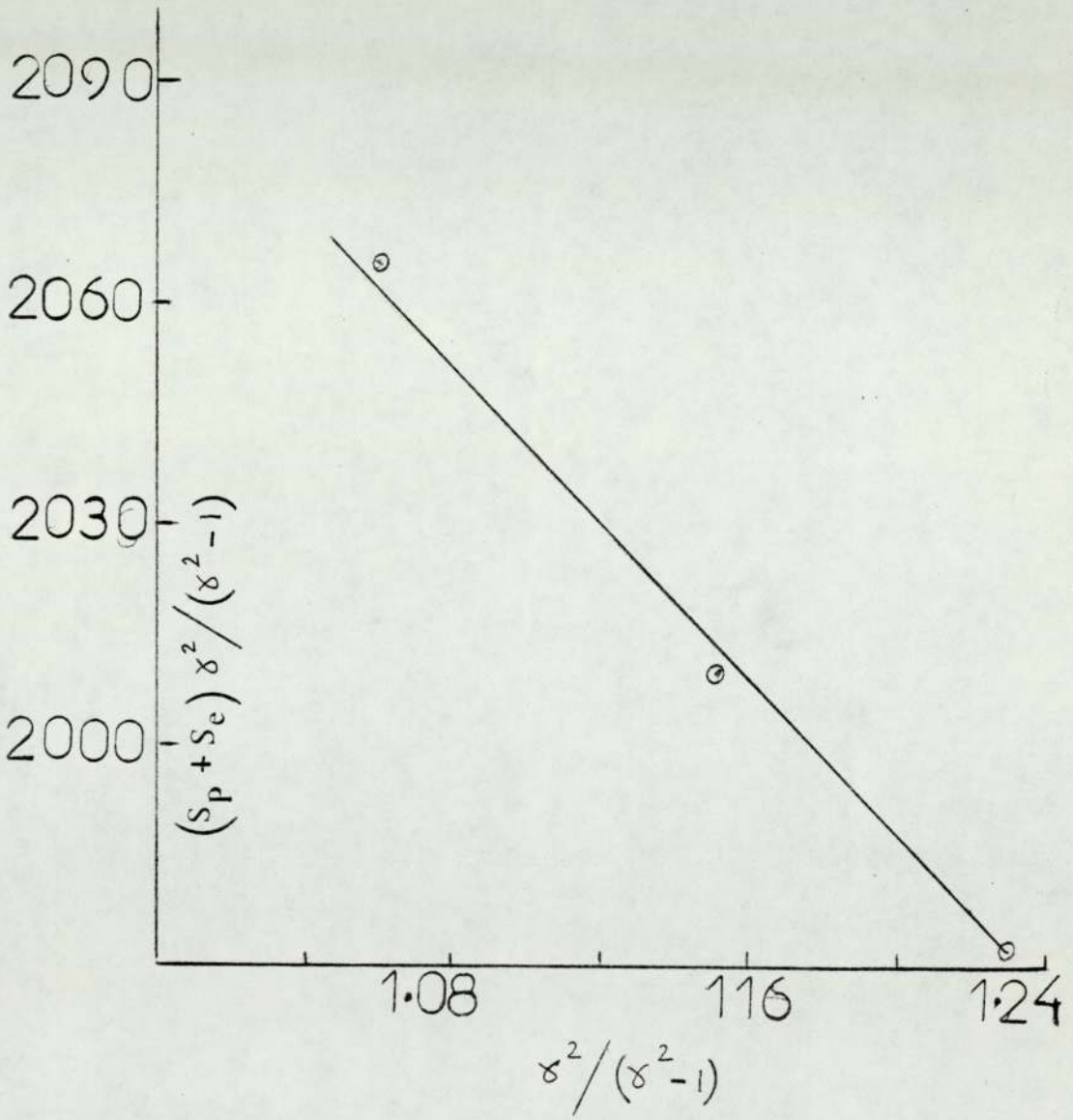

Determination of K_ξ for Rb at 2300 $^{\circ}$K

FIG 8-7

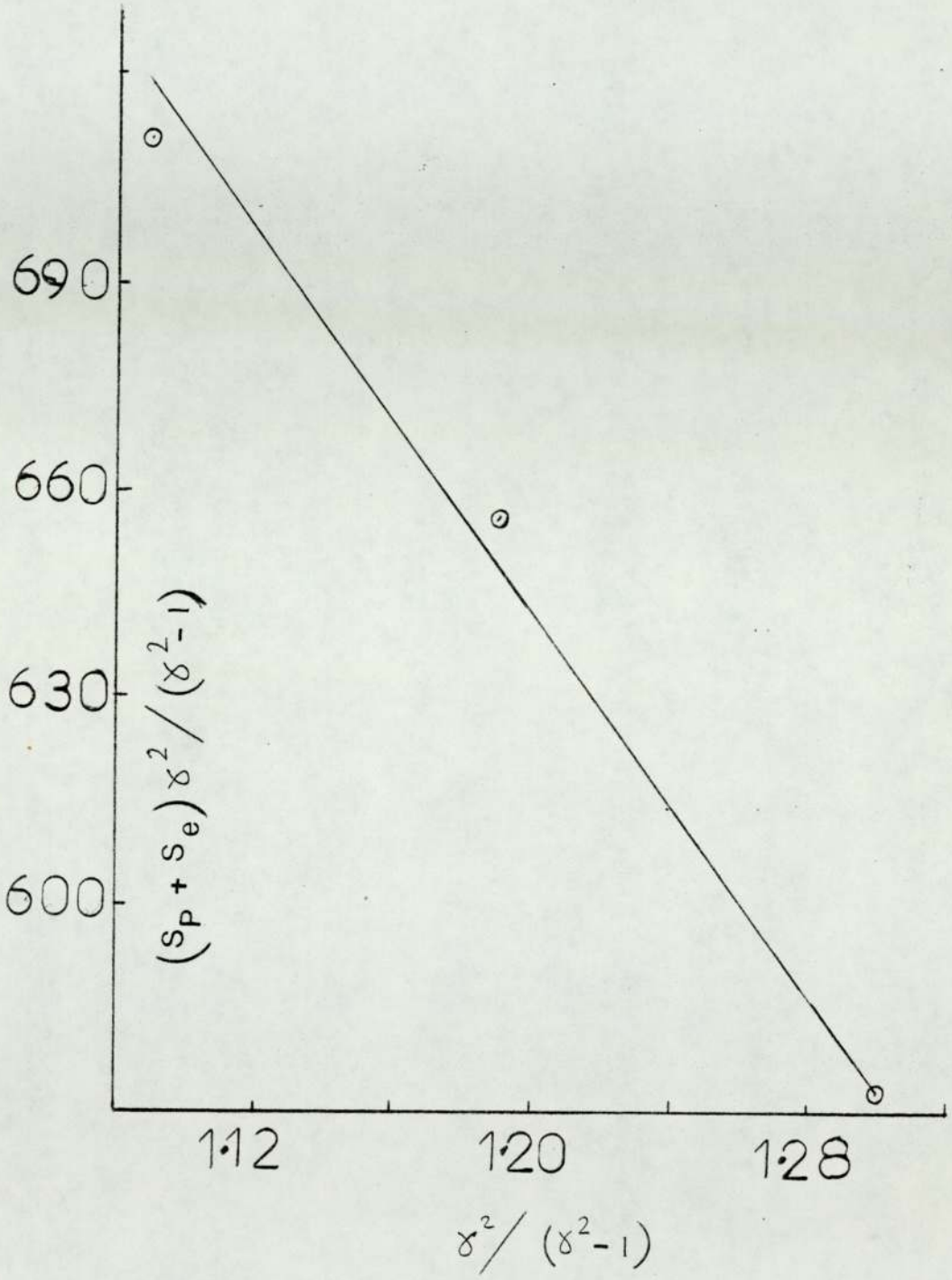

Determination of K_ξ for Rb at 2500 °K

FIG 8·8

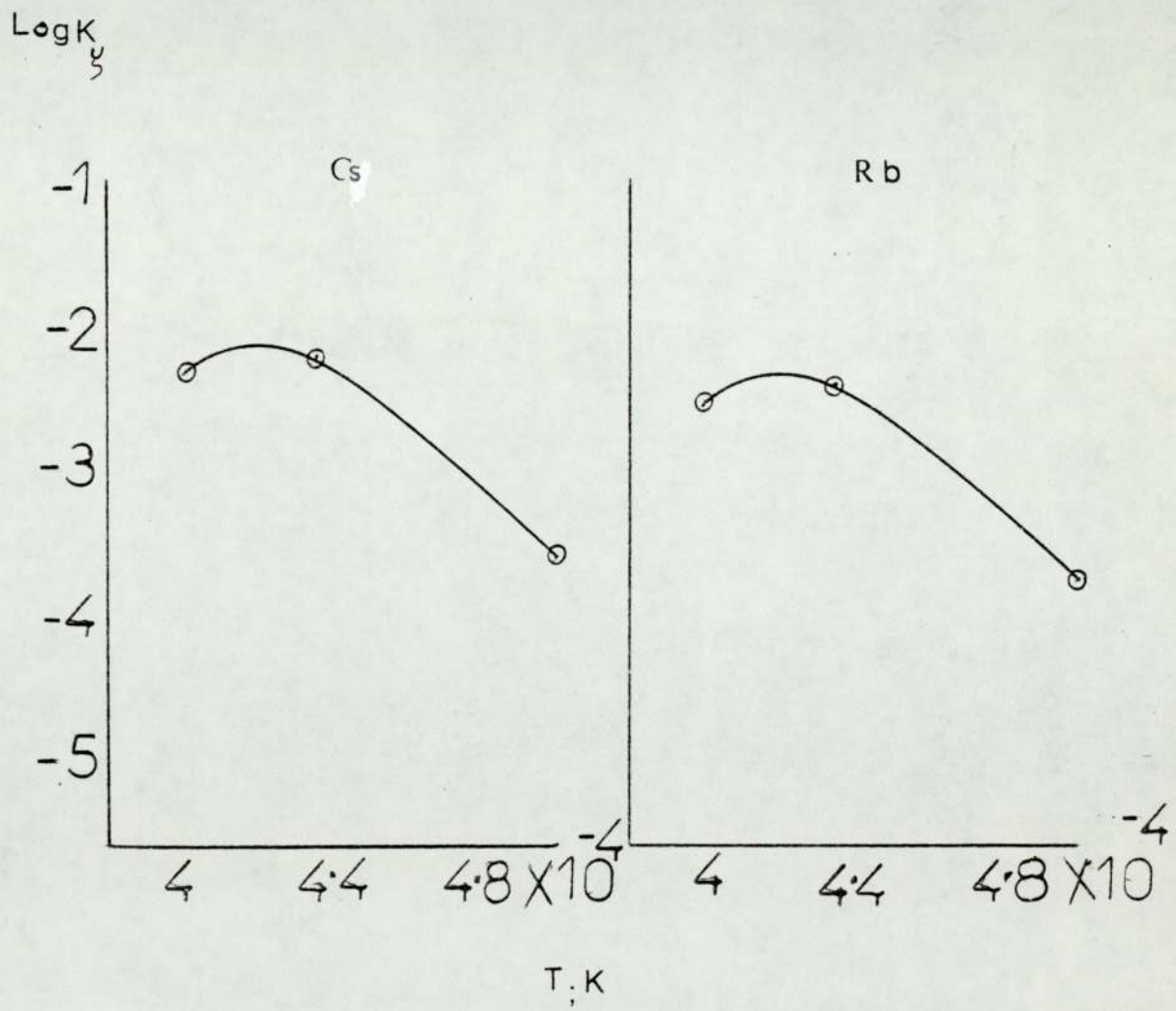

Graphical determination of the bond energy of AB

$$\frac{A_o}{I} \alpha\ 1 + \xi + \phi$$

The plot of $\frac{1}{T}$ against $[B]_o$ (Figure 7.4) shows a straight line, the slope of which (S*) is a function of $(1 + \xi + \phi)$.

Since $\xi = \frac{AB}{B} = \frac{B}{k_\xi}$

and $B_o = B + HB$

$= B\ (1+\theta)$

and since HPO_2 may only be a small fraction of B_o, we can generalise $(1+\theta)$ to mean $\frac{[Y]}{B}$,

Therefore $B = \frac{[Y]}{1+\theta} = \xi\ K_\xi$

$\xi = [Y]/K_\xi\ (1+\theta)$

$K_\xi(1+\theta) = \xi/[Y]$

the value of $(1+\theta)$, which here has the meaning (total phosphorus added)/(phosphorus present as PO_2) is close to 1 since Calcote et al[25] have shown PO_2 is the dominant species, therefore:

$1/K_\xi = S^*\ (1+\phi)$.

K_ξ could be obtained as shown in Table (8.5), taking $\phi_{C_S} = 2.1$ and $\phi_{Na} = 0.08$ as tabulated[73], and calculating ϕ at the different temperature through the relation:

$$\phi_T = \frac{OH_T}{OH_o} \cdot \frac{K_o}{K_T} \cdot \phi_o$$

where OH_o, K_o and ϕ_o are the reference parameters.

Table (8.5)

Metal	Temp, ^{o}K	K_{ξ}	$\log_{10}K_{\xi}$
Cs	2000	3.98×10^{-4}	- 3.4
	2300	7.9×10^{-4}	- 3.1
	2500	1.4×10^{-3}	- 2.85
Na	2000	1.1×10^{-3}	- 2.96
	2300	1.6×10^{-3}	- 2.8
	2500	1.9×10^{-3}	- 2.7

These results differ from those obtained in more complex ionisation studies and being more direct are more reliable. They are in general agreement as to order of magnitude.

The relative values of K_{ξ} indicate that A is less strongly bound to B in the case of Na than it is in the case of Cs.

In the case of Na, the temperature dependence is less than that in the case of Cs. This means that the enthalpy required to break the A-B bond in the case of Na is less than in the case of Cs.

To interpret the results in terms of a mechanism, the essential point is that whereas alkali atoms A are ionised by collisional processes with third bodies X in the absence of phosphorus:

$$A + X \rightleftharpoons A^+ + e^- + X, \qquad (8.4)$$

the presence of phosphorus (B) allows the following possible reactions to be catalysed:

$$A \longrightarrow A^+ + e^-$$
$$B+A \longrightarrow B^- + A^+$$
$$BA \longrightarrow B + A$$
$$B+e \longrightarrow B^-$$
$$B^-+H \longrightarrow HB + e^-$$
$$HB+H \longrightarrow B + H_2$$

These reactions would tend to produce a steady state given by their resultant (algebraic sum).

$$A + BA + 2H \longrightarrow 2A^+ + B^- + e + H_2 \qquad (8.5)$$

In hydrogen-rich flames, since $[H]$ will be well above its equilibrium value $[H]_e$, while $[H_2]$ will not be far from equilibrium concentration (being a bulk constituent) the balance (8.4) will give a higher steady state $[e^-]$ than the thermal equilibrium (8.4). The mechanism is not competitive as a direct reaction with (8.4) being too slow[41].

The addition of phosphorus must catalyse the production of electrons as well as removing them, and at sufficient low temperatures, or short times, the speed of the removal falls below the speed of the production. This appears to be a function of the alkali metal.

The positive ion concentration measurements show that

the removal of the positive ions may occur (by three body collisions or recombination of positive and negative ions) to form a stable complex for at least 40 μs.

As was the case for each of the analogous additives examined previously, such as halogens[41], the introduction of a P- containing compound to flames containing electrons results in the formation of negative ions and a corresponding decrease in electron density. Therefore, the substances present in the interconal gases during an experiment may be grouped into four classes[9]

(i) Molecules:

The bulk of the flame gases will consists of the molecules H_2, N_2 and H_2O, but some other important molecules are the alkali hydroxides AOH, the salts AB, and the compounds responsible for the flame gas parameter θ, which will usually be the hydrides HB.

(ii) Atoms and radicals:

In the burnt gas of $H_2/O_2/N_2$ flames considerable excess of atomic hydrogen (and hydroxyl radicals) persist well downstream of the reaction zone, the approach to flame gas equilibrium being limited by the relatively slow 3-body recombinations:

$$H + H + X \longrightarrow H_2 + X$$
$$H + OH + X \longrightarrow H_2O + X$$

To those arising from the flame gases, such as H, OH, and O, must be added the alkali metal atoms A, and the atoms or radicals of the electron acceptor B.

(iii) Positive ions:

The only such ion of importance is the alkali metal ion A^+.

(iv) Negative ions:

The ones to be considered are the hydroxide ion OH^-, the ion of the electron acceptor B^-, and the electron.

In general, electron acceptors reduce the number of free electrons produced by ionisation in a flame by the production of both salt and negative ions, and the magnitude of the reduction may usually be estimated accurately by considering the various chemical equilibria, using the thermodynamic equilibrium constants for the reactions involved.

It is worth noting that all the experiments to measure the concentration of positive ions with different alkali metals and at different temperatures confirm the similarity between sulfur and phosphorus in a way that both of them form compounds in the flame either extremely rapidly or extremely slowly.

The experimental evidence on the effect of phosphorus on the ionisation arising from a varity of different alkali metals has now been presented.

From the results obtained, it has been shown that phosphorus raises the ionisation while depressing the alkali emission. To discuss these observations let us consider a neutral alkali metal atom, A, that can be split into a positive ion, A^+, and a free electron, e. The ionisation and reverse recombination process are formally described by:

$$A \rightleftharpoons A^+ + e$$

At a given place in a stationary flame, the concentrations of these species will have stationary values which are [A], $[A^+]$ and [e], and are expressed in cm^{-3} or partial pressures. The degree of ionisation, δ_i, is now defined by

$$\delta_i = [A^+]/([A^+] + [A])$$

William J. Miller[25] has mentioned that recent work on the composition of fuel-rich flames seeded with small amounts of phosphorus compounds has shown that the predominant P-containing neutral species at equilibrium are PO, HPO_2 and PO_2. The presence of HPO_2 allows the ion production to be analysed in terms of a dissociative attachment equilibrium analogous to those established in the case of many other electrophiles, viz. attachment by an acid:

$$e + HPO_2 = PO_2^- + H \qquad (8.6)$$

The electron affinity of PO_2^- ($\simeq$ 3.1 eV) is sufficiently high to produce these ions in significant amounts. In the absence of strong electric fields we have generally that the local concentration of the free electrons (plus negative ions) equals that of the positive ions, because of charge balance.

The occurrence of these predominant PO_2^- ions in the flame reduces the value of [e] and thus enhances δ_i.

The stimulating influence of phosphorus on the degree of metal ionisation, owing to the removal of free electrons by PO_2^- formation, explains the aggravation of the disturbing ionisation effects when phosphorus increases in the flame. The concentration of PO_2^- ions in the flame gases depends on the concentration of free H radicals through the reaction (8.6).

From equation (8.6), the ratio $[PO_2^-]/[e^-]$ must vary proportionally to $[H]^{-1}$ at a given flame temperature and phosphorus supply.

The effect of phosphorus on electrons showed that the maxima, occurring at a lower level, and towards lower amounts of phosphorus with increasing distance from the burner

(lower γ), in general accord with equation (3.22).

To study the relation between E^2_{max} and γ, the equation (3.22) is expressed in the form:

$$E^2_{max} = \left(\frac{R_2}{1+\theta}\right)\left(1 - \frac{1}{\gamma^2}\right)\left(\frac{1}{(1+X[B_m]\bar{\gamma}^2)^2}\right)$$

$$\left(\frac{1}{(1+K_\eta/K_\xi^- + 2[B_m]/K_\eta K_\xi^-)}\right) \qquad (8.7)$$

In the 4th bracket, the terms could be considered as slowly varying functions, since the change of E^2_{max} depends more rapidly on γ^2 than it does on γ, and the terms within the bracket are less than unity.

For the 3rd bracket, there are two possibilities:

Case (1): $XB\gamma^{-2} << 1$

therefore, $E^2_{max} = A(1-\frac{1}{\gamma^2})$

hence $dE^2/d\gamma^2 = A^-/\gamma^4$

Case (2): $XB_\gamma^{-2} >> 1$

therefore, $E^2_{max} = C(\gamma^2 - 1)$

where $C = \frac{R_2}{XB_{max}(1+\theta)}\left(\frac{1}{(1+K_\eta/K_\xi^- + 2[B_m]/K_\eta K_\xi^-)}\right)$

Plots of E^2_{max} against γ^2 and against γ^{-2} show that most of the cases fit with case (1). The quantitative results for the example of Cs at 2000K show that when $\bar{\gamma}^2 = 0$, $\frac{R_2}{1+\theta} = 1.335$ as shown in Figure (8.9), according to equation (8.7).

Writing $X = R_2/K_\eta(1+\theta)$, R_2 has been found from equation (3.22) (considering $K_\xi \simeq K_\xi^-$) as 1.35, from which θ has been obtained as 0.015, which justifies the previous

FIG 8·9

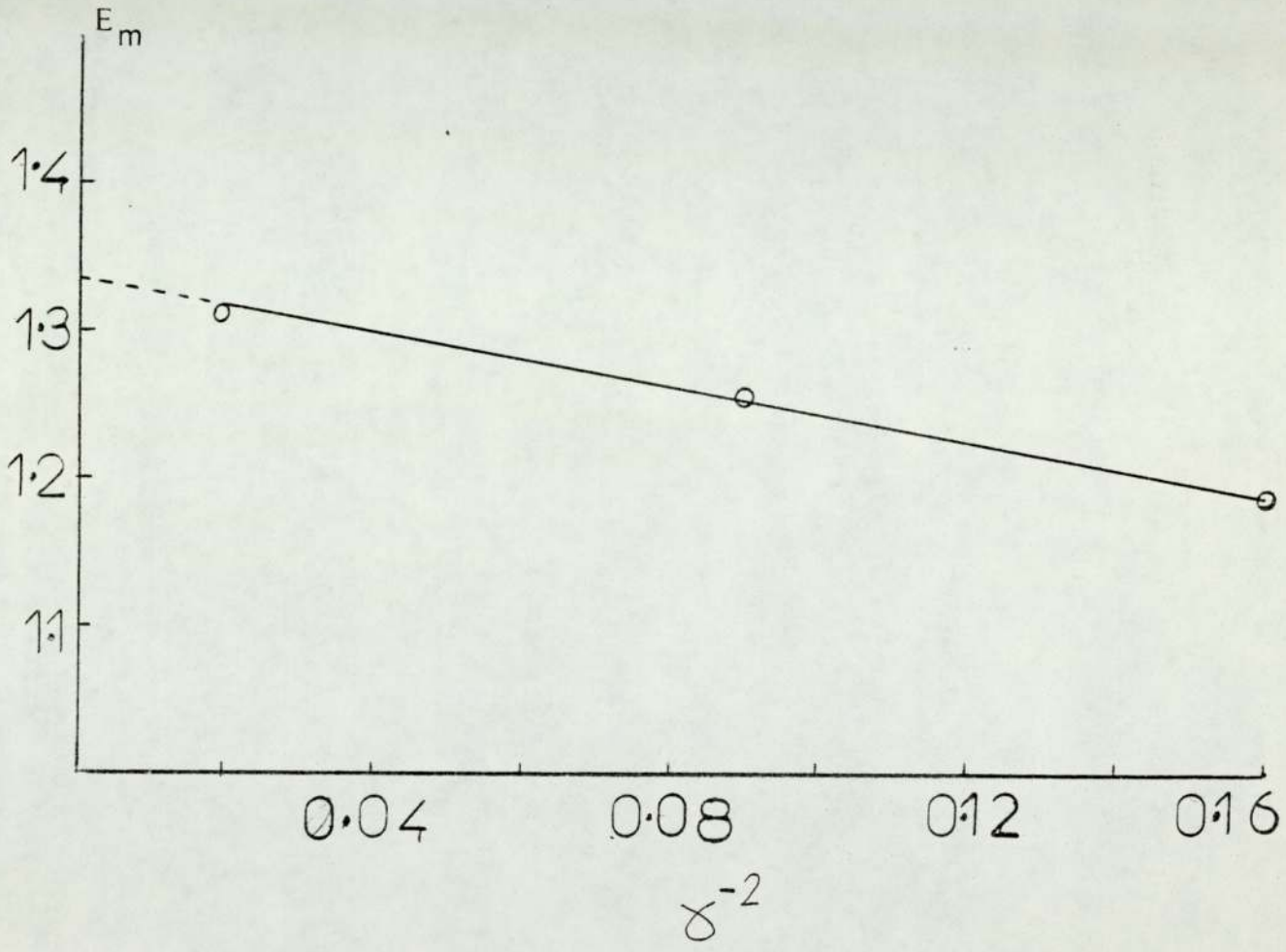

The dependence of E_{max} on γ^{-2} in the flame

assumption that $1+\theta \sim 1$. θ has also obtained for Rb at 2300^{o}K and K at 2300 ^{o}R to be 0.05 and 0.07 respectively.

It is obvious that there is an error for every individual point because of taking so many measurements and calculations with circular uncertainties. But using two different ways for obtaining both K_{η} and K_{ξ}, and finding the values of K_{η} are the same, and the values of K_{ξ} are in the same order of magnitude, indicating the applicability of the theory[4] which has been used during the work.

REFERENCES

The following special abbreviations have been used for some references:

C. & F.	Combusion and Flame
J.C.P.	J. Chem. Phys.
P.R.S.	Proc. Roy. Soc. Lond.A.
T.F.S.	Trans. Faraday Soc.
3rd Symposium to 17th Symposium	These refer to the biennial series of symposia (International) on Combustion. The 3rd, 4th and 8th symposia were published by Williams, Wilkins and Co., Baltimore; the 5th and 6th by Reinhold, New York; the 7th by Butterworths, London; the 9th by Academic Press, New York; and the 10th and subsequent ones by The Combustion Institute, Pittsburgh.

1. International Critical Tables, Vol. 5, Magraw-Hill Inc., (1933).
2. Lawton, J., and Weinberg, F.J., Electrical Aspects of Combustion, Clarendon Press., Oxford (1969).
3. Smith, F.T. and Gatz, C.R., Progress in Astronautics and Aeronautics, Vol. 12, K.E. Shuler Ed. Academic Press (1963).
4. Page, F.M., Physical Chemistry of Fast Reactions, Vo. 1, Chapter 3, Plenum Press, London and New York (1973).
5. Rolla, L. and Piccardi, G., Atti. Accad. Lincei, V.I, 2 29 (1925).
6. Rolla, L. and Piccardi, G., Atti. Accad. Lincei, V.I, 2 128, 173, 334 (1925).
7. Rolla, L. and Piccardi, G., Atti. Accad. Lincei V.I, 3 410, 489 (1926).

8. Rolla, L. and Piccardi, G., Atti. Accad. Lincei, V.I, 5 818 (1927).
9. Page, F.M., Dissertation, Cambridge (1955).
10. Wilson, H.A., Rev. Mod. Phys. 3, 156 (1931).
11. Saha, M.N., Phil. Mag. 40, 472 (1920).
12. Sugden, T.M. and Wheeler, R.C., Disc. Farad. Soc. 19, (1955).
13. Wheeler, R.C., Thesis, Cambridge (1954).
14. Karmen, A., Anal. Chem, 36, 1416 (1964).
15. Karmen, A., and Giuffrida, L., Nature, 201, 1204 (1964).
16. Giuffrida, L. J. Assoc. Anal. Chemists, 47, 293 (1964).
17. Karmen, A., Advances in Chromatography, Vol. 2, Dekker, New York (1966).
18. Aue, W.A., and Gehrke, C.W., Spectral Characteristic of the "thermionic" detector, American Chemical Society, New York (1966).
19. Saturno, T.T. and Cooke, W.D., American Chemical Society, New York (1966).
20. Padley, P.J., Page, F.M. and Sugden, T.M., T.F.S., 57, 1552 (1961).
21. Page, F.M. and Woolley, D.E., Anal. Chem. Vol. 40, 210 (1968).
22. Guest, J., Dip. Tech. Thesis, Aston (1961).
23. Miller, R., Dip. Tech. Thesis, Aston (1963).
24. Fenimore, C.P. and Jones, G.W., C. & F., 8, 133 (1964).
25. Miller, W.J., J.C.P., 69, 8, (1978).
26. Friedman, R., 3rd Symposium, p.110 (1949).
27. Semenov, N.N., Some Problems of Chemical Kinetics and Reactivity, Pergamon, London, Vol. 2, 149 (1959).

28. Dixon-Levis, G. and Williams, A., Nature, 196, 1309 (1962).

29. Lewis, B. and Von Elbe, G., Combustion, Flames and Explosions of Gases, Academic Press, New York (1951).

30. Ribaud, G., and Seferian, D. Chaleur et Industrie 167, 130 (1934).

31. Potter, A.E. and Berlad, A.L., J. Phys. Chem, 60, 97 (1956).

32. Fenimore, C.P. and Jones, G.W., J. Phys. Chem. 63, 1834 (1959).

33. Hartley, W.N., Phil. Trans. Roy. Soc., 185A, 161 (1894).

34. Hartley, W.N., P.R.S. 79, 242 (1907).

35. Gaydon, A.G., The Spectroscopy of flames, Chapman and Hall, London, (1974).

36. Fowler, R.H., Statistical Mechanics, 2nd Ed., Cambridge University Press, Cambridge, (1936).

37. Rose, J., Dynamic Physical Chemistry, Pitman & Sons, London (1961).

38. Unsöld, A., Physik der Sternatmosphären, 2nd Ed., Springer Verlag, Berlin (1955).

39. Foster, W.H., Ph.D. thesis, Massachusetts Institute of Technology (1959).

40. Page, F.M. and Sugden, T.M., T.F.S., 53, 1092 (1957)

41. Hayhurst, A.N. and Sugden, T.M., T.F.S., 63, 1375 (1967).

42. James and Sugden, T.M., P.R.S., A227, 212 (1955).

43. Griffiths, E. and Awbery, J.H., P.R.S., A123, 401 (1929).

44. Gaydon, A.G. and Wolfhard, H.G., Flames, Chapman and Hall Ltd., London (1979).

45. deVos, Physica, 20, 690 (1954).

46. Andrew, E. Axford, D.W.E. and Sugden, T.M., T.F.S., 44, 427 (1948).

47. Belcher, H. and Sugden, T.M., P.R.S., 202A 17 (1950).

48. Margenau, H., Phys. Rev. 69, 508 (1946).

49. Belcher, H. and Sugden, T.M., P.R.S., 201A, 840 (1950).

50. Sugden, T.M., 5th Symposium, P.406 (1955).

51. Padley, P.J. and Sugden, T.M., 8th Symposium, p.164 (1962).

52. Sugden, T.M. and Thrush,B. Nature, 168, 703 (1951).

53. Shuler, K.E. and Weber, J., J.C.P., 22, 491 (1954).

54. Wooley, D.E., Dissertation, Aston (1968).

55. Smith, H. and Sugden, T.M., P.R.S., 211A, 31 (1952).

56. Balwanz, W.W., Headrick, J.M. and Anerr, J.A., U.S. Naval Research Lab. Report No. AC.SIL/57/529 (1956).

57. Schneider, J. and Hofman, F.W., Phys. Rev., 116, 244 (1959).

58. Bulewicz, E.M. and Padley, P.J., J.C.P., 22, 491 (1954).

59. Sugden, T.M., 10th Symposium, p.636 (1965).

60. Kay, J., and Page, F.M., T.F.S., 62, 3081 (1966).

61. Page, F.M., Disc. Faraday Soc., 19, 87 (1955).

62. Bulewicz, E.M. and Padley, P.J., 9th Symposium, p 638 (1963)

63. Adler, J., Applied Phys., 20, 1125 (1949).

64. Lamont, "Waveguides", 3rd Ed., Menthuen (1950).

65. Horsfield, A., Ph.D. thesis, University of Cambridge (1957).

66. Padley, P.J. and Sugden, T.M., 8th Symposium, p 164 (1962).

67. Jensen, D.E. and Padley, P.J., 11th Symposium, p 351 (1967).

68. Knewstubb, P.F. and Sugden, T.M., T.F.S., 54, 372 (1958).

69. Williams, H., 8th Symposium, p.179 (1962).

70. Borgers, A.J., 10th Symposium, p 627 (1965).

71. Golant, Sou, phys. Tech. Phys, 5, 1197 (1961).

72. Ragan, "Microwave Transmission Circuits", McGraw-Hill (1948).

73. Jensen, D.E. and Padley, P.J., T.F.S., 62, 2132 (1966).

74. Soundy, R.G. and Williams, H. AGARD Conf. Proc. No. 8, 1, p.165 (1965).

75. Kelly, R. and Padley, P.J., T.F.S., 65, 355 (1969).

76. Cozens, J.R. and Von Engels, A., Nature, 202, 480 (1964).

77. Cozens, J.R. and Von Engels, 10th Symposium, p 670 (1965).

78. Williams, H. 10th Symposium, p 669 (1965).

79. Calcote, H.F., 8th Symposium, p 184 (1962).

80. Langmuir, I., General Electric Review, 26, 731 (1923).

81. Langmuir, I., and Mott-Smith, H., General Electric Review, 27, 449 (1924).

82. Mott-Smith, H.M. and Langmuir, L., Phys. Rev., 28, 727 (1926).

83. Heumann, T. Spectro Chim. Acta, 1, 293 (1940).

84. Kinbara, T., Nakamura, J. and Ikegami, H., 7th Symposium p 263, (1959).

85. King, I.R. and Calcote, H.F., J.C.P., 23, 2203 (1955).

86. Calcote, H.F. 9th Symposium, p 622 (1963).

87. King, I.R., J.C.P., 27, 817 (1957).

88. Wortberg, G., 10th Symposium, p 651 (1965).

89. Travers, B.E.L. and Williams, H., 10th Symposium, p 657 (1965).

90. Langmuir, I., J. Franklin Inst., 196, 754 (1923).

91. Johnson, E.O. and Malter, L., Phys. Rev. 80, 58 (1950).

92. Bills, D.G., Holt, R.B. and McClure, B.T., J. Appl. Phys. 33, 29 (1962).

93. Oskam, H.J., Carlson, R.W. and Oknda, T., Aeronaut. Res. Labs. Report No. A.R.L. 62-417 (1962).

94. Calcote, H.F. and King, I.R. 5th Symposium, p423 (1955).

95. Knewstubb, P.F. and Sugden, T.M., Nature, 196, 1312, (1962).

96. Padley, P.J., 9th Symposium p 635 (1963).

97. Shultz, R.G. and Brown, S.C., Phys. Rev. 98, 19 (1955).

98. Bohm, D., Burhop, E.H.S. and Massey, H.S.W., "The Characteristics of Electrical Discharges in Magnetic Fields". Chapter 2, McGraw-Hill (1949).

99. Jensen, D.E. and Kurzius, S.C., C. & F., 13, 219 (1969).

100. Boyd, F.L.F., Proc. Phys. Soc. B.64, 795 (1951).

101. Su. C.H. and Lam, S.H., Phys. Fluids, 6, 1479 (1963).

102. Cohen, I.M., J. Phys. Fluids, 6, 10, 1492 (1963).

103. Banta, H.E., Phys. Rev. 33, 211 (1929).

104. Clements, R.M. and Smy, P.R., J. Appl. Phys, 40, 4553 (1969).

105. Clements, R.M. and Smy, P.R., J. Appl. Phys. 41, 3745 (1970).

106. Lam, S.H., A.I.A.A.J., 2, 256 (1964).

107. Thomas, D.L., J. Phys. Fluids, 12, 56 (1969).

108. Kimura, I., Negishi, N. and Nakahara, M., 17th Symposium, in press (1978).

109. Arthur, J.R., Nature, 164, 537 (1949).

110. Bulewicz, E.M., James, C.G. and Sugden, T.M., P.R.S., 235A, 89 (1956).

111. Bulewicz, E.M. and Sugden, T.M., T.F.S., 52, 1475 (1956).

112. Bulewicz, E.M. and Sugden, T.M., T.F.S., 52, 1481 (1956).

113. James, C.G. and Sugden, T.M., P.R.S., 248A, 238 (1958).

114. Bulewicz, E.M. and Sugden, T.M., T.F.S., 54, 1855 (1958).

115. See Lewis, B. and Von Elbe, G. Combustion, Flames and Explosions of Gases. Academic Press, New York, p 206 (1951).

116. McWilliam, I.G. and Dewar, R.A., in "Gas Chromatography, 1958" (D.H.Desty, Ed.) pp 142-146. Academic Press, New

York (1958).

117. Thompson, A.E., J. Chromatog, 2, 148 (1959).

118. Calcote, H.F., C. & F., 1, 385 (1957).

119. Knewstubb, P.F., and Sugden, T.M., P.R.S. A255, 520 (1960).

120. DeJaegere, S., Deckers, J. and Van Tiggelen, A., 8th Symposium, p 155 (1960).

121. Condon, E.U. and Odishaw, H., Handbook of Physics, 2nd Ed., McGraw-Hill (1967).

122. Miller, E.R., Disseration, Aston (1969).

123. Newman, R.N., Dissertation, Aston (1971).

124. Calcote, H.F. and King, I.R., J.C.P., 23, 2203 (1955).